Received 22 May 2024; accepted 21 June 2024. Date of publication 3 July 2024; date of current version 1 August 2024.

Digital Object Identifier 10.1109/OJCOMS.2024.3422801

A Survey on Orthogonal Time Frequency Space Modulation

MAHMOUD ALDABABSA[1] (Senior Member, IEEE), SERDAR ÖZYURT[2], GÜNEŞ KARABULUT KURT[3] (Senior Member, IEEE), AND OĞUZ KUCUR[4]

[1]Department of Electrical and Electronics Engineering, Nisantasi University, 34481742 Istanbul, Türkiye

[2]Department of Electrical and Electronics Engineering, Ankara Yıldırım Beyazıt University, 06010 Ankara, Türkiye

[3]Department of Electrical Engineering, Polytechnique Montréal, Montreal, QC H3T 1J4, Canada

[4]Department of Electronics Engineering, Gebze Technical University, 41400 Gebze, Türkiye

CORRESPONDING AUTHOR: G. KARABULUT KURT (e-mail: gunes.kurt@polymtl.ca)

This work was supported in part by the Natural Sciences and Engineering Research Council of Canada (NSERC) Discovery Program.

ABSTRACT Orthogonal time frequency space (OTFS) modulation is strongly considered as a promising solution for high-mobility communications. In contrast to conventional modulation techniques, wherein information symbols are multiplexed in a one-dimensional time or frequency domain, OTFS employs a two-dimensional modulation scheme by multiplexing information symbols in the delay-Doppler domain. This paper presents a comprehensive survey of OTFS. It starts with an overview of OTFS, its advantages over conventional air interface techniques, general block diagrams, and implementations. Subsequently, the paper explores the potential integration of multiple-input multiple-output and OTFS techniques. The paper further discusses the feasibility of integrating OTFS into multiple access techniques as a solution for maintaining acceptable performance in high-mobility scenarios. Then, widespread applications of OTFS in satellite communications are highlighted. Also, the potential utilization of OTFS modulation in integrated sensing and communications paradigm is thoroughly treated. In addition, the survey covers further applications of OTFS in deep learning, index modulation, underwater acoustic, and unmanned aerial vehicle communications. The paper concludes by pointing out numerous challenging and promising directions for future OTFS research.

INDEX TERMS Orthogonal time frequency space (OTFS), delay-Doppler domain, multiple-input multiple-output, multiple access techniques, satellite communications, integrated sensing and communications, deep learning, index modulation, underwater acoustic, unmanned aerial vehicle.

I. INTRODUCTION

IN THE next few years, sixth-generation (6G) will bring a substantial revolution in communication technologies. It will enable the Internet of Everything (IoE) and provide significant development in performance superior to the emerging 5G [1], [2], [3]. The 6G has been envisioned to support different usage scenarios, summarized and depicted in Fig. 1, such as further enhanced mobile broadband (FeMBB), ultra-massive machine-type communications (umMTC), enhanced ultra-reliable and low-latency communications (eURLLC), long-distance and high-mobility communications (LDHMC), and extremely low power communications (ELPC) [1]. It has been anticipated that 6G would have extraordinary requirements to support the aforementioned great applications. Particularly, 6G has been expected to offer a peak data rate of at least one terabit per second ($\geq$ 1 Tbps), a user-experienced data rate of more than one gigabit per second ($\geq$ 1 Gbps), a connectivity density to reach millions of devices/users per km^2, a reduction in communication latency to small fractions of milliseconds (0.01-0.1 ms), an increase in the mobility speed to a minimum of 1000 kilometers per hour ($\geq$ 1000 kmph), a network energy efficiency of 10-100 times, a spectrum efficiency of 5-10 times, and reliability of 10 times those of 5G [1]. Notably, these requirements are critical challenges of their own. However, the most challenging 6G requirement

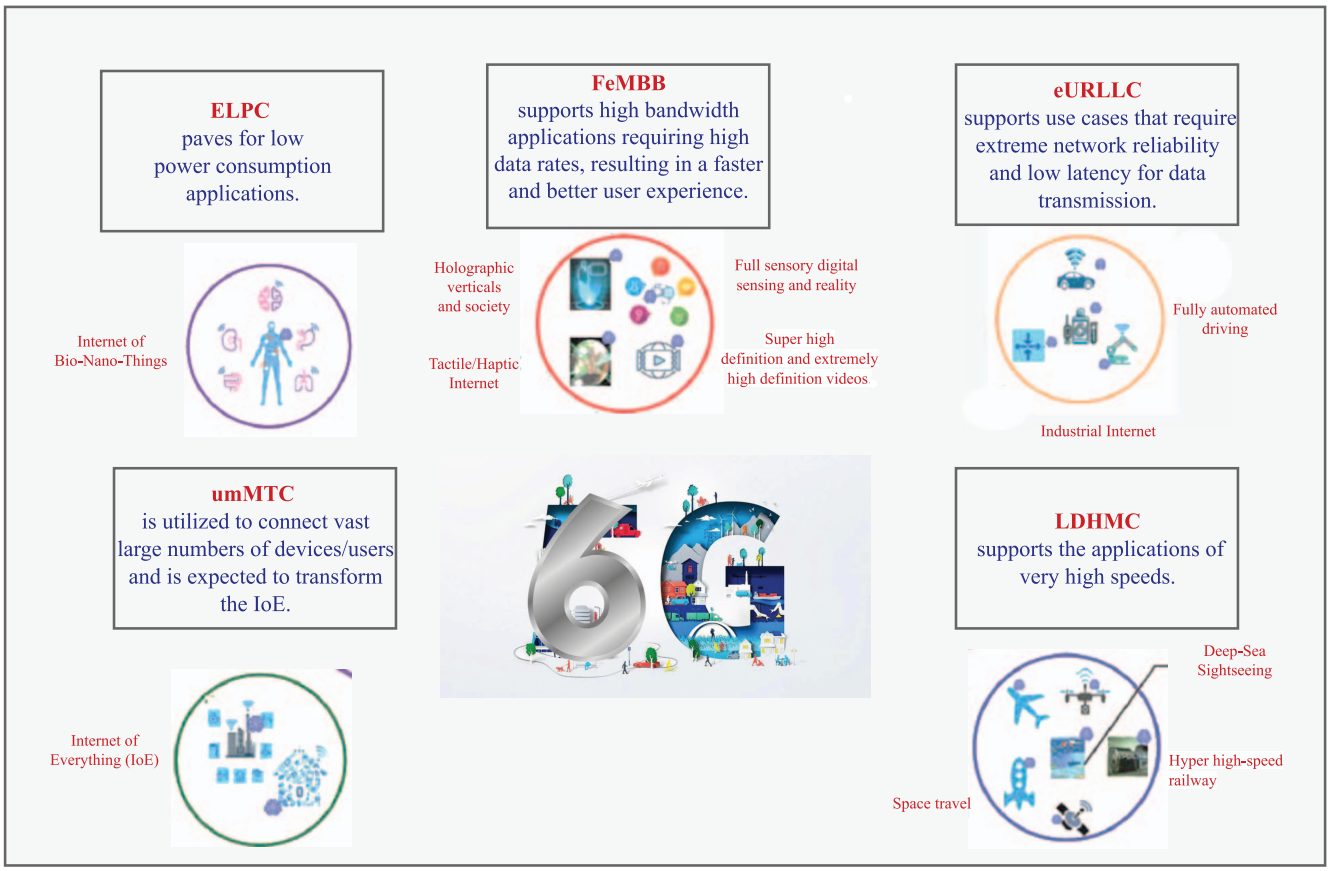

FIGURE 1. Potential usage scenarios for 6G (inspired by Fig. 1 of [1]).

is driven by the usage scenarios, in which it is expected to provide reliable communications in high-mobility environments.

Wireless communications operating at the high carrier frequency (f_c) in high-mobility environments experience fast time-variation of fading channels caused by the large Doppler spread[1] [4]. This will significantly deteriorate the performance of the system. Generally speaking, the wireless channel is doubly dispersive and has many paths. For each path, there are associated delay and Doppler values. Thus, the wireless channel can be easily depicted as a plurality of reflectors in the two-dimensional delay-Doppler (DD) domain. The wireless channels are categorized as linear time-invariant (LTI) channels, in which Doppler values are considered zeros, and linear frequency-invariant channels, where delay values are assumed to be zero. The system performance will significantly degrade once both delay and Doppler effects are present. It means that a waveform that is DD invariant is highly desired. Nevertheless, it can be noted that the spectrum of the 6G will be in the multi-THz range, and its mobility will be as high as thousands of kmph. This means that the Doppler impact is inevitable in the 6G, and if it is not taken into account for system design, the 6G will suffer from significant performance degradation over high-mobility channels. Fortunately, an increasing amount of research has recently been dedicated to high-mobility communications of next-generation wireless networks. To cope with the high-mobility problem, the researchers think more deeply about the radio resource element, which carries information signals from source to destination over the air. They have raised a crucial question, *do the existing air interface techniques and associated waveforms support diverse challenging requirements and usage scenarios of the 6G?* or *is it time to introduce a new air interface?*

The air interface has undergone notable changes over the generations of mobile communication systems. It was frequency division multiple access (FDMA), time division multiple access (TDMA), and code division multiple access (CDMA) in the 1G, 2G, and 3G networks, respectively. In 4G and 5G networks, respectively, the air interface was orthogonal frequency division multiple access (OFDMA), which exploited the orthogonality principle, and is the modified version of orthogonal frequency division multiplexing (OFDM), where the subcarrier bandwidth and cyclic prefix (CP) interval are made flexible. Unfortunately, the OFDM used in the emerging 5G networks will not satisfy the 6G

[1]Doppler spread is defined as the difference in shift frequencies associated with the multiple propagation paths when there is relative motion between the transmitter and the receiver.

requirements with high system performance. Additionally, it will not be a well-suited solution for offering reliable communications in high-mobility environments. The reasons behind that can be summarized as follows:

- In the OFDM, the channel is assumed to be quasi-static frequency-selective fading, which means that the channel remains constant over one OFDM symbol period. Nevertheless, the channel will change inside one OFDM symbol in high-mobility environments. Thus, the fading time-variation will destroy the orthogonality among subcarriers and introduce inter-carrier interference (ICI) due to carrier frequency offset (CFO). This will significantly deteriorate the system's performance.
- In the OFDM, a significant channel estimation overhead is necessary due to the limited coherence time of the time-frequency (TF) domain channel. For example, consider an OFDM system with a carrier frequency of $f_c = 3.5$ GHz, a subcarrier spacing of $\Delta f = 15$ KHz, and a relative velocity of $v = 300$ kmph. OFDM symbol duration (including a 20% CP) is 80 ms. Accordingly, the maximum Doppler shift is $\nu_{\max} \approx 0.97$ KHz, and the channel's coherence time is around 257 ms. Therefore, one channel coherence interval can only accommodate at most three OFDM symbols, which means a pilot symbol is inserted every three OFDM symbols, leading to a large overhead [8].

Recently, orthogonal time frequency space (OTFS) modulation has been suggested as a promising candidate for high-mobility communications [5], [6]. Compared to the conventional modulation techniques, in which the information symbols are multiplexed in a one-dimensional time-domain or frequency-domain, the OTFS is a two-dimensional modulation scheme, where the information symbols are multiplexed in the DD-domain. With special features, the OTFS has been recognized as a strong candidate among all modulation interface techniques to overcome high-mobility communications challenges and to achieve the requirements of the next mobile communication systems. The essential benefits of the OTFS can be remarked as follows.

1) *Delay- and Doppler-resilience:* The OTFS can radically transform a random fading channel within the TF frame into a stationary, deterministic, and non-fading channel. All information symbols in one OTFS frame experience the same static channel response. As a result, the OTFS can easily track time-varying fading, especially in high-speed mobile communications, which means that OTFS is resilient to both delay and Doppler shifts.
2) *Robust against CFO:* In high-mobility environments, the Doppler shift leads to CFO, which means that the oscillators' frequencies at the source and destination are mismatched. The CFO will destroy the orthogonality among the subcarriers and introduce ICI in multi-carrier systems such as OFDM. Since the Doppler shifts in high-mobility systems are a function of time, the CFO is time-varying, which means that the OFDM finds it challenging to track and compensate the CFO. However, due to Doppler-resilience benefits, the OTFS is more robust against the CFO than the OFDM.
3) *Low idle time:* The guard intervals are merely needed between consecutive OTFS frames rather than between time slots. Thus, the associated idle time is significantly reduced.
4) *Low number of pilot symbols for channel estimation training overhead:* In high-mobility environments, the channel envelope fluctuates violently, even for a short time. However, the DD response of wireless channels is much more sparse than the TF response, and the rate of change of the channel will be slower. In addition, multiplexing information in the DD-domain turns a time-varying channel into a quasi-static channel in the DD-domain. This might significantly reduce the amount of signaling overhead required for channel estimation. Hence, for channel estimation, the OFDM needs to send more times of pilots than the OTFS.
5) *Compatibility with the existing communication systems:* The OTFS can be implemented as a pre- and post-processing block to the OFDM systems. This enables the OTFS to have architectural back-compatibility with existing communication systems.
6) *Full diversity and reliability:* In contrast to the existing one-dimensional time-domain or frequency-domain modulation techniques, the OTFS is a two-dimensional modulation technique. The data symbols are multiplexed in the DD-domain, and each symbol is spread across the entire TF-domain. This leads to attaining maximum achievable diversity or transmission over doubly dispersive channels, provided that each time-domain and frequency-domain sample experiences independent fading. Note that the number of independently fading resolvable paths in the DD-domain determines the maximum attainable diversity order. Therefore, the OTFS has the potential to offer full diversity, which is the key to support reliable communications.
7) *Useful choice for different communications systems:*
   - Massive multiple-input multiple-output (MIMO) systems: As known, multiantenna systems suffer from the problem of channel estimation, which results in significant performance degradation. However, since the OTFS operates in the DD-domain, where the channel can be characterized in a very compact form, the OTFS can enable dense and flexible packing of reference signals. This means that the OTFS can provide accurate channel estimation. Therefore, the OTFS can support large antenna arrays in massive MIMO applications.
   - Millimeter-Wave (mm-Wave) systems: Regarding that mm-Wave systems utilize high carrier

frequencies, Doppler effects will be significantly amplified. However, the OTFS can easily handle the Doppler effect. This means the OTFS can be a beneficial choice for mm-Wave systems.

Although the advantages mentioned above render the OTFS eminently suitable for high-mobility and high-carrier scenarios, the OTFS has different disadvantages, which can be summarized as follows.

1) *Latency:* The OTFS modulation spreads information over a more extended block than the OFDM to combat channel fluctuations. This can increase the overall latency. In particular, each OTFS signal's duration is N times that of an OFDM symbol, with the same number of subcarriers and the same subcarrier spacing. However, by increasing the subcarrier spacing or reducing N at the expense of a reduced Doppler resolution, the OTFS's latency can be identical to that of the OFDM.
2) *Fractional Doppler:* In the case of fractional Doppler, the DD-domain requires particular channel estimation and detection algorithms. Otherwise, the performance may significantly degrade.
3) *Fractional delay:* Fractional delay can cause symbols to overlap in time, leading to inter symbol interference (ISI). Moreover, fractional delay complicates channel estimation and equalization processes in OTFS systems. It introduces additional phase shifts and distortions, making it challenging to estimate the channel response and apply appropriate equalization techniques accurately. As a result, the receiver may struggle to recover the transmitted symbols correctly, leading to increased error rates. Overall, fractional delay can degrade the performance of OTFS systems in terms of data rate, error rate, and spectral efficiency.

In [7], the authors introduced the concept of OTFS, including the key characteristics of the DD-domain channel, DD-domain multiplexing, and OTFS transceiver architecture. They then discussed the significant issues of OTFS, such as channel estimation, efficient data detection, and coding/decoding, and presented relevant initial results. Finally, they discussed the potential applications of OTFS and proposed several promising research directions. In [8], [9], [10], the authors created a three-part series of tutorials. The first paper [8] focused on two implementations of OTFS modulation. The second [9] provided a comprehensive overview of OTFS transceiver design. Lastly, [10] discussed OTFS-based integrated sensing and communications (ISAC), which is expected to be a powerful technology. In [11], the authors introduced an overview of the OTFS modulation for the Internet of Things (IoT). They discussed the OTFS's transceiver design, its advantages, challenges, and future design principles. In [12], the authors presented an in-depth review of OTFS technology in the context of the 6G era, encompassing fundamentals, recent advancements, and future directions. The authors in [13] provided a comprehensive summary and analysis of OTFS techniques and also illustrated the advantages of OTFS modulation from the level of multicarrier modulation comparison.

Differing from the aforementioned survey papers, this paper provides a more detailed guide for the research on OTFS. The main contributions of this paper can be highlighted as follows:

- provides an overview of OTFS, its advantages over conventional air interface techniques, general block diagrams, and implementations. Then, it reviews the literature on standard OTFS in terms of low-complexity signal detection, channel estimation, peak-to-average power ratio (PAPR), system design, and performance analysis.
- explores the potential integration of MIMO and OTFS techniques. It starts by demonstrating the MIMO-OTFS transceiver block diagram. Then, it highlights the related literature on MIMO-OTFS.
- discusses the feasibility of integrating OTFS into multiple access techniques as a solution for maintaining acceptable performance in high-mobility scenarios. It focuses on related works that are interested in the combination of OTFS with orthogonal multiple access (OMA) and non-orthogonal multiple access (NOMA) techniques.
- shows widespread applications of OTFS in satellite communications.
- considers the potential of OTFS modulation in ISAC transmissions.
- presents further applications of OTFS in deep learning (DL), index modulation (IM), underwater acoustic (UWA), and unmanned aerial vehicle (UAV) communications.
- The paper concludes by pointing out numerous challenging and promising directions for future OTFS research. For example, when the DD domain channel parameters are time-variant within a frame duration, the adaptation of OTFS to such a scenario poses a challenging future research direction. Moreover, with the new perspectives OTFS offer, there is likely an increasing interest in OTFS from a security point of view. Furthermore, a comprehensive performance evaluation of OTFS-NOMA for any number of users under practical impairments over generalized fading channels constitutes a potential future research topic. In addition, the exploitation of machine learning approaches in OTFS systems will attract intense interest when they are utilized in different scenarios with distinct goals. Also, the synergy between OTFS and ISAC is expected to be explored further in the future.

The rest of this paper is organized as follows: Section II introduces OTFS, including its general block diagram, implementations, and comparison with OFDM. Section III presents

TABLE 1. List of symbols frequently used in the text.

Symbol	Definition
f_c	Carrier frequency
Δf	Subcarrier spacing
v	Relative velocity
ν	Doppler shift
c	Speed of light
$h(\tau, t)$	Impulse response of the LTV channels
P	Number of paths
$h_i(t)$	Complex channel coefficient of the i-th path
$\tau_i(t)$	Propagation delay of the i-th path
$h_{TF}(f, t)$	The channel in TF-domain
$h_{DD}(\tau, \nu)$	The channel in DD-domain
h_i	Channel coefficient of the i-th path
B_{OTFS}	Bandwidth of OTFS frame
T_{OTFS}	Time duration of OTFS frame
K	Number of subcarriers
L	Number of time slots
T	Time duration
$X_{DD}[l, k]$	Information symbols in DD-domain
$s(t)$	Time-domain transmit signal of the OTFS
$r(t)$	Received signal in the time-domain
$Y_{DD}[l, k]$	Received signal in the DD-domain
g_{tx}	Transmitter pulse shaping filter
g_{rx}	Receiver pulse shaping filter
$z(t)$	AWGN
$[\cdot]_W$	Modulo operation w.r.t. W
$H_{DD}[l, k, l', k']$	Discrete DD-domain channel
$Z_{DD}[l, k]$	Discrete DD-domain noise
$w(l, k, l', k', l_i, k_i)$	Sampling function

TABLE 2. List of abbreviations frequently used in the text.

Abbreviation	Explanation
6G	Sixth-generation
ADC	Analog-to-digital conversion
AMP	Approximate message passing
AWGN	Additive white Gaussian noise
BER	Bit error rate
BL	Bayesian learning
CDMA	Code division multiple access
CFO	Carrier frequency offset
CIR	Channel impulse response
CLT	Central limit theorem
CoDSC	Continuous-Doppler spread channel
CP	Cyclic prefix
CSI	Channel state information
CZT	Continuous Zak transform
DAC	Digital-to-analog conversion
DD	Delay-Doppler
DFrFT	Discrete Fractional Fourier Transform
DL	Deep learning
DoF	Degrees-of-freedom
DZT	Discrete Zak transform
ELPC	Extremely low power communications
EP	Expectation propagation
eURLLC	Enhanced ultra-reliable and low-latency communications
FDMA	Frequency division multiple access
FeMBB	Further enhanced mobile broadband
FSS	Fractionally spaced sampling
ICI	Inter-carrier interference
ICZT	Inverse continuous Zak transform
IDI	Inter-Doppler interference
IDZT	Inverse discrete Zak transform
IM	Index modulation
IoE	Internet of Everything
IoT	Internet of Things
ISAC	Integrated sensing and communication
ISFFT	Inverse symplectic finite Fourier transform
ISI	Inter symbol interference
LDHMC	Long-distance and high-mobility communications
LEO-Sat	Low earth orbit satellite
LMMSE	Linear minimum mean square error
LoS	Line-of-sight
LSMR	Least squares minimum residual
LTI	Linear time-invariant
LTV	Linear time-varying
MF-MPD	Matched filtering-based message-passing detector
MIMO	Multiple-input multiple-output
ML	Maximum likelihood
MLSE	Maximum-likelihood sequence estimation
MMSE	Minimum mean square error
mmWave	Millimeter-Wave
MP	Message passing
MSE	Mean square error
NOMA	Non-orthogonal multiple access
OFDM	Orthogonal frequency division multiplexing
OFDMA	Orthogonal frequency division multiple access
OP	Outage probability
OTFS	Orthogonal time frequency space
PAPR	Peak-to-average power ratio
PC	Probability clipping
PMP	Parallel message passing
SFFT	Symplectic finite Fourier transform
SNR	Signal-to-noise ratio
SP	Superimposed pilot
TD	Time-delay
TDMA	Time division multiple access
TF	Time-frequency
UAV	Unmanned aerial vehicle
umMTC	Ultra-massive machine-type communications
UWA	Underwater acoustic
w.r.t.	with respect to
ZF	Zero forcing
ZT	Zak transform

and reviews the combination of MIMO and OTFS techniques in the relevant literature. Section IV introduces the potential of integrating OTFS into multiple access techniques, such as NOMA, as a solution for maintaining acceptable performance in high-mobility scenarios. Section V introduces OTFS as a promising waveform technology for satellite communications and reviews related literature on the topic. Sections VI and VII present the application of OTFS-ISAC and other application scenarios, respectively. Challenges and future perspectives in OTFS are given in Section VIII. Finally, the paper is concluded in Section IX.

Kindly note that the lists of symbols and abbreviations frequently used in the text are given, respectively, in Tables 1 and 2.

II. OTFS FUNDAMENTALS

In this section, we begin by providing an overview of the wireless channel models. We then introduce OTFS, its general block diagram, its implementations and its comparison with OFDM. Lastly, we present a review of the literature on OTFS modulation.

A. WIRELESS CHANNEL

In general, the wireless channel is linear time-varying (LTV). When a signal goes through a typical wireless channel, it gets reflected and refracted from multiple scatterers. This multipath results in time-dispersion of the signal. In addition, these refractors and transceivers can be mobile, resulting in frequency-dispersion of the signal. In the following, we consider three scenarios, as depicted in Fig. 2, that clearly illustrate time-dispersive, frequency-dispersive, and doubly-dispersive channel models.

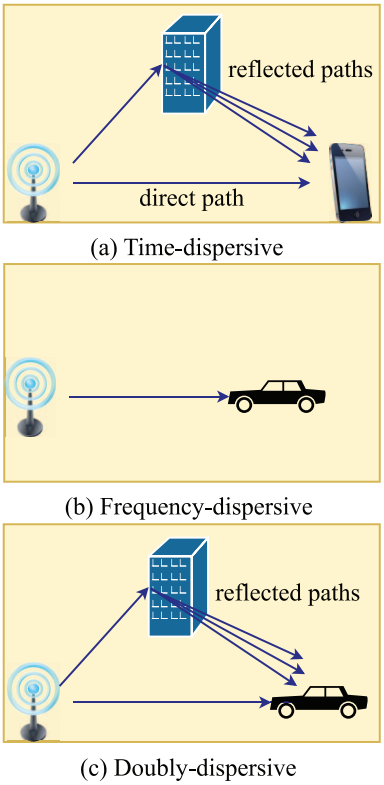

FIGURE 2. Illustration of wireless channel (a) Time-dispersive (b) Frequency-dispersive (c) Doubly-dispersive.

Consider the first scenario, where the transmitter and receiver are stationary, as shown in Fig. 2 (a). The difference in the propagation delay of the direct and reflected paths causes multiple copies of the transmitted signal to arrive at the receiver at different times. In this case, an LTI system can model the wireless channel. Hence, one-dimensional channel impulse response (CIR) in the delay-domain $h(\tau)$ is sufficient for characterizing the time-dispersive channel. The frequency response of this CIR is a frequency-selective channel transfer function. The frequency selectivity becomes more severe when the delay spread[2] increases significantly since the frequency-domain fades' separation is increasingly proportional to the CIR length.

Now consider the second scenario, where the receiver is a car moving towards the transmitter with a relative velocity v, as shown in Fig. 2 (b). The Doppler shift of the line-of-sight (LoS) due to the relative velocity is given by $\nu = \frac{vf_c}{c}$, where c denotes the light speed. In this case, an LTV system can model the wireless channel. The LTV channels give rise to frequency shifts due to the Doppler effect, yielding frequency-dispersive (time-selective) channels. Here, the separation of the channels' time-domain fades is increasingly proportional to the Doppler spread.

Finally, consider the last scenario (high-mobility scenario), which includes the multipath propagation and Doppler effects, as shown in Fig. 2 (c). Here, the LTV channels are doubly-dispersive due to the joint presence of multipath propagation and Doppler effects. The transmitted signals suffer from dispersions both in the time-domain and frequency-domain. Hence, two-dimensional CIR in the time-delay domain $h(\tau, t)$ is required for characterizing the time-dispersive and frequency-dispersive channels. The impulse response of the LTV channels can be written as

$$h(\tau, t) = \sum_{i=1}^{P} h_i(t)\delta(\tau - \tau_i(t)), \tag{1}$$

where P is the number of paths, and $h_i(t)$ and $\tau_i(t)$ are the complex channel coefficient and propagation delay of the i-th path, respectively.

The LTV channels can be equivalently depicted in either the TF- or DD-domain. The TF-domain channel, $h_{TF}(f, t)$, can be obtained by taking the Fourier transform of $h(\tau, t)$ with respect to (w.r.t.) delay τ. The TF-domain channel can be written as

$$\begin{aligned} h_{TF}(f, t) &= \int_{-\infty}^{\infty} h(\tau, t)e^{-j2\pi f\tau}d\tau \\ &= \int_{-\infty}^{\infty} \sum_{i=1}^{P} h_i(t)\delta(\tau - \tau_i(t))e^{-j2\pi f\tau}d\tau \\ &= \sum_{i=1}^{P} h_i(t)e^{-j2\pi f\tau_i(t)}. \end{aligned} \tag{2}$$

We can observe from (2) that $h_{TF}(f, t)$ is a complex channel transfer function coefficient at frequency f and time instant t. On the other hand, the DD-domain channel, $h_{DD}(\tau, \nu)$ can be obtained by taking the Fourier transform of $h(\tau, t)$ w.r.t. t. The DD-domain channel can be expressed as

$$\begin{aligned} h_{DD}(\tau, \nu) &= \int_{-\infty}^{\infty} h(\tau, t)e^{-j2\pi ft}dt \\ &= \int_{-\infty}^{\infty} \sum_{i=1}^{P} h_i(t)\delta(\tau - \tau_i(t))e^{-j2\pi ft}dt. \end{aligned} \tag{3}$$

With some mathematical calculations, the complex channel response in the DD-domain can be stated as

$$h_{DD}(\tau, \nu) = \sum_{i=1}^{P} h_i\delta(\tau - \tau_i)\delta(\nu - \nu_i), \tag{4}$$

where $\tau_i \in [0, \tau_{\max}]$ and $\nu_i \in [-\nu_{\max}, \nu_{\max}]$ denote the delay and Doppler shifts of the i-th path, respectively. Here, $\tau_{\max}$ and $\nu_{\max}$ denote the maximum delay and Doppler shifts in the considered high-mobility propagation environment, respectively. We can notice from (4) that the DD-domain channel $h_{DD}(\tau, \nu)$ characterizes the intensity of scatterers having a propagation delay of τ and Doppler frequency shift of ν.

Based on the TF-domain and DD-domain, we have the following observations:

1) With the limited coherence time and bandwidth of LTV channels in high-mobility scenarios, channel

[2]The delay spread is defined as the difference between the propagation delays of the longest and shortest paths, i.e., $\tau_{\max} - \tau_{\min}$.

acquisition in the TF-domain can be challenging, which may result in significant signaling overhead. On the other hand, the DD-domain channel responses fluctuate much slower than time-delay-domain or TF-domain channel responses since the DD-domain channel response changes only in the cases of remarkable changes in propagation path length or very high moving speed. This will reduce the signaling overhead and give an advantage to DD-domain over TF-domain to represent LTV channels in high-mobility scenarios.

2) The LTV channel in the DD-domain has valuable features that significantly facilitate channel estimation and data detection. These features can be highlighted below.
   - Separability: The DD-domain of wireless channels can separate the propagation paths with the same delay, thereby revealing the total number of channel degrees-of-freedom (DoF) available.
   - Stability: The DD-domain channel response is much more stable than that of time-delay-domain or TF-domain channel responses, as it only changes significantly when there is a significant difference in the propagation path length or when the speed of the moving object is very high.
   - Compactness: Generally, the maximum delay and Doppler values of a wireless channel are such that $\tau_{\max}\nu_{\max} \leq \frac{1}{4}$. Accordingly, $h_{DD}(\tau, \nu)$ has a compact DD-domain support within the intervals $[0, \tau_{\max}]$ and $[-\nu_{\max}, \nu_{\max}]$ along the delay and Doppler dimensions, respectively.
   - Potential Sparsity: When there are few moving scatterers in the propagation environment, the DD-domain channel will have a sparse response.

B. OTFS AND ITS IMPLEMENTATIONS

We assume an OTFS frame with a bandwidth of B_{OTFS} and a time duration of T_{OTFS}, defined in the TF-domain. The bandwidth is divided into L subcarriers with subcarrier spacing $\Delta f = \frac{B_{\text{OTFS}}}{L}$ and time duration is divided into K time slots with slot duration $T = \frac{T_{\text{OTFS}}}{K}$. As illustrated in Fig. 3, at the transmitter side of the OTFS, we assume that a set of LK information symbols $\{X_{DD}[l, k]\}$ are mapped into the two-dimensional DD-domain from the modulation alphabet to be transmitted over the OTFS time duration T_{OTFS} and OTFS bandwidth B_{OTFS}. Here, $l \in \{0, 1, \ldots, L-1\}$ and $k \in \{0, 1, \ldots, K-1\}$ are the delay and Doppler indices, respectively. In addition, we define $s(t)$ as the time-domain transmit signal of the OTFS. On the other hand, we define $r(t)$ and $Y_{DD}[l, k]$ as the received signal at the OTFS receiver in the time-domain and DD-domain, respectively.

We notice from Fig. 3 that the key function of the OTFS modulation is to transform the DD-domain signals, $X_{DD}[l, k]$, into a time-domain signal, $s(t)$, for transmission. On the other hand, the OTFS demodulation transforms the received time-domain signal, $r(t)$, into a DD-domain signal $Y_{DD}[l, k]$.

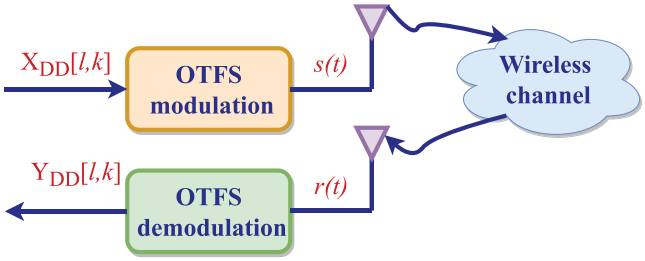

FIGURE 3. OTFS transceiver block diagram.

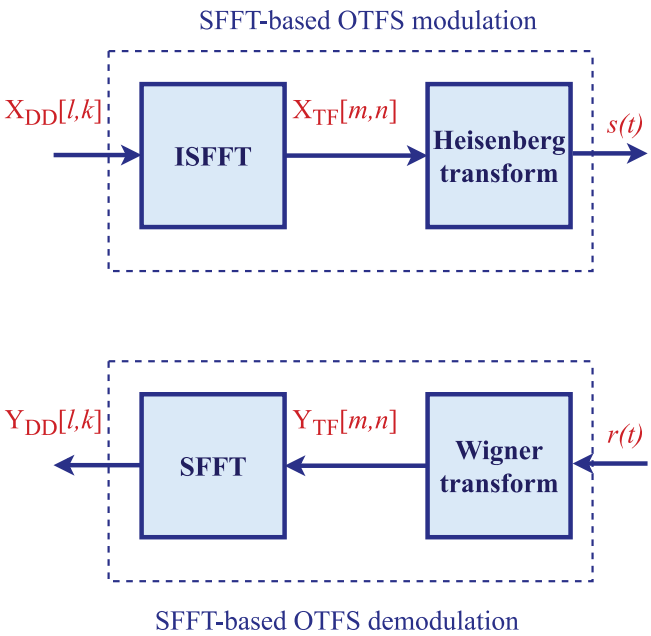

FIGURE 4. SFFT-based OTFS modulation and demodulation block diagrams.

The OTFS modulation/demodulation can be implemented commonly via two typical implementations named *symplectic finite Fourier transform (SFFT)-based OTFS* [8], and *Zak transform (ZT) (discrete ZT (DZT) [8] and continuous ZT (CZT) [14], [15], [16])-based OTFS*. In general, the SFFT-based OTFS modulation maps the DD-domain information symbols first to the TF-domain and then to the time-domain. On the other hand, the ZT-based OTFS modulation directly transforms the DD-domain information symbols into the time-domain. In the following, we will review both implementations in more detail and finally show their similarities and differences.

1) SFFT-BASED OTFS

As shown in Fig. 4, the SFFT-based OTFS modulation and demodulation are produced by a cascade of a pair of two-dimensional transforms at both the transmitter and receiver. The following steps can summarize this:

- At the transmitter, the modulator first utilizes the *ISFFT* to map the information symbols in the DD-domain to samples in the TF-domain.

- Next, the modulator applies the *Heisenberg transform* to create the time-domain signal to be transmitted over the wireless channel.
- At the receiver, the demodulator uses *Wigner transform* (the inverse of the Heisenberg transform) to map the received time-domain signal to the TF-domain.
- Finally, the demodulator exploits the *SFFT* to transform the TF-domain signal to the DD-domain signal.

Now, let us explain each part in SFFT-based OTFS modulation and demodulation deeply.

By using the ISFFT, the DD-domain symbol $X_{DD}[l,k]$ is transformed into TF-domain signal $X_{TF}[m,n]$, which can be written as

$$X_{TF}[m,n]=\frac{1}{\sqrt{LK}}\sum_{l=0}^{L-1}\sum_{k=0}^{K-1}X_{DD}[l,k]e^{j2\pi\left(\frac{k}{K}m-\frac{l}{L}n\right)}, \quad (5)$$

where $m\in\{0,1,\ldots,K-1\}$ and $n\in\{0,1,\ldots,L-1\}$ are the time slot and subcarrier indices, respectively. Note that $X_{TF}[m,n]$ in (5) can be rewritten as

$$X_{TF}[m,n]=\underbrace{\frac{1}{\sqrt{K}}\sum_{k=0}^{K-1}X_{DD}\left[\tilde{l},k\right]e^{\frac{j2\pi k}{K}m}}_{\text{IDFT}} \times\underbrace{\frac{1}{\sqrt{L}}\sum_{l=0}^{L-1}X_{DD}\left[l,\tilde{k}\right]e^{-\frac{j2\pi l}{L}n}}_{\text{DFT}}, \quad (6)$$

where $\tilde{l}$ and $\tilde{k}$ refer to the fixed l-th delay and k-th Doppler, respectively. We can observe from (6) that the $X_{TF}[m,n]$ can be calculated by taking the IDFT of the Doppler and DFT of the delay of $X_{DD}[l,k]$, respectively. Therefore, we can produce a set of LK symbols of X_{TF} by taking the K-point IDFT of the rows of X_{DD} and L-point DFT of the columns of X_{DD}, respectively. In other words, the ISFFT can be produced by taking the IDFT of the Doppler, which produces the time-domain, and the DFT of the delay, which produces the frequency-domain. To sum up, as illustrated in Fig. 5, the ISFFT corresponds to a two-dimensional transformation which takes a K-point IDFT of the rows of X_{DD} and an L-point DFT of the columns of X_{DD}. Accordingly, the ISFFT transforms the signal from the DD-domain to the TF-domain.

Next, the SFFT-based OTFS applies Heisenberg transform to create the time-domain transmit signal $s(t)$, which can be stated as

$$s(t)=\sum_{m=0}^{K-1}\sum_{n=0}^{L-1}X_{TF}[m,n]g_{tx}(t-mT)e^{j2\pi n\Delta f(t-mT)}, \quad (7)$$

where $g_{tx}(t)$ is the transmitter pulse shaping filter. We can notice from (7) that the Heisenberg transform converts the TF domain signal $X_{TF}[m,n]$ to a continuous time-domain waveform $s(t)$ using a transmit waveform $g_{tx}(t)$. This can be similar to performing multicarrier modulation on the TF domain signal $X_{TF}[m,n]$ to obtain $s(t)$, which is illustrated in Fig. 6.

Then, the signal $s(t)$ will be transmitted through LTV wireless channel. The time-domain received signal can be expressed as

$$r(t)=\int_{-\infty}^{\infty}\int_{-\infty}^{\infty}h_{DD}(\tau,\nu)e^{j2\pi\nu(t-\tau)}s(t-\tau)d\tau d\nu+z(t), \quad (8)$$

where $z(t)$ denotes the additive white Gaussian noise (AWGN) in the time-domain. Substituting (4) into (8) and using

$$\int_{-\infty}^{\infty}\int_{-\infty}^{\infty}s(t-\tau)\delta(\tau-\tau_i)\delta(\nu-\nu_i)e^{j2\pi\nu(t-\tau)}d\tau d\nu =s(t-\tau_i)e^{j2\pi\nu_i(t-\tau_i)}, \quad (9)$$

Then

$$r(t)=\sum_{i=1}^{P}h_i s(t-\tau_i)e^{j2\pi\nu_i(t-\tau_i)}+z(t). \quad (10)$$

At the OTFS receiver, Wigner transform is performed to map the received time-domain signal $r(t)$ to the TF-domain. The TF-domain received signal for the mth time slot and nth subcarrier can be written as

$$Y_{TF}[m,n]=\int_{-\infty}^{\infty}r(t)g_{rx}^{*}(t-mT)e^{-j2\pi n\Delta f(t-mT)}dt, \quad (11)$$

where $g_{rx}(t)$ is the receiver filter. This can be similar to performing multicarrier demodulation on the time-domain signal $r(t)$ to obtain $Y_{TF}[m,n]$, as shown in Fig. 6. Then, the TF-domain received signal is transformed into the DD-domain by the SFFT. The resulting DD-domain received signal is given by

$$Y_{DD}[l,k]=\frac{1}{\sqrt{LK}}\sum_{m=0}^{K-1}\sum_{n=0}^{L-1}Y_{TF}[m,n]e^{j2\pi\left(-\frac{m}{K}k+\frac{n}{L}l\right)}. \quad (12)$$

Note that $Y_{DD}[l,k]$ in (12) can be rewritten as

$$Y_{DD}[l,k]=\underbrace{\frac{1}{\sqrt{K}}\sum_{m=0}^{K-1}Y_{TF}\left[m,\tilde{n}\right]e^{-j2\pi\frac{m}{K}k}}_{\text{DFT}} \times\underbrace{\frac{1}{\sqrt{L}}\sum_{n=0}^{L-1}Y_{TF}\left[\tilde{m},n\right]e^{j2\pi\frac{n}{L}l}}_{\text{IDFT}}, \quad (13)$$

where $\tilde{m}$ and $\tilde{n}$ refer to the fixed mth slot and nth subcarrier, respectively. We can observe from (13) that the $Y_{DD}[l,k]$ can be calculated by taking the DFT of the time and IDFT of the frequency of $Y_{TF}[m,n]$, respectively. Therefore, we can obtain a set of LK symbols of Y_{DD} by taking the L-point IDFT of the rows and K-point DFT of the columns of Y_{TF} respectively. In other words, the SFFT can be produced by taking the DFT of the time, which produces the Doppler-domain, and the IDFT of the frequency, which produces the delay-domain. To sum up, as illustrated in Fig. 5, the SFFT corresponds to a two-dimensional transformation which takes

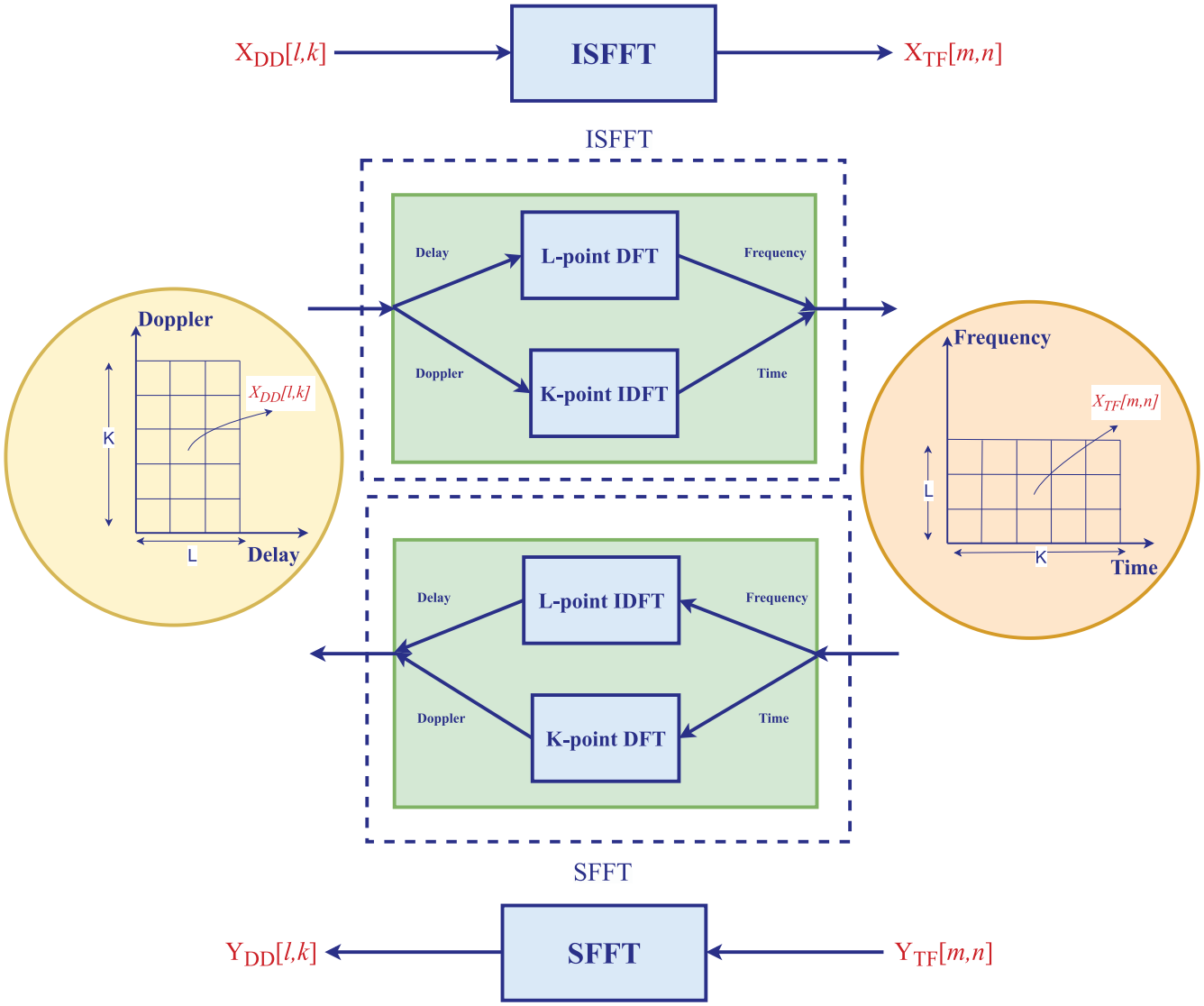

FIGURE 5. ISFFT and SFFT block diagrams.

a K-point DFT of the columns of Y_{TF} and an L-point IDFT of the rows of Y_{TF}. Accordingly, the SFFT transforms the signal from the TF-domain to the DD-domain.

2) DZT-BASED OTFS

As shown in Fig. 7, in the DZT-based OTFS modulation, the DD-domain information symbols are transformed directly into the time-domain signal by utilizing the IDZT. On the other hand, in the DZT-based OTFS demodulation, the time-domain signal is transformed directly into the DD-domain symbols by applying the DZT. Given that χ is a periodic sequence with period LK. Then, the DZT and IDZT can be defined, respectively as

$$\mathcal{ZAK}_{\chi}[l,k] = \frac{1}{\sqrt{K}} \sum_{n=0}^{K-1} \chi[l+nL] e^{-j2\pi \frac{n}{K} k}, \tag{14}$$

and

$$\chi[l+nL] = \frac{1}{\sqrt{K}} \sum_{k=0}^{K-1} \mathcal{ZAK}_{\chi}[l,k] e^{j2\pi \frac{n}{K} k}, \tag{15}$$

where $l \in \{0,1,\ldots,L-1\}$, $k \in \{0,1,\ldots,K-1\}$ and $n \in \{0,1,\ldots,K-1\}$. At the transmitter, the time-delay (TD)-domain sequence, which can be obtained by applying the IDZT to the DD-domain symbols, can be written as

$$X_{TD}[l+nL] = \sqrt{L} \sum_{k=0}^{K-1} X_{DD}[l,k] \mathcal{ZAK}_{g_{tx}}[l,k] e^{j2\pi \frac{n}{K} k}, \tag{16}$$

where $\mathcal{ZAK}_{g_{tx}}[l,k]$ is the DZT of the periodically extended sampled transmitter pulse shape $g_{tx}(\frac{[k]_{LK}}{L}T)$, where $[\,\cdot\,]_W$ denotes the modulo operation w.r.t. W and T is the periodic time. Taking the digital-to-analog conversion (DAC) of

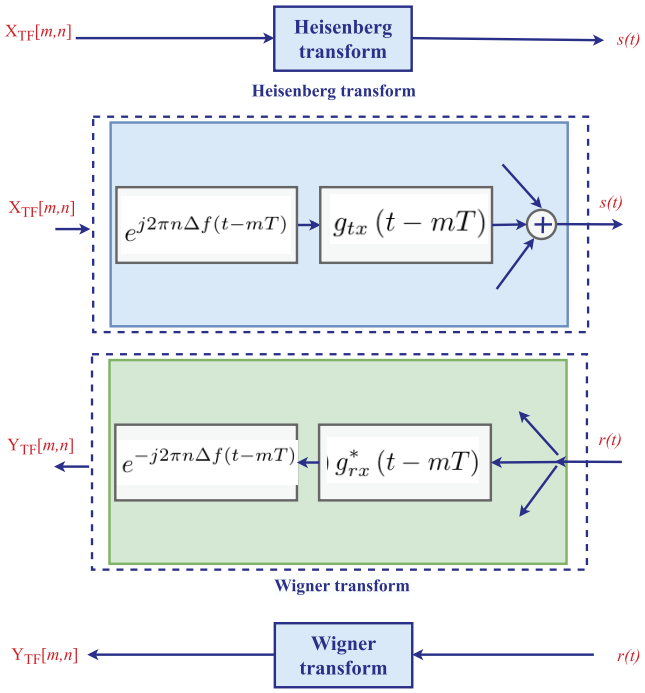

FIGURE 6. Heisenberg and Wigner transforms block diagrams.

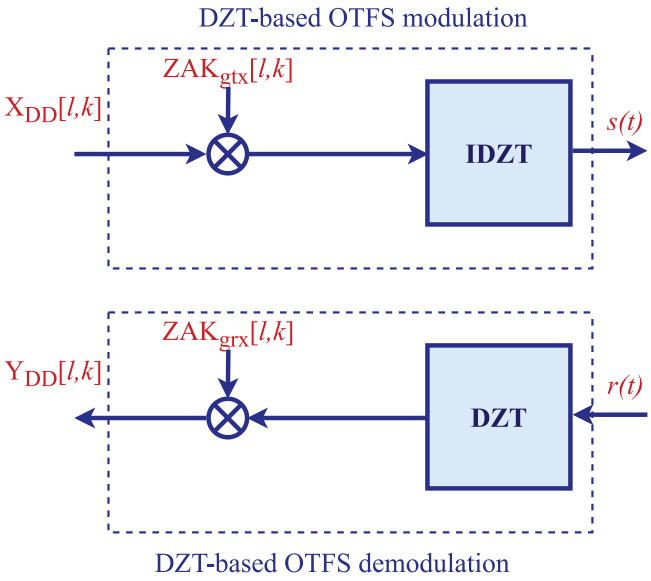

FIGURE 7. DZT-based OTFS modulation and demodulation block diagrams.

$X_{TD}[l+nL]$, the OTFS transmit signal $s(t)$ in time-domain is obtained as

$$s(t) = X_{TD}[l+nL], \tag{17}$$

where $t \in [\frac{l-0.5}{L}T + nT, \frac{l+0.5}{L}T + nT]$.

At the receiver, TD-domain received signal, which is an output of the analog-to-digital conversion (ADC) of time-domain received signal $r(t)$, can be written as

$$Y_{TD}[l+nL] = r(t)|_{t=\frac{l}{L}T+nT}. \tag{18}$$

Then, by conducting the DZT on the TD-domain received signal, the DD-domain received signal is expressed as

$$Y_{DD}[l,k] = \sqrt{LK}\mathcal{ZAK}_{Y_{TD}}[l,k]\mathcal{ZAK}^*_{g_{rx}}[l,k], \tag{19}$$

where $\mathcal{ZAK}_{Y_{TD}}[l,k]$ is the DZT of $Y_{TD}[l+nL]$ and $\mathcal{ZAK}_{g_{rx}}[l,k]$ is the DZT of the periodically extended sampled receiver filter $g_{rx}(\frac{[k]_{LK}}{L}T)$.

3) CZT-BASED OTFS

Due to the discrete nature of DZT, the DZT-based OTFS exhibits a degraded performance when the DD resolutions are not sufficient (fractional delay and Doppler). As a result, CZT-based implementation of OTFS has been proposed in [14], [15], [16]. Let $x(t)$ be a complex-valued time-continuous function. Then, for $-\infty < \tau < \infty$ and $-\infty < \nu < \infty$, the CZT and ICZT of $x(t)$ are defined, respectively, as

$$\mathcal{Z}_x(\tau,\nu) = \sqrt{T}\sum_{i=-\infty}^{\infty} x(\tau+iT)e^{-j2\pi i\nu T}, \tag{20}$$

and

$$x(t) = \sqrt{T}\int_0^{\frac{1}{T}} \mathcal{Z}_x(\tau,\nu)d\nu. \tag{21}$$

In the CZT-based OTFS, shown in Fig. 8, the information symbols are arranged as a two-dimensional array $X[l,k]$, and encoded as a discrete DD-domain information signal, i.e.,

$$X_{DD}[l+nL, k+mK] = X[l,k]e^{2\pi n\frac{k}{K}}. \tag{22}$$

Note that $X_{DD}[l,k]$ is a quasi-periodic function on the information grid with period L along the delay axis and period K along the Doppler axis, i.e.,

$$X_{DD}[l+nL, k+mK] = X_{DD}[l,k]e^{j2\pi n\frac{k}{K}}. \tag{23}$$

The discrete DD-domain signal is then lifted to a continuous DD-domain signal, i.e.,

$$X_{DD}(\tau,\nu) = \sum_{l,k} X_{DD}[l,k]\delta\Big(\tau - l\frac{\tau_p}{L}\Big)\delta\Big(\nu - k\frac{\nu_p}{K}\Big), \tag{24}$$

where τ_p and ν_p are the Delay and Doppler period of CZT-based OTFS modulation, respectively. Note that $X_{DD}(\tau,\nu)$ is quasi-periodic, i.e.

$$X_{DD}\big(\tau+n\tau_p, \nu+m\nu_p\big) = X_{DD}(\tau,\nu)e^{j2\pi n\nu\tau_p}. \tag{25}$$

The twisted convolution of the transmit pulse $w_{tx}(\tau,\nu)$ with $X_{DD}(\tau,\nu)$ gives the DD-domain transmit signal, i.e.,

$$X^{w_{tx}}_{DD}(\tau,\nu) = w_{tx}(\tau,\nu) * X_{DD}(\tau,\nu), \tag{26}$$

where $*$ denotes the twisted convolution operation. Using (21), the ICZT of $X^{w_{tx}}_{DD}(\tau,\nu)$ gives the time domain signal $s_{TD}(t)$ which is then transmitted. Without any additive noise, the received time domain signal $r_{TD}(t)$ is given by

$$r_{TD}(t) = \int\int h_{phy}(\tau,\nu)s_{TD}(t-\tau)e^{j2\pi\nu(t-\tau)}d\tau d\nu, \tag{27}$$

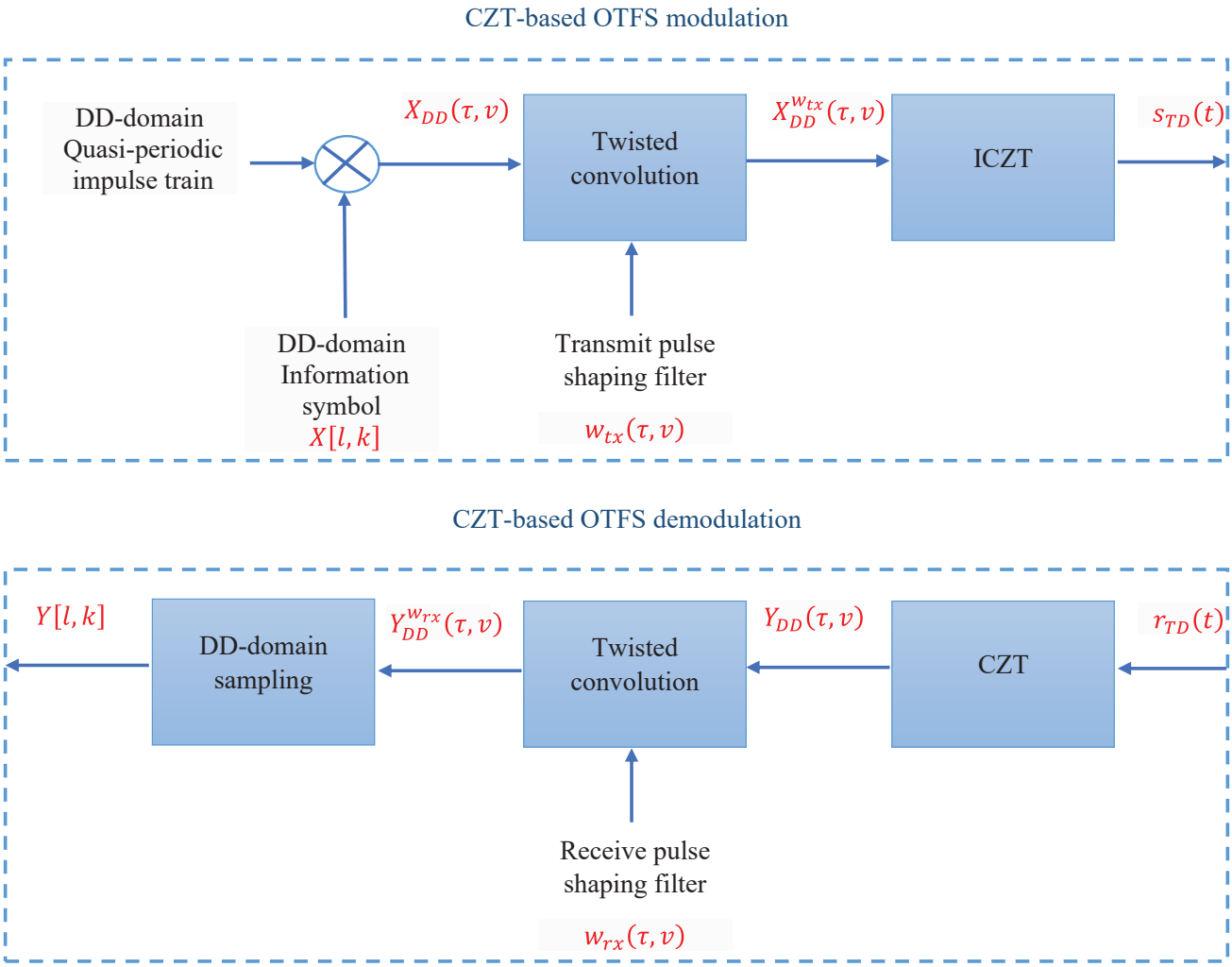

FIGURE 8. CZT-based OTFS modulation and demodulation block diagrams.

where $h_{phy}(\tau,\nu)$ is the DD representation/spreading function of the underlying physical channel. The received time domain signal is converted to its DD-domain representation $Y_{DD}(\tau,\nu)$ via the CZT in (20). The channel acts on $X_{DD}^{w_{tx}}(\tau,\nu)$ by twisted convolution so that

$$Y_{DD}(\tau,\nu) = h_{phy}(\tau,\nu) * X_{DD}^{w_{tx}}(\tau,\nu). \tag{28}$$

After twisted convolution of $Y_{DD}(\tau,\nu)$ with a receive DD pulse $w_{rx}(\tau,\nu)$, we obtain

$$Y_{DD}^{w_{rx}}(\tau,\nu) = w_{rx}(\tau,\nu) * Y_{DD}(\tau,\nu). \tag{29}$$

Finally, we sample this continuous output signal to obtain a discrete DD domain output signal, i.e.,

$$Y_{DD}[l,k] = Y_{DD}^{w_{rx}}\Big(\tau = l\frac{\tau_p}{L}, \nu = k\frac{\nu_p}{K}\Big). \tag{30}$$

4) COMPARISON BETWEEN SFFT AND DZT-BASED OTFS

Based on the above analyses for both SFFT-based OTFS and DZT-based OTFS, we have the following observations.

(1) Although the OTFS has two different implementations, both of them have the same DD-domain input-output relationship in the case of rectangular transmitter and receiver filters, integer delays and Doppler shifts. This can be clearly displayed as follows.

For the SFFT-based OTFS, the DD-domain input-output relationship can be written as

$$Y_{DD}[l,k] = \sum_{l'=0}^{L-1}\sum_{k'=0}^{K-1} X_{DD}\big[l',k'\big]H_{DD}\big[l,k,l',k'\big] + Z_{DD}[l,k], \tag{31}$$

where $H_{DD}[l,k,l',k']$ and $Z_{DD}[l,k]$ are the discrete DD-domain channel response and noise, respectively. The discrete DD-domain channel response can be expressed as

$$H_{DD}\big[l,k,l',k'\big] = \sum_{i=1}^{P} h_i w\big(l,k,l',k',l_i,k_i\big)e^{-j2\pi\nu_i\tau_i}, \tag{32}$$

where $k_i = \nu_i LT$ and $l_i = \tau_i K\Delta f$. Here, the values of k_i and l_i determine the integer and fractional Doppler,

and delay scenarios. Additionally, $w(l, k, l', k', l_i, k_i)$ in (32) refers to the sampling function for analog DD-domain channel response, which captures joint effects of delay and Doppler shifts, transmitter pulse shaping filter, and receiver filter. Now, assume that k_i and l_i are integers, and the transmitter and receiver filters are rectangular filters, i.e.,

$$g_{tx}(t) = g_{rx}(t) = \begin{cases} 1, & 0 \leq t \leq T \\ 0, & \text{otherwise.} \end{cases} \tag{33}$$

Then, (31) will be simplified to two dimensional circular convolution input-output relationship, which can be stated as

$$Y_{DD}[l, k] = \sum_{i=1}^{P} h_i X_{DD}[[l - l_i]_L, [k - k_i]_K] + Z_{DD}[l, k]. \tag{34}$$

Now, for the DZT-based OTFS, assume that the transmitter and receiver filters are rectangular filters. Then,

$$\mathcal{ZAK}_{g_{tx}}[l, k] = \mathcal{ZAK}_{g_{rx}}[l, k] = \frac{1}{\sqrt{LK}}. \tag{35}$$

With the integer delays and Doppler shifts, the DD-domain input-output relationship can be obtained as (34). This means that though the OTFS has two different implementations, both of them have the same DD-domain input-output relationship.

(2) The SFFT-based OTFS can be more compatible with the conventional OFDM. On the other hand, the DZT-based OTFS has a lower computational complexity. This can be interpreted as follows.

If we assume that $K = 1$ in (6) and (13), then the OFDM modulation and demodulation are obtained, respectively. Therefore, the OFDM is a special case of SFFT-based OTFS, which means that SFFT-based OTFS is compatible with the OFDM. Based on (6) and (13), LK-point IDFT and DFT are required at both the OTFS transmitter and receiver. On the other hand, based on (16) and (19), only L-point IDFT and DFT are required at the OTFS transmitter and receiver, respectively. Therefore, the DZT-based OTFS has a lower computational complexity than the SFFT-based OTFS.

C. COMPARISON BETWEEN OTFS AND OFDM

Recall from (34) that the input-output relation in the DD domain is a two dimensional convolution and it can be rewritten as

$$\mathbf{y} = \mathbf{H}\mathbf{x} + \mathbf{z}, \tag{36}$$

where $\mathbf{y} \in \mathbb{C}^{LK\times 1}$, $\mathbf{x} \in \mathbb{C}^{LK\times 1}$ and $\mathbf{z} \in \mathbb{C}^{LK\times 1}$ are respectively Y_{DD}, X_{DD} and Z_{DD} in vectorized form and $\mathbf{H} \in \mathbb{C}^{LK\times LK}$ is the fading channel coefficient matrix. Using the zero forcing (ZF) detection algorithm, the $\mathbf{x}$ can be detected. The detected signal can be expressed as

$$\hat{\mathbf{x}} = \mathbf{H}^{-1}\mathbf{y}. \tag{37}$$

Fig. 9 plots the bit error rate (BER) versus signal-to-noise ratio (SNR) for OTFS and OFDM. It can be noticed that the OTFS outperforms the OFDM. During the simulation, we use the parameters labeled in Table 3 for both OFDM and OTFS. Note that the OFDM is a special case of OTFS when $K = 1$.

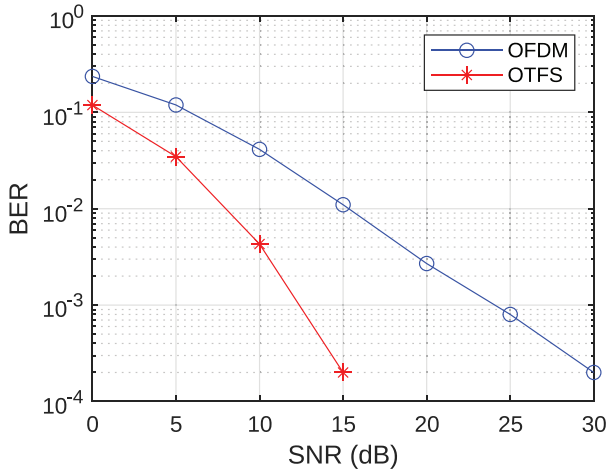

FIGURE 9. Comparison between OTFS and OFDM.

TABLE 3. Simulation parameters.

Parameter	Value
Number of delay bins	$L = 8$
Number of Doppler bins	$K = 8$
Modulation	Quadrature phase-shift keying (QPSK)
Channel model	Rayleigh distribution 4 taps ($P = 4$) of uniform power.
Delay taps	$[0, 1, 2, 3]$
Doppler taps	$[0, 1, 2, 3]$
Power profile	$\frac{1}{\sqrt{4}}[1, 1, 1, 1]$
Detection scheme	ZF

D. LITERATURE REVIEW

1) LOW-COMPLEXITY SIGNAL DETECTION

In [17], the authors presented a design of low-complexity modulator and demodulator structures for the OFDM-based OTFS system. The complexity analysis revealed that combining the ISFFT/SFFT and OFDM modulator/demodulator blocks in OTFS systems can save an incredible amount of computational complexity. In [18], the authors compared the performance of OTFS systems with ideal pulse-shaping waveforms that satisfy the bi-orthogonality conditions and rectangular waveforms which do not. They found that the ideal pulse-shaping waveforms caused inter-Doppler interference (IDI). On the other hand, the rectangular waveforms caused additional ICI and ISI. To address this, the authors proposed a low-complexity message passing (MP) algorithm for joint interference cancellation and symbol detection. This algorithm uses phase shifting to eliminate the ICI and ISI, and adapts the MP algorithm to mitigate the IDI. The results showed that the OTFS with rectangular

waveforms was superior to the OTFS with ideal pulse-shaping waveforms. In [19], the authors studied a low complexity linear minimum mean square error (LMMSE) receiver for OTFS. The LMMSE takes advantage of the sparsity and quasi-banded structure of the matrices involved in the demodulation process. This resulted in a log-linear order of complexity without any reduction in the BER performance. In [20], the authors studied the transmission of OTFS signals over a continuous-Doppler spread channel (CoDSC). To address the interference caused by the CoDSC, they proposed a low-complexity equalizer using the mathematical least squares minimum residual (LSMR) algorithm. They then developed an iterative OTFS receiver, which incorporated a reliability-based dynamic detector and block-wise interference eliminator, based on the LSMR equalization. In [21], the authors explored a joint radar parameter estimation and communication system that used OTFS modulation. They developed a simplified maximum likelihood (ML) parameter estimation approach and provided bounds and close approximations for the radar detector's mean square error (MSE). Additionally, they proposed a practical low-complexity soft-output detector for OTFS-separated detection and decoding based on MP. In [22], the authors proposed a low-complexity linear equalizer for OTFS modulation. This approach takes advantage of the block circulant structure of the OTFS channel matrix to reduce complexity. The proposed technique provides exact minimum mean square error (MMSE) and ZF solutions with lower complexity than the traditional matrix inversion approach. In [23], the authors suggested to use a low-complexity time-domain matrix inversion-based low-complexity expectation propagation (EP) detection to enhance the error performance of the OTFS and reduce the computational load. In [24], the authors proposed a new cross-domain iterative detection technique for OTFS modulation. They analyzed the state evolution of the proposed algorithm and studied its detection performance, including the MMSE performance and the DD-domain effective SNR. They demonstrated that the proposed algorithm can achieve the same error performance as maximum-likelihood sequence estimation (MLSE) detection, even in complex fractional Doppler shifts, but requires much less detection complexity. In [25], the authors proposed a new type of OTFS detector based on the approximate message passing (AMP) and the unitary AMP (UAMP). This detector takes advantage of the structure of the channel matrix, resulting in an efficient implementation. Furthermore, the UAMP-based detector includes the estimation of noise variance. In [26], the authors proposed a novel low-complexity parallel message passing (PMP) detection scheme for OTFS modulation. This scheme synchronizes the detection of all symbols and optimizes the structure of the symbol detection algorithm, resulting in a significant reduction in detection time. The authors of [27] suggested a turbo equalizer called doubly iterative sparsified MMSE. It can iteratively exchange the extrinsic information between a soft-input-soft-output MMSE estimator and a soft-input-soft-output decoder. This equalizer is not affected by short loops and can reach the same performance as the near-optimal symbol-wise maximum a posteriori (MAP) algorithm. In [28], the authors proposed a matched filtering-based message-passing detector (MF-MPD) with a novel probability clipping (PC) solution. The proposed algorithm has low complexity and reduced storage requirements due to the matched filtering processing.

The low-complexity detection techniques used in OTFS systems can be summarized in Table 4.

2) CHANNEL ESTIMATION

In [29], the authors proposed embedded pilot-aided OTFS channel estimation techniques. They organized pilot, guard, and information symbols in the DD grids to prevent interference between pilot and data symbols. These arrangements were designed for OTFS with ideal and rectangular pulses over channels with integer or fractional Doppler paths. At the receiver, channel estimation is carried out using a threshold method and the estimated channel information is used for data detection via the ML algorithm. In [30], the authors introduced a time-domain channel estimation technique for CP-OTFS systems with DD-domain embedded pilots. This method has a lower complexity than DD-domain channel estimation due to the increased sparsity of the channel matrix when residual synchronization errors are present. In [31], the authors studied a superimposed pilot (SP)-based channel estimation and data detection framework for OTFS systems. This framework superimposes low-powered pilots onto data symbols in the DD-domain. Two channel estimation and data detection designs were proposed for SP-OTFS systems. The first design estimates the channel by treating data as interference, which reduces its performance at the high SNR. The second design improves this issue by iteratively alternating between channel estimation and data detection. Both designs detect data using a MP algorithm which takes advantage of the OTFS channel sparsity and thus has low computational complexity. In [32], the authors proposed a data-aided channel estimation algorithm for OTFS with the SP and data transmission scheme. First, they coarsely estimated the channel based on the pilot symbol. Then they used an iterative process to detect the data symbols and refine the channel estimates. In [33], the authors introduced a Bayesian learning (BL) framework for channel state information (CSI) acquisition. This frame utilizes the sparsity of the DD-domain to enhance the estimation accuracy compared to the traditional MMSE-based approach. In [34], the authors suggested a new channel estimation technique (smoothness regularized channel main diagonal estimation (SR-CMDE)) with the capability of reducing signal leakage for OTFS modulation. This approach increases channel estimation accuracy while decreasing the amount of signaling required.

The channel estimation techniques used in OTFS systems can be summarized in Table 5.

TABLE 4. A summary of low-complexity detection techniques in OTFS systems.

Reference	Technique	Feature
[17]	ISFFT/SFFT and OFDM modulator/demodulator	Saves an incredible amount of computational complexity.
[18]	MP algorithm	Eliminates the ICI and ISI, and mitigates the IDI.
[19]	LMMSE	Exploits the sparsity and quasi-banded structure of the matrices involved in the demodulation process.
[20]	LSMR algorithm	Addresses the interference caused by the CoDSC.
[21]	Soft-output detector	Exploits efficiently the channel sparsity in the DD-domain.
[22]	Linear equalizer	Exploits block circulant structure of the OTFS channel matrix.
[23]	Time-domain matrix inversion-based EP detection	Enhances the error performance and reduces the computational load.
[24]	Cross-domain iterative detection	Achieves the same error performance as MLSE detection, even in complex fractional Doppler shifts, but requires much less detection complexity.
[25]	AMP and UAMP	Exploits the structure of the channel matrix, resulting in an efficient implementation.
[26]	PMP	Synchronizes the detection of all symbols and optimizes the structure of the symbol detection algorithm.
[27]	Doubly iterative sparsified MMSE	It is a turbo equalizer that is not affected by short loops and can reach the same performance as the near-optimal symbol-wise MAP algorithm.
[28]	MF-MPD	Reduces storage requirements due to the matched filtering processing.

TABLE 5. A summary for channel estimation techniques used in OTFS systems.

Reference	Technique	Feature
[29]	Embedded pilot-aided channel estimation	Pilots are arranged in the DD grids to prevent interference between pilot and data symbols. The channel estimation is carried out using a threshold method.
[30]	Embedded pilot-based time domain channel estimation	It has a lower complexity than DD-domain channel estimation due to the increased sparsity of the channel matrix when residual synchronization errors are present.
[31]	SP-based channel estimation	Superimposes low-powered pilots onto data symbols in the DD-domain. It estimates the channel by treating data as interference or iterates between channel estimation and data detection.
[32]	Data-aided channel estimation	It coarsely estimates the channel based on the pilot symbol. Then an iterative process is used to detect the data symbols and to refine the channel estimates.
[33]	Bayesian learning	Utilizes the sparsity of the DD-domain to enhance the estimation accuracy.
[34]	SR-CMDE	Reduces signal leakage for OTFS modulation.

3) PEAK-TO-AVERAGE POWER RATIO

In [35], the authors investigated the PAPR of the OTFS modulation waveform. They derived an upper bound on the PAPR of the OTFS signal and demonstrated that the maximum PAPR increases linearly with the number of Doppler bins. In [36], an efficient PAPR reduction method based on the iterative clipping and filtering framework was proposed for pilot-embedded OTFS modulation. This method

allowed the guard symbols to be padded with signals of small magnitudes. The clipping noise other than the clipped signal was then filtered. The filtering coefficients for the clipping noises in the data-plus pilot region and guard region were set to different values to achieve a good trade-off between PAPR and BER performance. In [37], the authors studied the PAPR of OTFS signals when the amount of data is large in the DD-domain. They found that when the number of data points is very large, the complex-valued OTFS signals tend to follow a Gaussian distribution due to the central limit theorem (CLT). Furthermore, the extremal theory of the Chi-squared process for stationary OTFS signals was used to derive an accurate expression for the PAPR distribution.

4) SYSTEM DESIGN

The authors of [38] studied the input and output relation of an OTFS system when using a variety of pulse-shaping waveforms. They demonstrated that the OTFS has a direct sparse input-output relation, which allows to use low-complexity detection algorithms. In [39], the authors proposed an OTFS system design developed on the Discrete Fractional Fourier Transform (DFrFT) based OFDM system. It was designed to be more efficient than the traditional OTFS system while having the same design complexity. In [40], the authors investigated the design of receivers for OTFS with fractionally spaced sampling (FSS). They derived a general channel input-output relationship for OTFS in DD-domain without relying on unrealistic assumptions such as ideal bi-orthogonal pulses. Next, they proposed two equalization algorithms, iterative combining MP and turbo MP, to detect symbols by exploiting the DD channel sparsity and the channel diversity gain through FSS. In [41], the authors inspected a receiver design based on the basis expansion model (BEM) OTFS. A low-order generalized complex exponential BEM (GCE-BEM) was initially used to estimate the channel with minimal pilot overhead. The accuracy of the estimation was then improved by iteratively refining the channel estimation and equalization, using a high-resolution GCE-BEM model with a large BEM order and exploiting the detected data symbols as pseudo-pilots. In [42], the authors studied the effects of using a window at the transmitter or receiver for OTFS modulation. They found that any window can provide the same performance in effective channel estimation. Additionally, the transmitter window can be seen as a power allocation in the TF-domain, while the receiver window can create colored noise. In [43], the authors proposed a two-stage equalizer system that processes the received signals in two domains. Initially, a sliding window-assisted minimum mean square error (SW-MMSE) equalizer is used in the TF-domain to reduce the ICI. Then, the DD-domain equalizer is applied to the output of the first stage to reduce the residual ISI. The authors in [44] introduced a new OTFS structure, which adapts the full-CP (FCP) structure used in OTFS modulation. This approach utilizes the FCP structure in the DD-domain to decode the data in the CP block instead of discarding it, thus improving the system's performance. In [45], waveform design is considered along with channel estimation based on unique-word and CP-free transmission. It is shown that for highly time-varying channels, it is advantageous to suppress the CP so that the channel estimation can be improved. A framework is developed to choose the waveform and frame parameters, such as the number of subcarriers and subblocks. For the CP-free transmission, it is shown that the waveforms that spread symbols energy in the time-domain per sub-block are the most resilient ones due to equal interference levels of the symbols. The authors in [46] presented a generic modulation framework for robust wireless communications over doubly dispersive channels. This robustness is achieved by spreading the symbols over time and frequency so that they experience the same channel gain. By exploiting an additional degree of freedom enabled by the generic framework, the authors proposed a low-complex waveform based on the sparse Walsh-Hadamard transform.

5) PERFORMANCE ANALYSIS

The authors of [47] derived a closed-form BER expression for the ZF-OTFS receiver in the presence of both perfect and imperfect receive channel information. In [48], the authors obtained a closed-form expression for the outage probability (OP) of the OTFS-based low earth orbit satellite (LEO-Sat) transmission. In [49], the authors investigated the error performance of rectangular pulse-shaped OTFS modulation with a practical receiver. In [50], the error performance of coded OTFS modulation over high-mobility channels was inspected. In [51], the authors proposed precoders for OTFS systems with linear equalizers to improve the BER. These precoders are designed to optimally distribute the power among the sub-channels with different gains in the DD-domain. In [52], the authors studied the security performance of an uplink LEO-Sat system, in which a cooperative UAV is used to send interference signals to a reconnaissance satellite. The OTFS technique was employed in the uplink transmission to counter the severe Doppler effect caused by the high-mobility of the LEO-Sat. In [53], the authors studied the OTFS performance over static multipath channels.

III. MULTIANTENNA OTFS SYSTEMS

As compared to the conventional single-input single-output (SISO) approaches, MIMO technology paves the way for dramatically improved spectral and energy efficiency performance at a manageable cost by counting on the available spatial degrees of freedom. Specifically, MIMO enables linear scaling of the channel capacity with the rank of the channel matrix. Due to its versatility and ease of integration, MIMO methods have been widely embraced in contemporary and emerging transmission systems under distinct scenarios. The existence of multiple antennas can mainly be leveraged in two distinct ways: spatial multiplexing for boosting the spectral efficiency and spatial diversity for improving the transmission reliability. Single and multiuser MIMO, massive (large-scale) MIMO, cooperative MIMO, distributed MIMO,

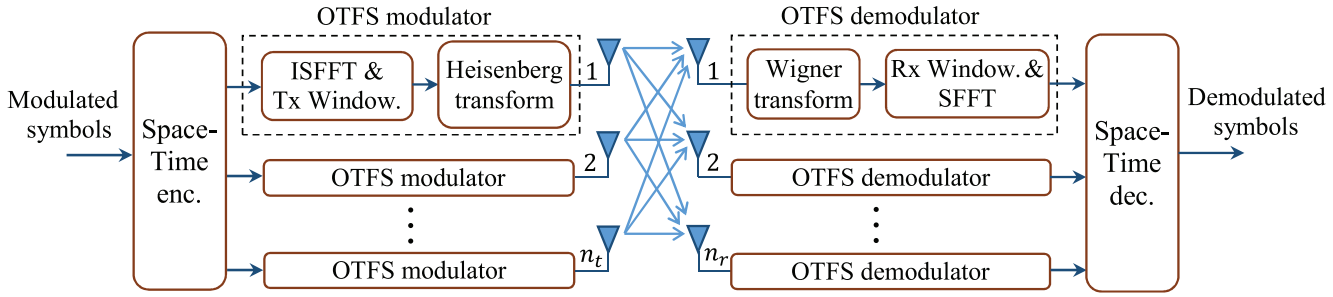

FIGURE 10. MIMO-OTFS transceiver block diagram.

transmit/receiver beamforming, space-time coding, physical layer security, mmWave MIMO, MIMO radar (for joint communications and sensing), and interference alignment are among some such applications of smart antenna technologies.

As a recently introduced DD domain transmission scheme, OTFS is proven to bring about promising performance over high-mobility frequency-selective fading channels. In order to attain robust resilient performance over doubly-dispersive channels, the combination of MIMO and OTFS techniques has attracted significant attention with the objective of reaping the advantages of both approaches. A transceiver block diagram of MIMO-OTFS is sketched in Fig. 10 where n_t and n_r represent the number of transmit and receive antennas, respectively. Appropriate space-time encoding (enc.) and decoding (dec.) processes are invoked at the transmitter and receiver, respectively. OTFS modulator is comprised of a respective application of ISFFT, transmitter windowing (Tx Window.), and Heisenberg transform operations. In addition, Wigner transform, receiver windowing (Rx Window.), and SFFT operations are implemented in the given order within OTFS demodulator. When the transmit antennas are used for the purpose of spatial multiplexing, OTFS modulated signal vectors are independently transmitted from the transmit antennas in a parallel and simultaneous fashion. Assuming a far-field scenario, the channel gain between the kth transmit antenna and lth receive antenna corresponding to delay τ and Doppler ν in the DD domain can be written as

$$h_{lk}(\tau, \nu) = \sum_{i=1}^{P} h_{lki}\delta(\tau - \tau_i)\delta(\nu - \nu_i) \tag{38}$$

for $k \in \{1, 2, \ldots, n_t\}$ and $l \in \{1, 2, \ldots, n_r\}$ where P denotes the number of resolvable multipath components in either the delay or Doppler dimension. Also, we further assume that the adjacent antennas at either side are placed half a wavelength apart. The probability density function of the random variable h_{lki} is determined by the underlying small-scale fading type. For instance, it has a zero-mean complex Gaussian distribution under Rayleigh fading. In this section, a review of the relevant studies on MIMO-OTFS is provided.

In [54], the input/output relation is formulated in a vectorized fashion for the MIMO-OTFS system. The obtained model allows to employ a number of signal detection algorithms. The authors present a low-complexity iterative MP algorithm for the detection process and show that it remarkably outperforms the traditional MIMO-OFDM scheme in terms of BER performance for a 2×2 MIMO system over doubly-dispersive channels. The introduced algorithm attains solid BER performance even at high Doppler frequencies (e.g., 1880 Hz resulting from a speed of 507.6 km/h at a carrier frequency of 4 GHz). In addition, a channel estimation scheme where DD impulses are utilized as pilots in the DD domain is presented. A discrete-time analysis of MIMO OFDM-based OTFS modulation is performed in [55]. A precise description of the ergodic capacity is presented and it is shown that both OFDM- and OTFS-based approaches accomplish the same ergodic capacity. In [56], the diversity level of OTFS is investigated and it is demonstrated that the asymptotic diversity order of the single-antenna OTFS (as SNR $\rightarrow \infty$) equals unity. Also, the authors introduce a phase rotation (PR) method that extracts full diversity of P in the DD domain. Here, P stands for the number of resolvable multipath components in either the delay or Doppler dimension. The idea relies upon that the minimum rank of the symbol difference matrix is augmented to P by means of multiplying the OTFS transmit vector with a diagonal PR matrix with different transcendental numbers. In addition, it is proven that the asymptotic diversity order is equal to n_r for an $n_t \times n_r$ MIMO-OTFS scenario where n_t independent OTFS signal vectors are simultaneously transmitted in a parallel manner. By generalizing the PR method, it is also shown that the presented MIMO-OTFS system can attain the full diversity of Pn_r. The use of space-time coding (STC) for a MIMO-OTFS setup is initially investigated in [57]. By adopting the well-known Alamouti code, the authors show that full spatial and DD diversity of $2P$ can be achieved in a 2×1 STC-OTFS system with the PR operation. The work in [58] evaluates the spectral efficiency of a 2×2 MIMO-OTFS scheme and confirms that the capacity can be doubled in this case as compared to a SISO-OTFS scenario. The diversity performance of receive antenna selection (RAS) (based on the maximum channel Frobenius norm in the DD domain) for a number of MIMO-OTFS arrangements is studied in [59]. The findings indicate that when combined with

a PR scheme, single-input multiple-output OTFS (SIMO-OTFS) and STC-OTFS systems with RAS can extract the full spatial and DD diversity. On the other hand, MIMO-OTFS system with RAS is shown to extract the full DD diversity only (not the full receive diversity) as a result of rank deficiency even under the PR approach. In [60], the diversity performance of transmit antenna selection (TAS) is inspected for an $n_t \times n_r$ MIMO-OTFS system with only one resolvable path in the DD domain, i.e., $P = 1$. By assuming a limited feedback from the receiver to the transmitter, TAS is performed based on the maximum channel Frobenius norm in the DD domain. It is proven that full spatial diversity of $n_t n_r$ is accomplished when only a single transmit antenna is selected. On the other hand, the diversity order equals n_r when TAS activates more than one transmit antenna. An OTFS system with multiple transmit antennas is investigated in [61] by precluding the bi-orthogonal assumption in the ideal pulse shaping. The rectangular pulse shaping is considered and the guard symbols, the pilot symbols, and the information symbols are accordingly allocated to achieve the transmit diversity. In [62], the authors present cyclic delay-Doppler shift technique (in time-domain and modulation-domain forms) for MIMO-OTFS systems to extract transmit diversity over doubly-selective channels. The main idea relies on introducing DD shifts at distinct transmit antennas such that the number of effective propagation paths in the wireless channel is increased. It is shown that the introduced scheme can yield full transmit diversity gain in certain cases. Analytical BER upper bounds for MIMO-OTFS systems are obtained in [63] with ideal and generalized waveforms by utilizing miscellaneous kinds of guard intervals.

The spectral efficiency of an uplink MIMO-OTFS system is inspected in [64] with delay division multiple access (DDMA) and Doppler division multiple access (DoDMA) schemes where MMSE combining is adopted at the receive side. The authors numerically demonstrate the performance enhancement of MIMO-OTFS over MIMO-OFDMA systems. In [65], the DD domain Tomlinson-Harashima precoding is studied for a downlink MIMO-OTFS system where a base station (BS) with multiple antennas simultaneously communicates with various single-antenna users. The presented technique does not necessitate any matrix decomposition or inversion. The authors conclude that the sum-rate increases logarithmically with the number of antennas and linearly with the number of users. By utilizing the block circulant structure of the effective DD MIMO channel matrix, ZF and MMSE equalizers with low-complexity are proposed in [66] for a 2×2 MIMO-OTFS system. In [67], a downlink MIMO-OTFS system is inspected where a BS with a large number of antennas simultaneously communicates with multiple single-antenna users. It is shown that separate demodulation of each DD domain information symbol at the users is possible by using a multiuser precoder at the BS and a low-complexity detection algorithm at the users. The proposed MIMO-OTFS scheme is demonstrated to attain notably better spectral efficiency as compared the OFDM-based approach over high-mobility channels. The authors design a low-overhead and low-complexity receiver structure for the OTFS system in [68] by deploying a large-scale antenna array at the receive side to decouple the received signals from distinct angles of arrival into multiple parallel signal branches. The proposed scheme encompasses the pilot pattern design, the channel estimation, the symbol detection, and the carrier frequency offset compensation. In [69], a downlink MIMO-OTFS system is considered where a BS transmits information to multiple users at the same time. Assuming that each node is equipped with multiple antennas, two low-complexity precoding algorithms are introduced and shown to have significantly reduced computational complexity with a limited performance loss as compared to the high-complexity block diagonalization precoding. The authors in [70] devise low-complexity ZF and MMSE receivers for MIMO-OTFS systems by considering both perfect and imperfect CSI scenarios. The complexity reduction is performed by utilizing the doubly-circulant structure of the MIMO-OTFS channel matrix. In [71], a tight signal-to-noise-plus-interference-ratio (SINR) approximation for the receiver structures in [70] is analytically determined under imperfect receive CSI. Based on the inherent channel sparsity and the channel-agnostic form of matrices involved in the detection process, the work in [72] presents a low-complexity linear minimum mean squared error (LMMSE) receiver structure for practical-pulse-shaped MIMO-OTFS systems. It is shown that the proposed scheme with only a log-linear complexity yields precisely the same solution, and therefore the same BER performance as compared to the traditional LMMSE receiver which has a cubic order of complexity. A low-complexity deep neural networks (DNN) model is proposed in [73] for OTFS signal detection under both single-antenna and multiantenna cases. It is demonstrated that when the additive noise at the receive side differs from the conventional independent and identically distributed Gaussian model, the DNN-based detector can outperform the standard ML and MMSE detection approaches. In [74], the authors present a linear-complexity detection scheme for MIMO-OTFS with rectangular pulse-shaping waveform. The introduced method exploits maximum-ratio combining (MRC) at the receiver and is shown to accomplish enhanced performance as compared to LMMSE and MP detectors. Relying on the sparsity of the channel matrix, a LSMR channel equalizer and an enhanced data detection technique are introduced for MIMO-OTFS in [75]. It is demonstrated that the presented scheme can effectively and robustly demodulate the superimposed high-order quadrature amplitude modulation (QAM) symbols even under high-mobility. In [76], the authors propose a low-complexity MMSE receiver for the uplink of a rectangular pulse-shaped massive MIMO-OTFS system. The presented approach makes use of the sparsity of the channel matrix and the MMSE expression matrix structure. It is shown that as compared to its traditional counterparts, the recommended

receiver has a considerably lower computational complexity without any degradation in the BER performance.

In [77], [78], the BER performance of MIMO-OTFS modulation is investigated with decode-and-forward relaying in high-mobility environments where all the nodes are equipped with multiple antennas. The communication between the transmit and receive ends takes place in two hops through a single relay and through multiple selected relays respectively in [77] and [78]. The achievable asymptotic diversity order is determined and a PR approach on the transmitted OTFS frames is proposed to increase the diversity level under both cases.

In [79], a new path division multiple access technique is proposed for massive MIMO-OTFS networks for both downlink and uplink scenarios. The efficacy of the introduced scheme is established through a number of simulation results. An uplink massive MIMO-OTFS system is considered in [80] where multiple single-antenna users simultaneously transmit their symbols to a multiantenna BS, which applies ZF beamforming to decode the users' signals. A rigorous performance analysis is also provided. In [81], the spectral efficiency of cell-free massive MIMO-OTFS is studied by considering the impact of channel estimation. Analytical expressions are derived for the spectral efficiency under both downlink and uplink cases. The numerical results exhibit the advantage of the MIMO-OTFS system in yielding enhanced data rates over high-mobility channels as compared to the traditional MIMO-OFDM approach. The downlink spectral efficiency of a cell-free massive MIMO-OTFS is inspected in [82] where every receiver relies on MMSE-based successive interference cancellation (SIC) operation. The authors present a max-min fairness resource allocation scheme based on per-user spectral efficiency. It is demonstrated by simulation results that as compared to a full power transmission case, the introduced approach can considerably enhance the spectral efficiency at each user. The authors of [83] investigate the grant-free random access in LEO satellite communications by embracing massive MIMO-OTFS where numerous Internet-of-Things devices desire to communicate with a LEO satellite in a sporadic manner. In order to estimate the channel and to detect active devices, a novel method relying on the channel sparsity in the DD-angle domain is introduced. Assuming an URLLC scenario with ideal pulse shape functions and fractional delay and Doppler shifts, an uplink MIMO-OTFS system is inspected in [84] where a set of single-antenna users communicate with a BS with multiple antennas. The BS initially applies MRC and subsequently invokes the ML decoding rule to decode the desired symbols. A number of conclusions are drawn on the achievable rate and diversity of the system. In [85], a scenario where a single-antenna user transmits towards a BS with a massive number of antennas is treated for OTFS modulation. In order to entirely remove the CP and to break the corresponding limitation on the maximum Doppler frequency that can be tolerated, a time-reversal MRC with residual Doppler correction windowing method is developed. It is shown that when the maximum Doppler shift is within OTFS limits, doubly-dispersive channel effects even out in the large antenna regime. A joint radar sensing and data transmission system is introduced in [86] where a multiantenna BS equipped with a reduced number of RF chains and a radar receiver broadcasts data utilizing OTFS in mmWave frequency bands. Two modes of operation are separately inspected. The proposed approaches are shown to perform effectively in terms of detection and estimation quality. In [87], the authors make use of the radar sensing information about the users and the surrounding environment to assist the channel estimation for MIMO-OTFS systems. Numerical findings reveal that the introduced method performs better than the traditional orthogonal matching pursuit (OMP)-based approach regarding the normalized MSE for the channel estimation and the pilot overhead. The authors of [88] carry out a thorough study on signal modeling, performance analysis, algorithm design, and numerical evaluations for massive MIMO-OTFS-based simultaneous localization and communications. Initially, a massive MIMO-OTFS channel model is built by assuming the ultra-wide bandwidth mmWave signals and large antenna arrays. Cramer-Rao lower bounds are then obtained for channel estimation and localization results based on the new multipath wideband channel model. The joint radar and communication problem is studied in [89] by adopting multiuser MIMO scenarios. A new scheme named as non-uniform OTFS is introduced and its performance is compared with other related OTFS-based methods for monostatic MIMO radar applications and under standard 3GPP vehicular channel models. In [90], a MIMO-OTFS system with 19.3 bits/s/Hz spectral efficiency at a carrier frequency of 28 GHz is experimentally investigated in over-the-air and mobility environments. The superior robustness of MIMO-OTFS as compared to MIMO-OFDM is empirically demonstrated over time-variant channels. A LEO satellite communication system based on MIMO-OTFS is studied in [91] by taking spatial antenna correlation into account. In order to cope with the spatial correlation, the authors propose whitening transformations at the transmit and receive sides. These decorrelation operations are numerically shown to bring about important error performance enhancement. However, the whitening transform technique in [91] cannot completely cancel spatial correlation at the receiver. In order to remedy this problem, an alternative whitening technique is developed in [92] over a time-varying spatially correlated MIMO-OTFS system. An upper bound on the pairwise error probability (PEP) is obtained as a function of the diversity and coding gains and SNR. In [93], a high-Doppler airborne communication ad-hoc network case is investigated where relative mobile node speeds can be as high as 1200 m/s. It is shown that MIMO-OTFS has the potential to offer sufficiently reliable transmission under the considered scenario. A summary of the prominent MIMO-OTFS studies with a focus on the diversity level is provided in Table 6.

TABLE 6. A summary of the diversity-oriented multiantenna OTFS studies.

Focus of Interest	Main Ideas and References
Diversity analysis for $n_t \times n_r$ MIMO-OTFS where the transmit antennas are utilized for spatial multiplexing, i.e., layered transmission	The naive $n_t \times n_r$ MIMO-OTFS has a diversity order of n_r. P-fold increase in the diversity order (the full diversity) is possible by a PR technique [56].
Diversity analysis for $n_t \times n_r$ MIMO-OTFS where all the antennas are used for spatial diversity	The 2×1 Alamouti-OTFS scheme in [57] attains the full diversity of $2P$ after a PR operation. A MIMO-OTFS scheme based on the cyclic delay-Doppler shift transmission method in [62] can yield the full diversity of Pn_tn_r.
Diversity analysis for $n_t \times n_r$ MIMO-OTFS with RAS	The RAS approach applied to SIMO-OTFS and Alamouti-OTFS schemes with the PR can extract the full diversity of n_rP and $2n_rP$, respectively. MIMO-OTFS with RAS ($n_r \geq n_t \geq 2$) suffers from a rank deficiency and cannot provide full diversity even under the PR transformation [59].
Diversity analysis for $n_t \times n_r$ MIMO-OTFS with TAS	When P equals unity and only one single transmit antenna is activated, the TAS approach ensures the full spatial diversity of n_tn_r. If multiple transmit antennas are turned on by TAS, the maximum achievable diversity order is given by n_r with $P = 1$ [60].
Diversity analysis for two-hop layered MIMO-OTFS with decode and forward relaying (one relay) and PR where all the nodes have multiple antennas	The diversity order equals the minimum of n_qP_{sr} and n_rP_{rd} where P_{sr} and P_{rd} respectively stand for the number of resolvable DD domain paths between the transmitter to the relay and the relay to the receiver channels. Also, n_q and n_r are the numbers of antennas at the relay and at the receiver, respectively [77].
Diversity analysis for two-hop layered MIMO-OTFS with selective decode and forward relaying (K relays) and PR where all the nodes have multiple antennas	The diversity order is equal to the sum of n_rP_{sd} and $\sum_{k=1}^{K}\min\left(n_qP_{sr_k},n_rP_{r_kd}\right)$ where P_{sr_k} and P_{r_kd} represent the number of resolvable DD domain paths between the transmitter to the kth relay and the kth relay to the receiver channels, respectively. Also, n_q and n_r are the numbers of antennas at any relay and at the receiver, respectively [78].
Diversity analysis for uplink multiuser SIMO-OTFS with ideal pulse shaping and fractional delay and Doppler shifts	Only negligible diversity gain can be attained [84].
Diversity analysis for layered $n_t \times n_r$ MIMO-OTFS under spatial correlation	The diversity gain is equal to the product of the number of receive antennas and the minimum number of non-zero eigenvalues of a pairwise difference matrix whose entries depend on the correlated channel matrix as well as the transmitted symbols [91], [92].

The work in [94] treats the joint channel estimation and data detection problem in hybrid reconfigurable intelligent surface (HRIS) aided mmWave MIMO-OTFS systems. The authors determine a new transmission framework where some HRIS elements are alternatively activated throughout the pilot durations and HRIS stays in passive mode throughout each OTFS block duration such that the impinging signal is reflected without any absorption. A number of simulation results are drawn to confirm the strength of the introduced scheme under different scenarios. A point-to-point MIMO-OTFS scenario is covered in [95] and a low-complexity hybrid digital-analog beamforming transmission framework is proposed. It is confirmed by numerical results that the presented technique can attain near-optimal rate performance. In [96], the authors adopt an air-to-ground communications scenario and promote a low-complexity massive MIMO-OTFS hybrid precoding method with rectangular waveforms. Numerical results are used to show the superior BER performance of the introduced scheme as compared to the other related approaches. MIMO/SISO-OTFS systems with intelligent reflecting surface (IRS) assistance are investigated in [97] with MMSE detection. The authors offer a method to conclude a set of IRS phase shifts such that the received SNR is maximized. It is demonstrated that the presented technique outperforms its OFDM-based IRS-assisted counterpart in terms of BER performance.

In [98], massive MIMO-OTFS downlink channel estimation problem is studied. It is proven that the time-variant massive MIMO channel has three dimensional sparsity given by normal sparsity along the delay dimension, block sparsity along the Doppler dimension, and burst sparsity along the angle dimension. Building upon this fact, the estimation problem is converted into a sparse signal recovery problem which is then solved by resorting to a structured OMP algorithm. The work in [99] considers an uplink-aided high-mobility downlink channel estimation scheme for massive

MIMO-OTFS networks. The expectation-maximization (EM) based variational Bayesian framework is utilized to determine the uplink channel parameters including the angle, the delay, the Doppler frequency, and the channel gain for each physical scattering path. Then, using the angle, delay, and Doppler reciprocity between the uplink and the downlink (even under the frequency division duplex mode), downlink channel parameters as the angles, the delays, and the Doppler frequencies are recovered at BS. The authors in [100] address the channel estimation problem for mmWave massive MIMO-OTFS systems where the large OTFS symbol size and the massive number of antennas may seriously escalate the involved computational complexity. As a remedy, a tensor-based OMP method is presented by utilizing the channel sparsity in the DD-angle domain. Numerical results are used to confirm the superiority and robustness of the introduced algorithm. A CSI acquisition method is presented in [101] for downlink massive MIMO-OTFS systems under the effect of fractional Doppler. Deterministic pilot design and the determination of the channel estimation algorithm problems are covered. The simulation results verify the efficacy of the introduced technique in acquiring precise downlink CSI. The authors of [102] present a channel estimation technique for massive MIMO-OTFS systems with the aim of lessening ISI when the subtraction of the two delay paths is less than the resolution of the system. A 3D structured OMP approach is adopted by utilizing the fact that the inner product descent ratio difference of the traditional OMP algorithm has a maximum value near sparsity. Simulation results verify that the proposed method outperforms the related conventional algorithms under distinct scenarios. In [103], a sparse CSI estimation model for MIMO-OTFS systems is proposed. In order to achieve a reduction in terms of the training overhead, the pilot signals are directly transmitted over the time-frequency-domain grid to estimate the DD-domain CSI. It is shown that the corresponding DD-domain CSI turns out to be simultaneously row and group sparse. The authors present an OMP algorithm complemented by an enhanced Bayesian learning framework and a low-complexity linear detector. The performance advantages of the introduced techniques against the other related approaches are illustrated through simulation results. A DD-angular domain representation of the wireless channel is developed in [104] for MIMO-OTFS systems. By utilizing the intrinsic four dimensional sparsity, the authors devise a time-domain pilot aided channel estimation model which functions based on an OMP framework. A novel channel estimation method based on compressed sensing is introduced for MIMO-OTFS systems in [105] by taking advantage of the structured sparsity of the DD domain MIMO channel. The authors devise a row-block OMP algorithm and show that their approach yields better performance as compared to the similar methods relying on compressed sensing. In [106], the authors initially develop the DD-domain input-output relationship considering a DD-angular domain channel model for mmWave MIMO-OTFS systems. Then, both analog and hybrid beamforming scenarios are studied and a new two-step procedure is presented for transmit beamformer/precoder and receiver combiner design, and for estimating the DD-domain CSI. It is shown that the corresponding CSI exhibits sparsity and block sparsity under analog and hybrid beamforming cases, respectively. Bayesian learning is then resorted for CSI estimation. Simulation results affirm the improved CSI estimation performance of the introduced algorithm against other relevant sparse signal recovery techniques. In order to eliminate the channel estimation performance degradation due to the off-grid channel parameters, the authors of [107] establish a cross-domain channel estimation method for OTFS-based hybrid beamforming systems. By using the time-domain and DD-domain signal models, two parallel sparse recovery problems are built and solved. It is shown that the presented technique can attain superior performance as compared to the relevant schemes in the presence of the off-grid channel parameters. In [108], a cubature Kalman filter is used to address channel estimation problem in mmWave MIMO-OTFS systems. The authors adopt a beam-switching approach to minimize the tracking errors and show by simulations that the proposed method outperforms the prior relevant techniques. A CSI estimation framework based on an orthogonal affine-precoded superimposed pilot structure in DD domain is presented in [109] for CP-aided SISO- and MIMO-OTFS systems with arbitrary transmitter-receiver pulse shaping. The authors derive Bayesian Cramer-Rao bounds on the system performance and provide a number of BER simulation results to expose the enhanced performances of the proposed strategies in various settings. In [110], online Bayesian learning-assisted CSI estimation methods are developed for both SISO- and MIMO-OTFS modulated systems. Under the MIMO-OTFS scenario, the authors offer an online row and group sparse Bayesian learning method for channel estimation and a low-complexity detector relying on an iterative block matrix inversion approach. The work in [111] introduces a channel estimation method for MIMO-OTFS. The objective function is first expressed as a block sparse signal recovery problem and then a solution is determined by a block sparse Bayesian learning technique with block reorganization. Simulation results are used to show the superiority of the presented scheme in comparison with the other relevant methods. In [112], the pilot pattern construction problem is treated for channel estimation in MIMO-OTFS systems. As compared to the conventional approach, the authors' proposed pilot scheme is shown to exhibit similar BER performance with a lower pilot overhead. The authors of [113] study channel estimation problem in an asymmetrical massive MIMO-OTFS system where antenna array sizes differ in the uplink and downlink. A parametric channel estimation method called proximal gradient OMP is introduced and shown to enhance the precision of channel estimation as compared to the other methods that perform estimation directly from delay, Doppler, and angular domains. In [114], an iterative algorithm is introduced for channel estimation and data

detection in the DD domain for MIMO-OTFS systems. The presented scheme iterates between MP-aided data detection and data-aided channel estimation where two methods are recommended for the latter process. It is shown that the proposed approach outperforms the related schemes in [103] and [111] with regard to the channel estimation quality and BER performance.

IV. MULTIPLE ACCESS TECHNIQUES AND OTFS

5G and beyond (5G +) systems are envisaged to support high data rate and URLLC as well as massive and ubiquitous connectivity. Some of these systems are further expected to efficiently operate even under high-mobility conditions, e.g., under a speed of 500 km/h. However, in such cases, a corresponding Doppler shift is also coupled with each of the multipath components over the wireless channel which thereupon exhibits selective fading both in time and frequency domains. The transmitted signal is consequently exposed to Doppler spread together with delay spread.

In response to stringent quality of service requirements, multiple access techniques are designed with the purpose of maintaining high data rate and reliable communications to a multitude of users/equipments/terminals over a mutual channel. When a common entity such as a BS communicates with a number of users over a joint medium, the corresponding channel and system are respectively called a broadcast channel and a downlink system. On the other hand, the opposite scenario in which multiple users transmit data to a common receiver forms an uplink system over a multiple access channel. Multiple access methods and associated waveforms have traditionally played key roles during transition from one communications standard to another. Orthogonal multiple access (OMA) techniques have principally been adopted from the early generations to the currently deployed 5G systems which implement OFDMA. Orthogonal TF resource blocks are allocated to the users under OFDMA, which features some important assets given by its resilience against frequency-selective fading and its ease of implementation and integration in terms of backward compatibility. As a result of the first advantage, orthogonality among users can be retained at the receive side(s) even under the presence of delay spread due to the multipath propagation. However, as the mobility of the active terminals rises and Doppler spread becomes more pronounced, OFDMA's error probability performance starts declining and preserving the orthogonality among distinct signals at the receiver entails computationally complex equalization schemes.

Thanks to its robustness under both time- and frequency-selective fading, OTFS combined with an appropriate multiple access plan has the potential to offer a solution for maintaining acceptable performance over high-mobility scenarios. In contrast to OMA practice, NOMA approaches allocate more than one user in a unique resource unit such that a group of users simultaneously exploit the same frequency band [115]. Similarly, the modulated symbols are spread over the whole TF grid in OTFS. Hence, there exists an analogy between the two ideas and it is highly projected that the upcoming communication systems will promote both approaches. Recently, a great deal of interest has been concentrated on an adequate and effective combination of OTFS and multiple access techniques by exploiting TF, DD, space, power, and code domains. Fig. 11 exemplifies one such application of user multiplexing in DD domain with OTFS for downlink and uplink cases, respectively. In this section, a survey of prominent studies on OTFS with various orthogonal and non-orthogonal multiple access methods is provided.

In [116], an uplink multiple access technique is proposed for OTFS-based communication systems over doubly-dispersive fading channels. By subdividing delay and Doppler axes into equal-length portions in DD domain, a certain number of DD resource blocks are obtained. These are accordingly allocated to distinct users in DD domain such that non-overlapping localized portions of TF domain are assigned to different users without any interuser interference. The introduced scheme is shown to attain high sum spectral efficiency over doubly-dispersive fading channels with no guard band. The problem of devising a multiple access plan for an uplink OTFS system is studied in [117]. Depending on how DD resource blocks are distributed to users, three distinct techniques are considered. In the first and second schemes, users are respectively multiplexed along the delay and Doppler axes such that a single user's signal spans the whole TF plane. In the third scheme, DD resource blocks are allocated similar to [116] where any user's signal is constrained to span only a subdivision of TF plane. It is numerically shown that the first scheme outperforms the others as wells as OFDMA and single-carrier FDMA techniques in terms of BER. Also, a pilot-based channel estimation method with the first scheme is demonstrated to provide a performance close to that with perfect channel knowledge. In [118], the authors study DD channel estimation for an uplink system with OTFS where user multiplexing is applied in DD domain. In order to exploit the inherent sparsity of the channel in DD domain, a compressed sensing-based estimation method is implemented. The results indicate the superior performance of the proposed technique against an impulse-based channel estimation scheme reported for uplink OTFS systems. A novel path division multiple access scheme for both downlink and uplink massive MIMO-OTFS systems is introduced in [79], [119]. Modeling the received signal in the DD-angle domain, a path scheduling algorithm is conceived. In addition, MRC-based and beamforming-based detection schemes are designed respectively for uplink and downlink scenarios. Simulation results verify the efficiency of the presented technique. DDMA and DoDMA methods are studied for an uplink OTFS system in terms of achievable rate under MIMO and SISO scenarios in [64] and [120], respectively. It is asserted that a robust SINR performance can be attained thanks to a favorable channel

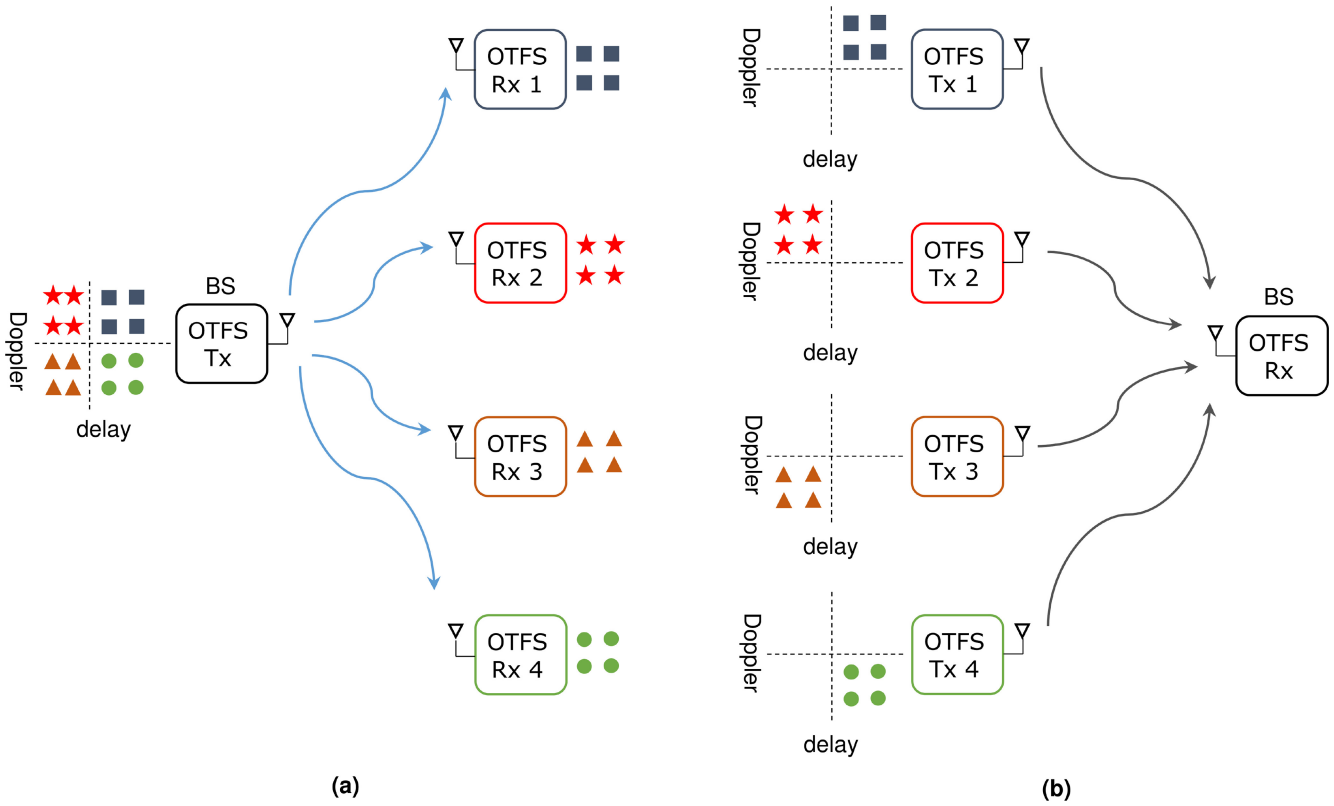

FIGURE 11. An example of user multiplexing in DD domain with OTFS for downlink and uplink scenarios, respectively.

hardening effect appearing as a result of DD domain signal processing. In addition, numerical results reveal a noteworthy enhancement in the users' achievable rates in comparison with the conventional OFDMA-based approach. The outage performance of OTFS modulation is analyzed in [121] for doubly-dispersive channels. Both the single-user transmission and the uplink multiuser transmission (relying on DDMA introduced in [64], [120]) scenarios are covered. A number of numerical results are provided to show that OTFS-based systems achieve considerably superior outage performance as compared to traditional OFDM-based approaches.

In [122], the authors focus on a multiuser uplink scenario with OTFS and introduce a user multiplexing scheme (called interleaved TF multiple access) where TF resource blocks allocated to distinct users are non-contiguous and interleaved. The simulation results reveal that as compared to the relevant method of [116], the proposed technique accomplishes better performance in terms of BER and PAPR. Several OMA methods are integrated with an uplink OTFS system in [123] where non-overlapping resource blocks in DD and/or TF domains are allocated to distinct users. Specifically, guard band based multiple access, interleaved DD multiple access, and interleaved TF multiple access techniques are investigated in terms of their spectral efficiency performances under practical rectangular pulses. Simulation results indicate that the sum spectral efficiency of the interleaved DD multiple access is noticeably higher than those of the other considered schemes.

A combination of OTFS and NOMA is presented in [124] for both uplink and downlink scenarios with heterogeneous user mobility profiles. User grouping is applied such that the ones with high-mobility get service in the DD plane with their signals being modulated by OTFS. The low mobility users, on the other hand, are served in TF plane such that their signals are modulated in a fashion analogous to conventional OFDM. It is demonstrated that both types of users enjoy from the introduced OTFS-NOMA method in terms of enhanced spectral efficiency and reduced latency. The beamforming design for an OTFS-NOMA downlink scenario is investigated in [125] by assuming that a BS simultaneously communicates with multiple low-mobility users along with one high-mobility user over the same frequency band. The findings assert that the presented beamforming scheme can yield an important performance advantage as compared to a scenario with random beamforming. In [126], an uplink DD-angle domain NOMA approach is inspected for massive MIMO-OTFS systems. The authors suggest to schedule multiple users with overlapped angle signatures within the same DD domain resource block. User clustering and optimal transmission strategy problems are also investigated. The efficiency of the presented scheme is confirmed by means of simulation results. An OTFS-NOMA system is treated in [127] by assuming that multiple high-mobility users all

served by OTFS are multiplexed in power-domain for both downlink and uplink scenarios. Various power allocation policies are devised to maximize the sum spectral efficiency under distinct cases. Performance comparisons reveal that the presented OTFS-NOMA scheme achieves a larger spectral efficiency as compared to OTFS-OMA. On the other hand, in comparison with OFDM-NOMA, outage spectral efficiency of the introduced OTFS-NOMA approach is enhanced at the expense of a reduction in average spectral efficiency. The authors of [128] present a coded uplink OTFS-NOMA architecture where sub-vector resources of Doppler and delay dimensions are respectively allocated to the stationary and mobile users. An iterative SIC receiver is devised for multiuser detection and decoding under intensive co-channel interference. The introduced iterative SIC turbo receiver is demonstrated to accomplish performance enhancement over other relevant receivers and to attain resilience against imperfect SIC and CSI uncertainty. By utilizing LEO satellite communications, grant-free NOMA is integrated with OTFS in [129], [130] to enable massive IoT connectivity in a terrestrial-satellite link scenario. The authors introduce a two-step successive active terminal identification and channel estimation algorithm along with a low-complexity multiuser signal detection technique. A number of numerical results are provided to show the superiority of the proposed approaches as compared to the other related schemes in terms of error probability performance and channel estimation quality. In [83], the authors study the grant-free random access in LEO satellite communications by adopting a massive MIMO-OTFS scenario where multiple IoT devices wish to communicate with a LEO satellite in a sporadic fashion. The input-output relationship is initially analyzed. Then, a novel method to estimate the channel and to detect active devices is introduced by relying on the channel sparsity in the DD-angle domain. Numerical results are used to verify that the proposed technique can obtain precise CSI and device activity status. A two-user downlink OTFS-NOMA system is addressed in [131] where a slow-mobile user with a better channel condition than a fast-mobile user performs SIC. This process is carried out as follows: the slow-mobile user initially decodes the fast-mobile user's signal in DD domain and cancels it from the aggregate signal. Subsequently, the slow-mobile user decodes its own signal in TF domain. The fast-mobile user, on the other hand, directly decodes its own signal in DD domain. The presented system is asserted to provide advantages in terms of overall latency and spectral efficiency. In [132], OTFS is combined with filter bank multi-carrier and NOMA techniques to attain massive connectivity and larger spectral efficiency over a mmWave channel. Novel user-pairing techniques are proposed by assuming a downlink scenario where a BS with massive number of antennas communicates with multiple single-antenna users. The introduced scheme is shown to outperform similar related works in terms of error probability performance. An OTFS-NOMA assisted cooperative multicast-unicast streaming scenario is covered in [133] where the authors present power allocation and relay selection methods to provide reliability and security. Numerical results signify that a notable enhancement can be achieved as compared to the relevant OFDM-NOMA techniques. In [134], [135], an iterative low-complexity method for equalization and detection in downlink OTFS-NOMA systems is introduced. The proposed approach exploits the least-squares with QR factorization algorithm for equalization and a novel reliability zone detection technique to detect the users' symbols. In addition, multiuser interference is eliminated in each step by interference cancellation. The presented method is numerically shown to outperform the existing MMSE SIC benchmark scheme in terms of symbol error rate performance. An uplink heterogeneous NOMA system is investigated in [136] where an iterative SIC-based detection algorithm is implemented with realizable rectangular pulses and without the assumption of ideal SIC. Users are divided into two groups where OFDM and OTFS are adopted by the low-mobility and high-mobility user groups, respectively. An extrinsic information transfer chart analysis is used to confirm that the introduced algorithm manifests fast convergence and provides the same performance as the detection with ideal SIC for sufficiently large SNR values. As a low-complexity extension of [83], the work in [137] relies on MIMO-OTFS for the grant-free random access in LEO satellite communications with large differential delay and Doppler shift. In order to estimate the channel and to detect active devices, a deep learning-based generalized approximate MP algorithm with cross-correlation-based Gaussian prior is utilized. In addition, the EM rule is used to learn the corresponding hyperparameters. Simulation results are provided to show that the presented scheme outperforms other related works in terms of channel estimation quality and device activity detection performance. In [138], a downlink OTFS-NOMA system is discussed by assuming the existence of both high-mobility and low-mobility user profiles. The authors focus on a resource allocation and user pairing problem to minimize average BER. The resulting mixed integer programming problem is initially solved for a case with two users and the solution is then generalized for the general scenario. The presented scheme is demonstrated to perform similarly to the optimal exhaustive approach. An OTFS-NOMA downlink scheme is investigated in [139] for coordinated direct and relay transmission system. Here, a source directly transmits to a close-by mobile terminal and sends information to a remote terminal with high-mobility by getting assistance from the nearby terminal as a relay. A number of closed-form expressions are derived on the outage probability and on the outage sum-rate assuming both perfect and imperfect SIC. Numerical results confirm the performance advantage of the introduced approach. A downlink OTFS-NOMA scenario is inspected in [140] where a BS communicates with multiple high-mobility users. The K-means clustering algorithm is implemented to classify the users into a number of distinct clusters while power-domain NOMA is applied on the cluster centers. In [141],

a novel OTFS-NOMA-assisted downlink ISAC method is presented where an UAV acts as an air BS to support multiple users. Initially, the UAV acquires the users' position and velocity information by utilizing the signal echo spread in the LoS channel and a 3D motion prediction topology is then executed to direct the NOMA transmission towards the multiple users. The proposed scheme is shown to accomplish superior achievable spectral efficiency as compared to the other related approaches.

A multiuser OTFS system relying on a code-domain NOMA method called sparse code multiple access (SCMA) is proposed in [142] for both downlink and uplink cases by judiciously positioning SCMA codewords in DD plane. The authors present proper detection techniques for both scenarios and demonstrate that the introduced OTFS-SCMA scheme attains better BER performance as compared to the combinations of OTFS with OMA and power-domain NOMA. In [143], the authors offer a two-dimensional downlink OTFS-NOMA approach where power-domain NOMA is adopted between one high-mobility user and multiple low-mobility users. In addition, SCMA is implemented for the users under the subgroup of low-mobility. The superior spectral efficiency performance of the presented scheme as compared to the other existing power-domain NOMA and OTFS combinations is verified by means of simulations. The work in [144] presents a channel estimation method for the uplink OTFS-SCMA scenario introduced in [142]. Exploiting the convolutional sparse coding approach, a minimal overhead equivalent to that of a single-user case is accomplished without compromising on the estimation error. The efficiency of the presented method is demonstrated via simulation results in terms of BER, normalized MSE, and spectral efficiency. The works in [145], [146] consider a downlink OTFS-SCMA scheme and introduce a cross-domain receiver architecture where OTFS symbol estimation and SCMA decoding operations are performed in a joint fashion by iteratively passing the extrinsic information between time and DD domains. It is demonstrated that the detector structure in [142] exhibits poor BER performance due to the fact that fractional Doppler shifts result in inferior channel equalization causing performance deterioration in the subsequent SCMA decoding. The proposed method in [145], [146] is shown to outperform the approach in [142] in terms of BER performance by bypassing the preceding effect. An uplink coordinated multipoint coverage case is addressed in [147] where numerous mobile user terminals are congregated for SCMA. These users simultaneously get service from remote radio heads before and behind them by exploiting OTFS. The authors offer practical receiver algorithms for centralized and decentralized detectors to reap the inherent channel diversity. The presented detector structures are demonstrated to yield effective and robust performance under CSI uncertainty. A simple yet functional resource hopping technique over delay or Doppler axis is proposed in [148] to suppress interference due to common jamming signals in OTFS-SCMA systems. The introduced idea is shown to provide BER performance enhancement under jamming as compared to conventional OTFS-SCMA systems. In [149], it is stated that the performance of conventional OTFS-based multiple access approaches heavily depends on the characteristics of the channel spreading function. In this sense, the traditional schemes with a limited spectrum resource and non-sparse non-compact channel spreading function suffer from a lack of capacity. The authors correspondingly propose a grant-free multiple access method called orthogonal time frequency code space modulation by exploiting orthogonal code domain resources. A number of simulation results are illustrated to validate the superiority of the introduced technique in terms of false alarm probability and BER performances. The performance of the preceding technique is evaluated for joint grant-free access and positioning of massive terminals with high-mobility over Internet of Vehicles networks in [150]. The numerical evaluations are performed for positioning error and BER of terminals under distinct scenarios. The proposed scheme is shown to outperform the conventional OFDM systems with orthogonal spreading. An uplink MIMO-OTFS SCMA system is investigated in [151] by introducing a memory AMP detector. The proposed approach is shown to bring about implementation advantage in terms of computational complexity with desired BER performance. In [152], an IRS-assisted OTFS-based uplink SCMA communications system is studied. Using an upper bound on the word error probability, the authors develop two IRS phase shift design algorithms based on the semidefinite relaxation and gradient ascent approaches. The performance of the presented scheme is inspected in terms of diversity and SNR gains.

In [153], tandem spreading multiple access (TSMA), which is a novel grant-free code-domain NOMA approach to yield a trade-off between the reliability and the user data rate [154], is combined with OTFS for smart high-speed railway massive IoT networks. Simulation results confirm that desired levels of high user connectivity and transmission reliability can be accomplished by the presented scheme. OTFS-TSMA approach in [153] is extended for a LEO satellite system based on differential Doppler shift in [155]. It is demonstrated that the presented scheme brings about enhanced connectivity as well as a reduction in the system resource consumption. In order to satisfy the low-latency, high-reliability, and massive connection requirements of 6G networks in high-mobility environments, a novel OTFS-based pattern division multiple access (PDMA) method is introduced in [156]. As a variant of NOMA, PDMA enables multiple number of users to commonly use orthogonal resources (time, frequency, space, DD domain resources) in a non-orthogonal fashion by a joint design of transmitter and receiver. Relying on the EP algorithm, the authors propose a combined detection scheme for the OTFS-PDMA system. Simulation results indicate that the presented method outperforms the traditional OTFS-OMA approaches.

The study in [157] considers an uplink OTFS scenario and presents a low-complexity detection method based on

decomposing the original large channel into parallel small sub-channels. The decomposition process is applied initially in space domain and then in time domain. The introduced scheme requires partial CSI feedbacks in terms of delay and Doppler shifts from the receiver to the transmitters and is shown to provide enhanced BER performance with lower complexity as compared to the existing related techniques. In [158], a new uplink multiple access method is presented where each user forms a coded QAM-modulated OFDM signal and then transmits it after upsampling and circular shifting operations, respectively, over a doubly-dispersive channel. It is proven that the aggregate received signal at the BS has the same form as the received signal in an equivalent single-user OTFS system. In addition, the authors propose multiuser SIC and turbo receivers to obtain diversity gain. The superior performance of the proposed scheme is numerically shown in comparison with the corresponding multiuser OFDM system. The authors of [159] inspect an OTFS-based uplink multiuser MIMO system by embracing practical rectangular pulses along with fractional delay and Doppler shifts. In the considered setting, multiple single-antenna users desire to simultaneously communicate with a multiantenna receiver under ML and nearest-neighbor decoding rules. It is demonstrated that the severe performance degradation in terms of PEP is induced with the adoption of the rectangular pulses.

V. APPLICATIONS OF OTFS IN SATELLITE COMMUNICATIONS

In recent years, the space networks have been evolving rather rapidly, with the deployments of LEO mega-constellations and lunar missions [160]. These networks introduce a number of unknowns regarding channel characteristics, such as the ambient noise conditions. In addition, the large delays associated with long propagation distances and high Doppler shifts due to the high speeds of LEO satellites (5-10 km/s [161]) render space networks, in particular LEO mega-constellations, very suitable for the use of OTFS modulation. The unique features of OTFS make it a promising waveform technology for satellite communications, providing robustness to time-varying channels, multipath fading, and high spectral efficiency with low computational complexity. This synergy is well-elaborated in the recent work [162], where the authors also use a case study to demonstrate the potential performance improvement that can be provided by OTFS. In [163], the authors also highlight the Doppler mitigation capabilities of the OTFS modulation.

The use of OTFS in varying mobility scenarios is first discussed in [124]. Inspired by the superior performance of OTFS in doubly dispersive channels, the authors use OTFS with NOMA to jointly harvest multipath and multiuser diversities in the presence of heterogeneous mobility profiles. The benefits of the proposed approach in terms of increased spectral efficiency and reduced latency are demonstrated numerically for both high-mobility and low-mobility users. Motivated by the suitability of the OTFS for high-mobility scenarios, the authors consider sub-6-GHz and millimeter-wave bands for satellite-to-ground channels with high-mobility [161]. Both LoS and non-LoS conditions are investigated. To improve the error performance, MMSE with successive detection is used instead of solely MMSE. The authors in [164] investigate the potential performance improvement in a dual satellite transmission system. The flexibility introduced by the OTFS is used to counteract the residual frequency offset from the varying inter-satellite distances. They make use of precoding the symbols of the distant satellite to compensate for differential delays and frequency shifts with respect to the closest satellite. Hence the proposed scheme allows the ground-based receiver to lock on to a single satellite.

The extension of the OTFS to MIMO scenarios for LEO satellites is proposed in [91], where the authors investigate the performance of the system in the presence of spatially correlated channels. Whitening transformations are proposed at the transmitter and the receiver to combat the spatial correlation and to enhance the error performance. In [165], the authors make use of the properties of the OTFS waveform to jointly estimate the DD channel vector and detect the transmitted data. Unknown symbols in an OTFS frame are used as 'virtual pilots' with the goal of improving the estimation performance. The use of IRS is also considered in space-air-ground integrated networks in [166], where the authors proposed to create "virtual" Doppler frequencies to facilitate the IRS configuration. It is also shown that the proposed IRS configuration helps overcome the error floors.

Another line of research focused on the use of OTFS between satellite-to-ground channels for IoT networks. Instead of classical grant-free random access schemes (that are not suitable for rapidly varying channel conditions), the authors in [129] proposed to use NOMA-OTFS. The investigated methodology offers multi-functionality by jointly performing active user detection and channel estimation based on the proposed OTFS data frame structure. The authors in [83] extended the work to MIMO settings. To exploit the sparsity of the channel, a sparse Bayesian learning-based channel estimation approach is presented. A novel grant-free random access scheme, TSMA is considered for OTFS-based satellite communication systems in [155]. The authors also consider smart railways as the application scenario where the ground stations can also be high-mobility nodes. They propose a differential Doppler shift-based TSMA-OTFS transmission scenario to enable service continuity and to control multiuser interference. The extended application of the grant-free access to scenarios where the differential delay is more than one symbol duration jointly with the differential Doppler shift exceeding one subcarrier spacing is considered in [137]. In this work, the authors estimate the channel in the delay dimension and decompose the 3D tensor for parallel computation. A DL-based generalized approximate MP is proposed, and the EM algorithm is used to learn the hyperparameters. The combination of grant-free NOMA and OTFS is also

studied in [167] where the authors compare different configurations, including the traditional frame structures, virtual oversampling lattices, and a proposed training sequence to demonstrate various configurations that provide a wide range of flexibility according to the target use case. Finally in [130] a two-stage successive active terminal identification and channel estimation is proposed for multiuser transmission that exploits the sparsity of satellite-to-ground channels. A least-squares-based parallel detection technique is also proposed to alleviate the detection complexity.

The performance of OTFS in satellite systems is also considered in [48], where the authors derive the closed-form expression for the OP. In addition, UAV cooperation is considered for increased performance. In [168], the authors investigate a mobile multi-UAV cluster that facilitates the communication between the satellite and the ground terminal by compensating the path loss and improving the coverage. The system OP is presented based on the analysis using stochastic geometry. The physical layer security performance of the OTFS-based satellite system is also investigated in [52]. The authors derive the secrecy OP and compare the performance of OTFS and OFDM. A cooperative-jamming UAV node is also considered to improve the secrecy performance.

Overall, the current literature solidifies the use of OTFS for satellite communication systems (See Table 7). Their use for inter-satellite communications and communication systems between spacecrafts remains an open issue.

TABLE 7. A summary of OTFS applications in satellite communications.

Application Area	Key Highlights and References
Performance Analysis for LEO Networks	OTFS's robustness to time-varying channels and high Doppler shifts makes it ideal for LEO networks [160]–[163].
OTFS in High-Mobility Scenarios	Superior performance in doubly dispersive channels, useful for high-mobility satellite-to-ground channels [124], [161].
Dual Satellite Transmission	Enhancing performance using precoding for differential delays and frequency shifts in dual satellite systems [164].
MIMO Extensions	Investigating OTFS performance in spatially correlated channels for MIMO in LEO satellites [91], [165].
IRS in Space-Air-Ground Networks	Utilizing IRS to create "virtual" Doppler frequencies and enhance performance in integrated networks [166].
Satellite-to-Ground IoT Networks	Development of NOMA-OTFS and TSMA-OTFS for IoT, focusing on high-mobility scenarios and channel sparsity [83], [129], [130], [137], [155], [167].
Performance Analysis	Studies on OTFS performance in satellite systems, including OP derivation and UAV cooperation [48], [52], [168].

VI. OTFS-ISAC

International Telecommunications Union (ITU) has clearly stated the expectation about the integration of sensing and communication systems to become a part of the IMT 2030 [169]. In line with this expectation, the recent literature has also concentrated on identifying OTFS's advantages for ISAC systems [10]. The preliminary work OTFS-ISAC is [170], which focuses on the vehicular network applications. The authors have shown that the slow time-varying delay-Doppler domain channel coefficients provide a significant advantage in accurately predicting the channel parameters. Following this, in [171], the authors propose a spatially spread OTFS to obtain an angular domain discretization. A beam tracking, angle estimation, and power allocation scheme is proposed for radar sensing by making use of the effective radar sensing matrix. In [172], the authors propose a matched filter-Fibonacci (MF-F) algorithm to improve the estimation of sensing parameters in an ISAC OTFS system. The MF-F method is verified through a software-defined radio implementation, and the authors show high precision and robustness in estimating parameters, potentially enhancing the efficiency and speed of the sensing and communication system. Reference [173] introduces a framework for OTFS-ISAC systems targeting high-mobility environments while maintaining high spectral efficiency. The proposed framework consists of sequential coarse and fine-tuning spectrum matching modules coupled with a constant false alarm rate target detection module, targeting to significantly enhance the detection performance and accuracy in target range and velocity estimation, as demonstrated by simulation results. Another recent work exploring a user state refinement algorithm within OTFS-ISAC systems particularly suitable for high-mobility networks where reliable data transmission is critical is [174], whereby leveraging a hybrid digital-analog architecture and a nested array-based technique, the authors propose an algorithm that refines initial coarse angle estimates, subsequently enhancing joint delay and Doppler shift estimations, as validated by numerical results, thus improving both radar and communication performance metrics.

[175] proposes the amplitude barycenter calibration (ABC) algorithm to address the challenge of fractional delay and Doppler effects in OTFS-ISAC systems, which may result in estimation errors due to non-integer multiples in channel resolutions. The proposed algorithm utilizes integer DD grid observations to calibrate estimates effectively, and its performance analysis, including error estimation and the

Cramer–Rao lower bound, shows significant improvements in sensing resolution for distance and velocity while maintaining robust communication performance. In [176], the authors offer a high-order spectra barycenter calibration algorithm by targeting some of the shortcomings in sensing resolution caused by limited bandwidth and frame time. The introduced technique outperforms the ABC approach by providing higher sensing accuracy even at low pilot SNR values. A method for joint radar sensing and communications using OTFS modulation is proposed in [177] precisely for detecting moving targets during digital wireless transmissions. The technique employs random pilot signals for channel impulse response estimation, which proves superior in identifying vehicle velocities in noisy conditions compared to the traditional methods. Simulations and field tests validate the effectiveness of this OTFS-based sensing approach, demonstrating its advantages over the conventional cross-ambiguity function radar processing in terms of target detection accuracy. Reference [141] introduces a network design that integrates NOMA for OTFS-ISAC, utilizing UAVs as air BSs to serve multiple users. The system leverages ISAC capabilities to extract user positional and velocity data from echo signals, optimizing power allocation for enhanced data rates, and incorporates a 3D motion prediction topology for effective NOMA transmission. The authors explore the enhancement of uplink transmission in a vehicular network using OTFS-ISAC in [178], focusing on the challenge of associating sensing parameters with transmitters to improve communication. A scheme that jointly handles parameter association, channel estimation, and signal detection is proposed as a constrained bilinear recovery problem, utilizing a bilinear unitary approximate message passing (Bilinear-UAMP) algorithm. Reference [179] introduces an OTFS-ISAC system that provides precise range-velocity profiles without requiring large bandwidths or extended transmission durations. The proposed system uses a single OTFS carrier with rectangular pulse shaping to estimate delays and Doppler shifts, thus determining range and velocity, while an innovative algorithm leverages the sidelobes of the pilot signal's physical pulse shape to detect radar targets beyond conventional resolution limits. MIMO extension of OTFS-ISAC is considered in [180] for the first time. The authors present a generalized likelihood ratio test based multi-target detection algorithm and delay-Doppler-angle estimation for MIMO-OTFS radar, which effectively handles ISI and ICI to enhance target detection. Additionally, they propose adaptive transmission strategies for OTFS ISAC in discovery and track modes, utilizing DD multiplexing for wide-ranging environmental probing and directional transmissions for optimal radar and communication performance. Finally, in [181], the authors present a joint design approach for an OTFS signal and a receiving filter, formulating the optimization problem as a minimization of the weighted integrated sidelobe level (WISL) and interference from the ISAC waveform, while maintaining SNR targets. The proposed majorization-minimization algorithm with alternating iterative minimization effectively reduces WISL and interference, enhancing data rates and detection performance as demonstrated by simulation results.

VII. OTHER APPLICATIONS AND SCENARIOS

A. UWA

Due to the low speed of acoustic waves and wideband characteristics, UWA communications undergo large time delay, Doppler shift and scale effects such that UWA communications is much more challenging than RF wireless communications. Since the UWA channels are both time-selective and frequency-selective, i.e., doubly dispersive, OFDM fails with ICI and thus OTFS being Doppler resilient and converting worse TF domain channels into better DD domain channels emerges as a good alternative. OTFS based UWA system has first been proposed in [182]. The authors showed by simulations that OTFS outperforms OFDM in terms of BER and spectral efficiency in different UWA channel conditions. In [183], OTFS is shown to provide better performance than OFDM when simulated in the Bellhop-based statistical UWA channel model for AWGN, complex noise, and real channel noise. References [184] and [185] also show the superiority of OTFS over OFDM with channel estimation errors and IM, respectively. To handle time scaling effect of UWA channels, OTFS-like orthogonal delay scale space modulation, outperforming OTFS and OFDM is developed with a low complexity receiver based on subcarrier-by-subcarrier equalization [186]. In [187], a two-step Doppler compensation to alleviate Doppler effects and a practical channel estimation method to avoid mathematical problem of fractional Doppler shifts are proposed. The simulation results obtained in different UWA channel environments verify the performance improvement as compared to OFDM. Reference [188] proposed a learned denoising based sparse adaptive channel estimation method enhancing the estimation performance significantly. In [189], a structured sparsity-based generalized AMP channel estimation algorithm, providing lower computational complexity and superior performance is developed for quantized OTFS systems. Several detection techniques such as DNN based signal detection [190], passive time reversal [191], LMMSE SIC detection [192] and unitary AMP based detection [193] are also studied in OTFS UWA communications.

B. UAV

Since UAVs are flexible in terms of maneuverability, altitude, deployment and of low cost, and provide LOS connectivity to ground users and establish ubiquitous and seamless connectivity of different communication devices and networks, UAV communications will be an indispensable part of 6G aiming to unify all terrestrial, non-terrestrial, RF and free space optical (FSO) communications. However, UAV applications require high mobility causing severe Doppler effects. Thus, OTFS appears to provide Doppler resilience in such non-terrestrial UAV communications. For such Doppler compensation, OTFS-based UAV communication system

has been proposed in [194]. The authors optimized UAV trajectory by minimizing the energy consumption under the constraints of BER and transmission rate, and showed the superiority of the system over OFDM based UAV system. Reference [195] proposes an emergency localization technique for UAV equipped with cellular BS to establish OTFS modulated physical random access channel (PRACH) transmission and reception scheme performing time-of-arrival measurements. The simulation results show that the proposed solution outperforms standard PRACH-based localization techniques. In [196], an iterative algorithm based on belief propagation and gradient descent optimization for localizing a swarm of UAVs communicating with each other and an edge server has been presented by using time difference of arrival measurements obtained through OTFS-modulated signals. The proposed algorithm increases the localization accuracy of the limited bandwidth systems. Reference [197] and also aforementioned works [48], [52], [168] deal with OTFS performance of satellite communication systems including UAV cooperation.

C. DL

Deep/machine learning (DL/ML) algorithms have been taking their roles in everyday daily routine with a plethora of diverse application scenarios. Their popularity can be credited to their ability in performing precise predictions in an iteratively improving fashion by learning from new data. Stimulated by their advantages, DL/ML techniques are currently being inspected for physical-layer of wireless communications as well. To that end, there exists a continuously increasing interest on the combination of DL/ML and OTFS schemes in order to collectively reap the benefits of both approaches. In [198], a damped generalized AMP algorithm is proposed to enhance the detection performance of OTFS systems with reduced complexity where the damping factors are optimized relying on DL techniques. In order to alleviate the PAPR problem in OTFS, an autoencoder based DL scheme is introduced in [199]. Using a two-stage training procedure, the presented technique reduces the PAPR considerably by yielding a reasonable compromise between BER and PAPR. The authors of [200] treat an autoencoder-based OTFS system within a DL framework. Considering a feed-forward neural network architecture for both encoding and decoding, it is shown that the detection performance of the recommended method outperforms the conventional OTFS with the MP-based detection at high SNR levels. In [201], a two-dimensional convolutional neural network based detection is studied for single-antenna OTFS systems. It is revealed by simulation results that the suggested technique brings about an enhanced BER performance over the traditional MP detector with a very low time complexity. As an extension of [201] for multiantenna scenarios, a low-complexity detection approach based on two-dimensional convolutional neural network is presented for MIMO-OTFS in [202] by only taking into account the received signal and an augmented dataset as input to the DNN. It is numerically demonstrated that as compared to the conventional detectors, the devised scheme has a better error performance when fractional Doppler effect exists. A neural network-based structure is examined in [203] for OTFS equalization problem. It is shown that ISI can be decreased noticeably by exploiting a reservoir computing-based neural network architecture with a particularly tailored training dataset. In [204], a Gaussian AMP based signal detection approach is designed for OTFS by expanding the standard Gaussian AMP into a corresponding DNN structure. The simulation results affirm that the presented model-driven detection scheme performs better than the standard Gaussian AMP by around 2 dB at a BER of 10^{-4}. The authors of [205] inspect an EP aided model-driven DL architecture for OTFS signal detection. In order to increase the speed of the convergence and to enhance the detection performance, every iteration is unfolded into a layer-wise network through embedding trainable parameters which can be optimized by offline training. Numerical results confirm that the introduced scheme can indeed enhance the signal detection performance with similar computational complexity in comparison with traditional EP approaches. The work in [206] considers a DL-based signal detector approach for RIS-aided OTFS systems. It is shown that the studied DL-based detector can achieve infinitesimally low BER at a lower SNR as compared to the traditional detectors. A DNN based fractional Doppler channel estimation method is conceived in [207] for an air-to-ground OTFS communication system. It is demonstrated that as compared to the conventional approach, a similar performance can be accomplished by the proposed technique with a lower pilot power. In [208], an OTFS-enabled URLLC scenario is inspected and a predictive precoder scheme with an unsupervised learning based DL mechanism is recommended with the purpose of enhancing the system reliability performance in terms of frame error rate. The performance of a DL-based OTFS system is investigated in [209] under the presence of practical hardware impairments such as in-phase and quadrature-phase component mismatch and DC offset. By applying data augmentation, the adopted DL-OTFS model is trained in an offline manner and subsequently implemented for online signal detection in the DD domain. The simulation results verify that the presented approach can attain enhanced BER performance in comparison with the traditional MP- and MMSE-based receiver structures. In [210], a graph neural network detection architecture is designed for OTFS systems. The authors utilize the Markov random field theory to effectively extract the hidden features of input data and to obtain more precise detection. An automatic modulation classification technique is developed for OTFS in [211] by utilizing a hybrid convolutional neural network and long short-term memory network with a residual stack. The numerical results show that the introduced approach accomplishes a classification precision over 98.5% for an SNR value of 20 dB and performs adequately at low SNR levels as well. In order to enhance the detection performance

in the presence of channel estimation errors for OTFS systems, the study in [212] investigates the performance of a model-driven DL based orthogonal AMP detection architecture. It is revealed by the simulation results that with much reduced complexity and much less parameters, the presented detector can attain better error performance under channel estimation errors as compared to other related nonlinear detectors. In [213], a learning-based channel estimation scheme for fractional DD domain channel for OTFS systems is proposed where the learning process is implemented in TF domain instead of DD domain. This is driven by the fact that the range of values in the TF channel matrix is more favorable for the training purposes as compared to the DD channel matrix values which may have large variance values and thus may not be suitable for the training process. Numerical results reveal that with a significantly lower complexity, the introduced idea can acquire almost the same performance as that of the best performing scheme available in the literature.

D. IM

Index modulation with its various forms enables an innovative low-complexity practice for the transmission of extra data bits by means of the indices of the available transmit resource blocks. With the purpose of attaining enhanced spectral efficiency over high-mobility channels, the integration of IM into OTFS systems is addressed in several works. As one of the pioneering studies on the application of IM to OTFS, the work in [214] aims to enhance BER performance while guaranteeing a certain spectrum efficiency level over doubly-dispersive channels. In addition to the constellation symbols, a number of extra bits are transmitted via indices bits on DD domain. Simulation results verify that the introduced OTFS-IM idea leads to superior BER performance as compared to the conventional OTFS approach. It is stated in [215] that OTFS-IM signal of [214] activates all the subcarriers when converted into TF domain. This, on the other hand, may result in an escalated BER especially with large numbers of active lattices. As a remedy, the authors of [215] offer a new approach called OTFS with improved IM where every index bit is transmitted two times. Numerical results confirm the performance gain in terms of BER as compared to the standard OTFS-IM. In [216], OTFS with dual-mode IM is introduced to attain an enhanced trade-off between the spectral efficiency and BER. Relying on the minimum Hamming distance criterion, the authors devise a modified log-likelihood ratio detector with low complexity, which is shown to perform almost identically as the ML approach. A symbol-by-symbol aided EP detection procedure is proposed in [217] for OTFS-IM. It is numerically demonstrated that the introduced idea can yield important performance gains beyond the other detection approaches such as MMSE [214] for OTFS-IM. A novel transmission method, called OTFS with in-phase and quadrature IM, is conceived in [218] where a number of extra information bits are conveyed by means of the grid index of OTFS block in in-phase and quadrature dimensions. The presented scheme is shown to perform better than the other related OTFS-IM techniques in terms of both BER and PAPR. In [219], it is articulated that the studies in [214] and [216] only activate independent delay-Doppler resources by adopting impractical bi-orthogonal OTFS pulses. Thus, they cannot perform well under ISI caused by the channel delay and Doppler shifts. As a solution, the authors of [219] offer two new block-wise OTFS-IM designs under a practical scenario by activating a block of delay/Doppler resource bins at the same time. Simulation results affirm the BER advantage of the investigated approaches against the other related techniques. A physical layer anti-eavesdropping idea is inspected in [220] for OTFS-IM systems under frequency-division duplexing mode. As no channel reciprocity exists under such a scenario, a secure mapping technique is crafted relying on a chaos sequence generated by utilizing the angular reciprocity of the legitimate link. Numerical findings reveal that the eavesdropper's BER can be increased significantly without seriously affecting the BER of the legitimate user. The authors in [221] indicate that the existing OFDM-IM methods implement a fixed-sized constellation on a number of activated grids in DD domain to avoid ambiguous detection. They accordingly offer a new OTFS-IM technique where the number of active grids transmitting modulation symbols from any cardinality of constellations is permitted to be altered. The ambiguous detection is prevented by transmitting a fixed length of information bits via joint-mapping. Simulation results show that the introduced idea enhances the BER performance of the standard OTFS-IM scheme. In [222], a block-wise OTFS-IM method is designed where, unlike [219], an OTFS frame can include subblocks that transmit information symbols in delay or Doppler bins at the same time and active resource blocks may implement different constellations. The presented approach is numerically demonstrated to outperform other related schemes in terms of BER performance. Two new detectors based on MMSE and vector-by-vector-aided MP approaches are introduced in [223] for OTFS-IM systems and are shown to bring about BER performance gain as compared to the standard OTFS-IM scheme. In [224], the performance of OTFS-IM is inspected in a two-hop decode-and-forward relay communication system with a single relay where each node has a single antenna. It is shown that the utilization of indexing enhances the performance of OTFS with decode and forward relaying and the diversity order of the system becomes equal to the minimum of the number of resolvable DD domain paths between the source-to-relay and the relay-to-destination links with a PR operation at the transmitter.

In [225], it is shown that the introduction of spatial modulation results in an increase in the overall spectral efficiency of MIMO-OTFS by the base-two logarithm of the number of transmit antennas. Similarly, a spatial multiplexing aided OTFS scheme with IM is devised in [226] by adopting vertical Bell Labs layered space-time approach for simultaneous and parallel transmission over

transmit antennas. It is shown that the introduced method can provide an important SNR gain as compared to its counterpart in [225] under the same data rate with lower computational complexity. The authors of [227] treat a MIMO-OTFS scheme with spatial modulation and provide a number of closed-form expressions on the error rate of the system by means of union bounding together with the moment-generating function approach. A space-time block coding aided MIMO-OTFS system with spatial modulation is investigated in [228]. The proposed scheme is demonstrated to outperform the corresponding similar techniques in terms of BER performance. A combination of spatial-index modulation and OTFS systems is inspected in [229], [230]. The authors suggest to use a three dimensional IM approach including the transmit antenna index in the spatial domain along with the delay and Doppler indices in the DD domain. The presented scheme is shown to yield superior BER performance as compared to the traditional approaches. In [231], a generalized spatial modulation combined MIMO-OTFS system is proposed together with a decision feedback detector. The introduced technique is shown to accomplish better BER performance as compared to the conventional MIMO-OTFS and OFDM-based approaches. The authors of [232] develop a spatial modulation-aided OTFS technique for high-Doppler cases. A low-complexity distance-based ordering subspace check detector is proposed by utilizing a priori information of the transmit symbol vector. Simulation results are used to reveal the superior BER performance of the introduced scheme as compared to the traditional SIMO-OTFS system. A transmission technique named as generalized space-delay-Doppler index modulated OTFS is introduced in [233] by taking advantage of multi-domain resources. Here, additional information bits are conveyed by means of the combined space-delay-Doppler resource units. The adopted idea is demonstrated to outperform the existing spatial-index modulation based and generalized spatial modulation based OTFS approaches in terms of BER performance. In [234], a low complexity two-step detector structure for the scheme in [233] is presented.

In [235], space-time shift keying-aided OTFS-based multiple access is introduced for a single-cell uplink communication scenario. By collectively invoking the DD, space and time domain resource blocks, multiple users simultaneously transmit to a common BS. Here, additional information bits are conveyed by the indices of the active dispersion matrices. The presented scheme is shown to enjoy enhanced diversity level and coding gain. The authors of [236] present an uplink multiple access scheme by relying on a combination of OTFS and IM over DD domain. All the users independently implement IM by activating subgroups of the available DD resource blocks. Here, it is possible that a certain resource block can be used simultaneously by multiple users. It is demonstrated that in spite of such probable collisions among user signals, the introduced idea provides improved BER performance as compared to other similar multiple access schemes with OTFS. With the purpose of augmenting spectral efficiency and decreasing BER, an OTFS-NOMA scheme with IM is devised in [237] for a two-user downlink scenario over a doubly-selective channel. Numerical findings indicate that the introduced system outperforms other related OTFS-based approaches with IM.

VIII. FUTURE CHALLENGES

In this section, we present several research directions of interest to the research community working on OTFS.

- It is conceivable that the prospective communication systems may include transceiver nodes with extremely high velocities. Under such cases, Doppler shift levels that are unprecedentedly large for the contemporary wireless communication systems will be experienced and the channel parameters associated with the multipath propagation such as delay, Doppler, and complex gain will alter at an excessive rate. When not dealt with appropriately, this can cause serious performance degradation in terms of BER. Hence, when the DD domain channel parameters are time-variant within a frame duration, the adaptation of OTFS to such a scenario poses a challenging future research direction.
- A number of works have recently studied possible utilization of the DD-domain signaling for security purposes. The efficacy of the traditional physical layer key generation schemes strictly depends on the stability of TF domain channel. Hence, these approaches severely suffer from performance loss under high-mobility (low coherence time) cases. Contrarily, under the same scenarios, a sparse and relatively stationary channel characterization can be accomplished in the DD domain by leveraging OTFS. Thus, with new perspectives OTFS offers, it is quite likely that there will be an increasing interest on OTFS from a security point of view.
- The number of nodes to be connected in IoT networks is expected to escalate in an exponential rate in the upcoming years. Hence, efficiency in time and frequency utilization has become particularly crucial in the emerging communication systems and standards. Non-orthogonal approaches for multiple access allow cost-effective usage of these resources and it is highly anticipated that they will be featured in the future standards. As such, the combination of OTFS and NOMA is being researched currently from distinct viewpoints including DD domain user multiplexing. In this sense, a comprehensive performance evaluation of OTFS-NOMA for any number of users and under practical impairments over generalized fading channels constitutes a potential future research topic.
- Cell-free massive MIMO technology is proven to support five- to ten-fold enhancement in 95%-likely per-user throughput as compared to the traditional cellular operation [238]. From the network design point of view, the cell-free massive MIMO idea can substantially change the conventional complex centralized processing approach. In addition, OTFS in a cell-free

massive MIMO network can respond to the stringent requirements in terms of spectral efficiency, coverage, connectivity, and mobility. On the other hand, such a system must deal with a number of emerging challenges, such as downlink channel estimation under frequency-division duplexing mode, which may require excessive overhead. The sparsity in the DD-domain channel characterization can be exploited in this case.

- Machine learning has been attracting intense interest and is being utilized in different scenarios with distinct goals. Thus, some very recent studies have investigated the exploitation of machine learning approaches in OTFS systems, especially for channel estimation and data decoding purposes. However, there still exist many pending issues to be resolved in terms of miscellaneous applications and practical implementations.
- OTFS is a promising candidate for future ISAC systems, offering a balanced approach to the dual demands of communication and sensing in dynamic and spectrum-constrained environments. This makes it a suitable choice for emerging applications in autonomous driving, UAV systems, and other areas requiring robust mobile communication and precise sensing. Cooperative distributed use of OTFS-ISAC still remains an open issue that should be addressed in the near future. The synergy between OTFS and ISAC is expected to be explored further in the future, as we discuss in Section VI.

IX. CONCLUSION

In this survey paper, OTFS, a promising solution for high-mobility communications towards 6G, is reviewed comprehensively. Its advantages over other competing techniques, implementations, and integration with MIMO, multiple access techniques, satellite communications, ISAC, DL, IM, UWA, and UAV are discussed in detail. Future challenges and open issues are also indicated.

REFERENCES

[1] Z. Zhang et al., "6G wireless networks: Vision, requirements, architecture, and key technologies," *IEEE Veh. Technol. Mag.*, vol. 14, no. 3, pp. 28–41, Sep. 2019.

[2] W. Saad, M. Bennis, and M. Chen, "A vision of 6G wireless systems: Applications, trends, technologies, and open research problems," *IEEE Netw.*, vol. 34, no. 3, pp. 134–142, May 2020.

[3] I. F. Akyildiz, A. Kak, and S. Nie, "6G and beyond: The future of wireless communications systems," *IEEE Access*, vol. 8, pp. 133995–134030, 2020.

[4] J. Wu and P. Fan, "A survey on high mobility wireless communications: Challenges, opportunities and solutions," *IEEE Access*, vol. 4, pp. 450–476, 2016.

[5] R. Hadani et al., "Orthogonal time frequency space modulation," in *Proc. IEEE Wireless Commun. Netw. Conf. (WCNC)*, San Francisco, CA, USA, 2017, pp. 1–6.

[6] R. Hadani and A. Monk, "OTFS: A new generation of modulation addressing the challenges of 5G," 2018, *arXiv:1802.02623*.

[7] Z. Wei et al., "Orthogonal time-frequency space modulation: A promising next-generation waveform," *IEEE Wireless Commun.*, vol. 28, no. 4, pp. 136–144, Aug. 2021.

[8] Z. Wei, S. Li, W. Yuan, R. Schober, and G. Caire, "Orthogonal time frequency space modulation—Part I: Fundamentals and challenges ahead," *IEEE Commun. Lett.*, vol. 27, no. 1, pp. 4–8, Jan. 2023.

[9] S. Li, W. Yuan, Z. Wei, R. Schober, and G. Caire, "Orthogonal time frequency space modulation—Part II: Transceiver designs," *IEEE Commun. Lett.*, vol. 27, no. 1, pp. 9–13, Jan. 2023.

[10] W. Yuan, Z. Wei, S. Li, R. Schober, and G. Caire, "Orthogonal time frequency space modulation—Part III: ISAC and potential applications," *IEEE Commun. Lett.*, vol. 27, no. 1, pp. 14–18, Jan. 2023.

[11] L. Xiao, S. Li, Y. Qian, D. Chen, and T. Jiang, "An overview of OTFS for Internet of Things: Concepts, benefits, and challenges," *IEEE Int. Things J.*, vol. 9, no. 10, pp. 7596–7618, May 2022.

[12] W. Yuan et al., "New delay Doppler communication paradigm in 6G era: A survey of orthogonal time frequency space (OTFS)," *China Commun.*, vol. 20, no. 6, pp. 1–25, Jun. 2023.

[13] M. Li, W. Liu, J. Lei, "A review on orthogonal time–frequency space modulation: State-of-art, hotspots and challenges," *Comput. Netw.*, vol. 224, Apr. 2023, Art. no. 109597.

[14] S. K. Mohammed, R. Hadani, A. Chockalingam, and R. Calderbank, "OTFS—A mathematical foundation for communication and radar sensing in the delay-Doppler domain," *IEEE BITS Inf. Theory Mag.*, vol. 2, no. 2, pp. 36–55, Nov. 2022.

[15] S. K. Mohammed, R. Hadani, A. Chockalingam, and R. Calderbank, "OTFS—Predictability in the delay- Doppler domain and its value to communication and radar sensing," *IEEE BITS Inf. Theory Mag.*, early access, Sep. 27, 2023, doi: 10.1109/MBITS.2023.3319595.

[16] S. Li, W. Yuan, Z. Wei, J. Yuan, B. Bai, and G. Caire, "On the pulse shaping for delay-Doppler communications," in *Proc. IEEE Glob. Commun. Conf. (GlobeCom)*, Kuala Lumpur, Malaysia, 2023, pp. 1–6.

[17] A. Farhang, A. RezazadehReyhani, L. E. Doyle, and B. Farhang-Boroujeny, "Low complexity modem structure for OFDM-based orthogonal time frequency space modulation," *IEEE Wireless Commun. Lett.*, vol. 7, no. 3, pp. 344–347, Jun. 2018.

[18] P. Raviteja, K. T. Phan, Y. Hong, and E. Viterbo, "Interference cancellation and iterative detection for orthogonal time frequency space modulation," *IEEE Trans. Wireless Commun.*, vol. 17, no. 10, pp. 6501–6515, Oct. 2018.

[19] S. Tiwari, S. S. Das, and V. Rangamgari, "Low complexity LMMSE receiver for OTFS," *IEEE Commun. Lett.*, vol. 23, no. 12, pp. 2205–2209, Dec. 2019.

[20] H. Qu, G. Liu, L. Zhang, S. Wen, and M. A. Imran, "Low-complexity symbol detection and interference cancellation for OTFS system," *IEEE Trans. Commun.*, vol. 69, no. 3, pp. 1524–1537, Mar. 2021.

[21] L. Gaudio, M. Kobayashi, G. Caire, and G. Colavolpe, "On the effectiveness of OTFS for joint radar parameter estimation and communication," *IEEE Trans. Wireless Commun.*, vol. 19, no. 9, pp. 5951–5965, Sep. 2020.

[22] G. D. Surabhi and A. Chockalingam, "Low-complexity linear equalization for OTFS modulation," *IEEE Commun. Lett.*, vol. 24, no. 2, pp. 330–334, Feb. 2020.

[23] Y. Shan, F. Wang, and Y. Hao, "Orthogonal time frequency space detection via low-complexity expectation propagation," *IEEE Trans. Wireless Commun.*, vol. 21, no. 12, pp. 10887–10901, Dec. 2022.

[24] S. Li, W. Yuan, Z. Wei, and J. Yuan, "Cross domain iterative detection for orthogonal time frequency space modulation," *IEEE Trans. Wireless Commun.*, vol. 21, no. 4, pp. 2227–2242, Apr. 2022.

[25] Z. Yuan, F. Liu, W. Yuan, Q. Guo, Z. Wang, and J. Yuan, "Iterative detection for orthogonal time frequency space modulation with unitary approximate message passing," *IEEE Trans. Wireless Commun.*, vol. 21, no. 2, pp. 714–725, Feb. 2022.

[26] Z. Yuan, M. Tang, J. Chen, T. Fang, H. Wang, and J. Yuan, "Low complexity parallel symbol detection for OTFS modulation," *IEEE Trans. Veh. Technol.*, vol. 72, no. 4, pp. 4904–4918, Apr. 2023.

[27] H. Li and Q. Yu, "Doubly- iterative spasified MMSE turbo equalization for OTFS modulation," *IEEE Trans. Commun.*, vol. 71, no. 3, pp. 1336–1351, Mar. 2023.

[28] H. Zhang and T. Zhang, "A low-complexity message passing detector for OTFS modulation with probability clipping," *IEEE Wireless Commun. Lett.*, vol. 10, no. 6, pp. 1271–1275, Jun. 2021.

[29] P. Raviteja, K. T. Phan, and Y. Hong, "Embedded pilot-aided channel estimation for OTFS in delay–Doppler channels," *IEEE Trans. Veh. Technol.*, vol. 68, no. 5, pp. 4906–4917, May 2019.

[30] S. S. Das, V. Rangamgari, S. Tiwari, and S. C. Mondal, "Time domain channel estimation and equalization of CP-OTFS under multiple fractional Dopplers and residual synchronization errors," *IEEE Access*, vol. 9, pp. 10561–10576, 2021.

[31] H. B. Mishra, P. Singh, A. K. Prasad, and R. Budhiraja, "OTFS channel estimation and data detection designs with superimposed pilots," *IEEE Trans. Wireless Commun.*, vol. 21, no. 4, pp. 2258–2274, Apr. 2022.

[32] W. Yuan, S. Li, Z. Wei, J. Yuan, and D. W. K. Ng, "Data-aided channel estimation for OTFS systems with a superimposed pilot and data transmission scheme," *IEEE Wireless Commun. Lett.*, vol. 10, no. 9, pp. 1954–1958, Sep. 2021.

[33] S. Srivastava, R. K. Singh, A. K. Jagannatham, and L. Hanzo, "Bayesian learning aided sparse channel estimation for orthogonal time frequency space modulated systems," *IEEE Trans. Veh. Technol.*, vol. 70, no. 8, pp. 8343–8348, Aug. 2021.

[34] A. Pfadler, T. Szollmann, P. Jung, and S. Stanczak, "Leakage suppression in pulse-shaped OTFS delay-Doppler-pilot channel estimation," *IEEE Wireless Commun. Lett.*, vol. 11, no. 6, pp. 1181–1185, Jun. 2022.

[35] G. D. Surabhi, R. M. Augustine, and A. Chockalingam, "Peak-to-average power ratio of OTFS modulation," *IEEE Commun. Lett.*, vol. 23, no. 6, pp. 999–1002, Jun. 2019.

[36] S. Gao and J. Zheng, "Peak-to-average power ratio reduction in pilot-embedded OTFS modulation through iterative clipping and filtering," *IEEE Commun. Lett.*, vol. 24, no. 9, pp. 2055–2059, Sep. 2020.

[37] P. Wei, Y. Xiao, W. Feng, N. Ge, and M. Xiao, "Charactering the peak-to-average power ratio of OTFS signals: A large system analysis," *IEEE Trans. Wireless Commun.*, vol. 21, no. 6, pp. 3705–3720, Jun. 2022.

[38] P. Raviteja, Y. Hong, E. Viterbo, and E. Biglieri, "Practical pulse-shaping waveforms for reduced-cyclic-prefix OTFS," *IEEE Trans. Veh. Tech.*, vol. 68, no. 1, pp. 957–961, Jan. 2019.

[39] R. Mallaiah and V. V. Mani, "A novel OTFS system based on DFrFT-OFDM," *IEEE Wireless Commun. Lett.*, vol. 11, no. 6, pp. 1156–1160, Jun. 2022.

[40] Y. Ge, Q. Deng, P. C. Ching, and Z. Ding, "Receiver design for OTFS with a fractionally spaced sampling approach," *IEEE Trans. Wireless Commun.*, vol. 20, no. 7, pp. 4072–4086, Jul. 2021.

[41] Y. Liu, Y. L. Guan, and G. David González, "Near-optimal BEM OTFS receiver with low pilot overhead for high-mobility communications," *IEEE Trans. Commun.*, vol. 70, no. 5, pp. 3392–3406, May 2022.

[42] Z. Wei, W. Yuan, S. Li, J. Yuan, and D. W. K. Ng, "Transmitter and receiver window designs for orthogonal time-frequency space modulation," *IEEE Trans. Commun.*, vol. 69, no. 4, pp. 2207–2223, Apr. 2021.

[43] C. Jin, Z. Bie, X. Lin, W. Xu, and H. Gao, "A simple two-stage equalizer for OTFS with rectangular windows," *IEEE Commun. Lett.*, vol. 25, no. 4, pp. 1158–1162, Apr. 2021.

[44] S. E. Zegrar and H. Arslan, "A novel cyclic prefix configuration for enhanced reliability and spectral efficiency in OTFS systems," *IEEE Wireless Commun. Lett.*, vol. 12, no. 5, pp. 888–892, May 2023.

[45] R. Bomfin, M. Chafii, A. Nimr, and G. Fettweis, "A robust baseband transceiver design for doubly-dispersive channels," *IEEE Trans. Wireless Commun.*, vol. 20, no. 8, pp. 4781–4796, Aug. 2021.

[46] R. Bomfin, A. Nimr, M. Chafii, and G. Fettweis, "A robust and low-complexity Walsh-Hadamard modulation for doubly-dispersive channels," *IEEE Commun. Lett.*, vol. 25, no. 3, pp. 897–901, Mar. 2021.

[47] P. Singh, K. Yadav, H. B. Mishra, and R. Budhiraja, "BER analysis for OTFS zero forcing receiver," *IEEE Trans. Commun.*, vol. 70, no. 4, pp. 2281–2297, Apr. 2022.

[48] J. Shi, J. Hu, Y. Yue, X. Xue, W. Liang, and Z. Li, "Outage probability for OTFS based downlink LEO satellite communication," *IEEE Trans. Veh. Technol.*, vol. 71, no. 3, pp. 3355–3360, Mar. 2022.

[49] C. Shen, J. Yuan, and H. Lin, "Error performance of rectangular pulse-shaped OTFS with practical receivers," *IEEE Wireless Commun. Lett.*, vol. 11, no. 12, pp. 2690–2694, Dec. 2022.

[50] S. Li, J. Yuan, W. Yuan, Z. Wei, B. Bai, and D. W. K. Ng, "Performance analysis of coded OTFS systems over high-mobility channels," *IEEE Trans. Wireless Commun.*, vol. 20, no. 9, pp. 6033–6048, Sep. 2021.

[51] J. Sun, Z. Wang, and Q. Huang, "A closed-form minimum BER precoder for orthogonal time frequency space systems," *IEEE Commun. Lett.*, vol. 26, no. 8, pp. 1898–1902, Aug. 2022.

[52] J. Hu, J. Shi, S. Ma, and Z. Li, "Secrecy analysis for orthogonal time frequency space scheme based uplink LEO satellite communication," *IEEE Wireless Commun. Lett.*, vol. 10, no. 8, pp. 1623–1627, Aug. 2021.

[53] P. Raviteja, E. Viterbo, and Y. Hong, "OTFS Performance on static multipath channels," *IEEE Wireless Commun. Lett.*, vol. 8, no. 3, pp. 745–748, Jun. 2019.

[54] M. K. Ramachandran and A. Chockalingam, "MIMO-OTFS in high-Doppler fading channels: Signal detection and channel estimation," in *Proc. IEEE Glob. Commun. Conf. (GLOBECOM)*, Abu Dhabi, UAE, 2018, pp. 206–212.

[55] A. RezazadehReyhani, A. Farhang, M. Ji, R. R. Chen, and B. Farhang-Boroujeny, "Analysis of discrete-time MIMO OFDM-based orthogonal time frequency space modulation," in *Proc. IEEE Int. Conf. Commun. (ICC)*, 2018, pp. 1–6.

[56] G. D. Surabhi, R. M. Augustine, and A. Chockalingam, "On the diversity of uncoded OTFS modulation in doubly-dispersive channels," *IEEE Trans. Wireless Commun.*, vol. 18, no. 6, pp. 3049–3063, Jun. 2019.

[57] R. M. Augustine, G. D. Surabhi, and A. Chockalingam, "Space-time coded OTFS modulation in high-Doppler channels," in *Proc. IEEE 89th Veh. Technol. Conf. (VTC)*, Kuala Lumpur, Malaysia, 2019, pp. 1–6.

[58] C. An and H.-G. Ryu, "High throughput mobile communication based on OTFS system with the delay-Doppler compensation," *Wireless Pers. Commun.*, vol. 106, pp. 473–486, May 2019.

[59] V. S. Bhat, S. G. Dayanand, and A. Chockalingam, "Performance analysis of OTFS modulation with receive antenna selection," *IEEE Trans. Veh. Technol.*, vol. 70, no. 4, pp. 3382–3395, Apr. 2021.

[60] V. S. Bhat and A. Chockalingam, "Performance analysis of OTFS modulation with transmit antenna selection," in *Proc. IEEE 93rd Veh. Technol. Conf. (VTC)*, Helsinki, Finland, 2021, pp. 1–6.

[61] D. Wang, B. Sun, F. Wang, X. Li, P. Yuan, and D. Jiang, "Transmit diversity scheme design for rectangular pulse shaping based OTFS," *China Commun.*, vol. 19, no. 3, pp. 116–128, Mar. 2022.

[62] H. Yin et al., "Cyclic delay-Doppler shift: A simple transmit diversity technique for delay-Doppler waveforms in doubly selective channels," in *Proc. IEEE Int. Conf. Acoust., Speech, Signal Process. Workshops (ICASSPW)*, Rhodes Island, Greece, 2023, pp. 1–5.

[63] S. Li, L. Xiao, Y. Liu, G. Liu, P. Xiao, and T. Jiang, "Performance analysis for orthogonal time frequency space modulation systems with generalized waveform," *China Commun.*, vol. 20, no. 4, pp. 57–72, Apr. 2023.

[64] R. Chong, M. Mohammadi, H. Q. Ngo, S. L. Cotton, and M. Matthaiou, "On the spectral efficiency of MMSE-based MIMO OTFS systems," in *Proc. Int. Symp. Wireless Commun. Syst. (ISWCS)*, Hangzhou, China, 2022, pp. 1–6.

[65] S. Li, J. Yuan, P. Fitzpatrick, T. Sakurai, and G. Caire, "Delay-Doppler domain Tomlinson-Harashima precoding for OTFS-based downlink MU-MIMO transmissions: Linear complexity implementation and scaling law analysis," *IEEE Trans. Commun.*, vol. 71, no. 4, pp. 2153–2169, Apr. 2023.

[66] G. D. Surabhi and A. Chockalingam, "Low-complexity linear equalization for 2×2 MIMO-OTFS signals," in *Proc. IEEE 21st Int. Workshop Signal Process. Adv. Wireless Commun. (SPAWC)*, Atlanta, GA, USA, 2020, pp. 1–5.

[67] B. C. Pandey, S. K. Mohammed, P. Raviteja, Y. Hong, and E. Viterbo, "Low complexity precoding and detection in multi-user massive MIMO OTFS downlink," *IEEE Trans. Veh. Technol.*, vol. 70, no. 5, pp. 4389–4405, May 2021.

[68] Y. Shan and F. Wang, "Low-complexity and low-overhead receiver for OTFS via large-scale antenna array," *IEEE Trans. Veh. Technol.*, vol. 70, no. 6, pp. 5703–5718, Jun. 2021.

[69] B. Cao, Z. Xiang, and P. Ren, "Low complexity transmitter precoding for MU MIMO-OTFS," *Digit. Signal Process.*, vol. 115, Aug. 2021, Art. no. 103083.

[70] P. Singh, H. B. Mishra, and R. Budhiraja, "Low-complexity linear MIMO-OTFS receivers," in *Proc. IEEE Int. Conf. Commun. Workshops (ICC Workshops)*, Montreal, QC, Canada, 2021, pp. 1–6.

[71] P. Singh, A. Gupta, H. B. Mishra, and R. Budhiraja, "Low-complexity ZF/MMSE MIMO-OTFS receivers for high-speed vehicular communication," *IEEE Open J. Commun. Soc.*, vol. 3, pp. 209–227, 2022.

[72] P. Singh, S. Tiwari, and R. Budhiraja, "Low-complexity LMMSE receiver design for practical-pulse-shaped MIMO-OTFS systems," *IEEE Trans. Commun.*, vol. 70, no. 12, pp. 8383–8399, Dec. 2022.

[73] A. Naikoti and A. Chockalingam, "Low-complexity delay-Doppler symbol DNN for OTFS signal detection," in *Proc. IEEE 93rd Veh. Technol. Conf. (VTC)*, Helsinki, Finland, 2021, pp. 1–6.

[74] T. Thaj and E. Viterbo, "Low-complexity linear diversity-combining detector for MIMO-OTFS," *IEEE Wireless Commun. Lett.*, vol. 11, no. 2, pp. 288–292, Feb. 2022.

[75] H. Qu, G. Liu, M. A. Imran, S. Wen, and L. Zhang, "Efficient channel equalization and symbol detection for MIMO OTFS systems," *IEEE Trans. Wireless Commun.*, vol. 21, no. 8, pp. 6672–6686, Aug. 2022.

[76] M. A. Sheikh, P. Singh, and R. Budhiraja, "Low-complexity MMSE receiver design for massive MIMO OTFS systems," *IEEE Commun. Lett.*, vol. 26, no. 11, pp. 2759–2763, Nov. 2022.

[77] V. S. Bhat and A. Chockalingam, "Performance analysis of MIMO-OTFS with decode and forward relaying," in *Proc. IEEE 98th Veh. Technol. Conf. (VTC)*, 2023, pp. 1–7.

[78] V. S. Bhat and A. Chockalingam, "Performance analysis of MIMO-OTFS with selective decode and forward relaying," in *Proc. IEEE 98th Veh. Technol. Conf. (VTC)*, 2023, pp. 1–6.

[79] M. Li, S. Zhang, F. Gao, P. Fan, and O. A. Dobre, "A new path division multiple access for the massive MIMO-OTFS networks," *IEEE J. Sel. Areas Commun.*, vol. 39, no. 4, pp. 903–918, Apr. 2021.

[80] J. Feng, H. Q. Ngo, M. F. Flanagan, and M. Matthaiou, "Performance analysis of OTFS-based uplink massive MIMO with ZF receivers," in *Proc. IEEE Int. Conf. Commun. Workshops (ICC Workshops)*, Montreal, QC, Canada, 2021, pp. 1–7.

[81] M. Mohammadi, H. Q. Ngo, and M. Matthaiou, "Cell-free massive MIMO meets OTFS modulation," *IEEE Trans. Commun.*, vol. 70, no. 11, pp. 7728–7747, Nov. 2022.

[82] M. Mohammadi, H. Q. Ngo, and M. Matthaiou, "Cell-free massive MIMO with OTFS modulation: Statistical CSI-based detection," *IEEE Wireless Commun. Lett.*, vol. 12, no. 6, pp. 987–991, Jun. 2023.

[83] B. Shen, Y. Wu, J. An, C. Xing, L. Zhao, and W. Zhang, "Random access with massive MIMO-OTFS in LEO satellite communications," *IEEE J. Sel. Areas Commun.*, vol. 40, no. 10, pp. 2865–2881, Oct. 2022.

[84] J. Feng, H. Q. Ngo, and M. Matthaiou, "OTFS-based massive MIMO with fractional delay and Doppler Shift: The URLLC case," in *Proc. IEEE 33rd Annu. Int. Symp. Pers., Indoor Mobile Radio Commun. (PIMRC)*, Kyoto, Japan, 2022, pp. 522–528.

[85] D. L. Li and A. Farhang, "OTFS without CP in massive MIMO: Breaking Doppler limitations with TR-MRC and windowing," in *Proc. IEEE Wireless Commun. Netw. Conf. (WCNC)*, Austin, TX, USA, 2022, pp. 2518–2523.

[86] S. K. Dehkordi, L. Gaudio, M. Kobayashi, G. Caire, and G. Colavolpe, "Beam-space MIMO radar for joint communication and sensing with OTFS modulation," *IEEE Trans. Wireless Commun.*, vol. 22, no. 10, pp. 6737–6749, Oct. 2023.

[87] S. Jiang and A. Alkhateeb, "Sensing aided OTFS massive MIMO systems: Compressive channel estimation," in *Proc. IEEE Int. Conf. Commun. Workshops (ICC Workshops)*, Rome, Italy, 2023, pp. 794–799.

[88] Z. Gong, F. Jiang, C. Li, and X. Shen, "Simultaneous localization and communications with massive MIMO-OTFS," *IEEE J. Sel. Areas Commun.*, vol. 41, no. 12, pp. 3908–3924, Dec. 2023.

[89] A. C. Serrano, N. Petrov, M. G. Huici, and A. Yarovoy, "MIMO OTFS with arbitrary time-frequency allocation for joint radar and communications," *IEEE Trans. Radar Syst.*, vol. 1, pp. 707–718, Nov. 2023.

[90] N. Tawa, T. Kuwabara, Y. Maruta, and T. Kaneko, "28 GHz over-the-air measurement using an OTFS multi-user distributed MIMO," in *Proc. 51st Eur. Microw. Conf. (EuMC)*, 2022, pp. 450–453.

[91] A. S. Bora, K. T. Phan, and Y. Hong, "Spatially correlated MIMO-OTFS for LEO satellite communication systems," in *Proc. IEEE Int. Conf. Commun. Workshops (ICC Workshops)*, 2022, pp. 723–728.

[92] A. S. Bora, K. T. Phan, and Y. Hong, "Mitigating spatial correlation in MIMO-OTFS," *IEEE Trans. Veh. Technol.*, vol. 73, no. 3, pp. 3608–3622, Mar. 2024.

[93] T. M. C. Chu, H. J. Zepernick, A. Westerhagen, A. Hook, and B. Granbom, "Performance assessment of OTFS modulation in high Doppler airborne communication networks," *Mobile Netw. Appl.*, vol. 27, pp. 1746–1756, Aug. 2022.

[94] M. Li, S. Zhang, Y. Ge, F. Gao, and P. Fan, "Joint channel estimation and data detection for hybrid RIS aided millimeter wave OTFS systems," *IEEE Trans. Commun.*, vol. 70, no. 10, pp. 6832–6848, Oct. 2022.

[95] M. Liu, S. Li, Z. Wei, and B. Bai, "Near optimal hybrid digital-analog beamforming for point-to-point MIMO-OTFS transmissions," in *Proc. IEEE Wireless Commun. Netw. Conf. (WCNC)*, 2023, pp. 1–6.

[96] Y. Yan, C. Shan, J. Zhang, and H. Zhao, "Low-complexity OTFS-based hybrid precoding in mmWave high mobility systems," *Digit. Signal Process.*, vol. 126, Jun. 2022, Art. no. 103496.

[97] A. S. Bora, K. T. Phan, and Y. Hong, "IRS-assisted high mobility communications using OTFS modulation," *IEEE Wireless Commun. Lett.*, vol. 12, no. 2, pp. 376–380, Feb. 2023.

[98] W. Shen, L. Dai, J. An, P. Fan, and R. W. Heath, "Channel estimation for orthogonal time frequency space (OTFS) massive MIMO," *IEEE Trans. Signal Process.*, vol. 67, no. 16, pp. 4204–4217, Aug. 2019.

[99] Y. Liu, S. Zhang, F. Gao, J. Ma, and X. Wang, "Uplink-aided high mobility downlink channel estimation over massive MIMO-OTFS system," *IEEE J. Sel. Areas Commun.*, vol. 38, no. 9, pp. 1994–2009, Sep. 2020.

[100] X. Wu, S. Ma, and X. Yang, "Tensor-based low-complexity channel estimation for mmWave massive MIMO-OTFS systems," *J. Commun. Inf. Netw.*, vol. 5, no. 3, pp. 324–334, Sep. 2020.

[101] D. Shi et al., "Deterministic pilot design and channel estimation for downlink massive MIMO-OTFS systems in presence of the fractional Doppler," *IEEE Trans. Wireless Commun.*, vol. 20, no. 11, pp. 7151–7165, Nov. 2021.

[102] G.-R. Wang and Z.-X. Wang, "3D-IPRDSOMP algorithm for channel estimation in massive MIMO with OTFS modulation," *IEEE Access*, vol. 11, pp. 94679–94690, 2023.

[103] S. Srivastava, R. K. Singh, A. K. Jagannatham, and L. Hanzo, "Bayesian learning aided simultaneous row and group sparse channel estimation in orthogonal time frequency space modulated MIMO systems," *IEEE Trans. Commun.*, vol. 70, no. 1, pp. 635–648, Jan. 2022.

[104] S. Srivastava, R. K. Singh, A. K. Jagannatham, and L. Hanzo, "Delay-Doppler and angular domain 4D-sparse CSI estimation in OTFS aided MIMO systems," *IEEE Trans. Veh. Technol.*, vol. 71, no. 12, pp. 13447–13452, Dec. 2022.

[105] A. Mohebbi, W.-P. Zhu, and M. O. Ahmad, "Compressive sensing-based channel estimation for MIMO OTFS Systems," in *Proc. Bienn. Symp. Commun. (BSC)*, Montreal, QC, Canada, 2023, pp. 71–76.

[106] S. Srivastava, R. K. Singh, A. K. Jagannatham, A. Chockalingam, and L. Hanzo, "OTFS transceiver design and sparse doubly-selective CSI estimation in analog and hybrid beamforming aided mmWave MIMO systems," *IEEE Trans. Wireless Commun.*, vol. 21, no. 12, pp. 10902–10917, Dec. 2022.

[107] Y. Yan, C. Shan, J. Zhang, and H. Zhao, "Off-grid channel estimation for OTFS-based mmWave hybrid beamforming systems," *IEEE Commun. Lett.*, vol. 27, no. 8, pp. 2167–2171, Aug. 2023.

[108] X. Qi and J. Xie, "Cubature Kalman filter based millimeter wave beam tracking for OTFS systems," *China Commun.*, vol. 20, no. 7, pp. 233–240, Jul. 2023.

[109] A. Mehrotra, S. Srivastava, A. K. Jagannatham, and L. Hanzo, "Data-aided CSI estimation using affine-precoded superimposed pilots in orthogonal time frequency space modulated MIMO systems," *IEEE Trans. Commun.*, vol. 71, no. 8, pp. 4482–4498, Aug. 2023.

[110] A. Mehrotra, S. Srivastava, S. Asifa, A. K. Jagannatham, and L. Hanzo, "Online Bayesian learning-aided sparse CSI estimation in OTFS modulated MIMO systems for ultra-high-Doppler scenarios," *IEEE Trans. Commun.*, vol. 72, no. 4, pp. 2182–2200, Apr. 2024.

[111] L. Zhao, J. Yang, Y. Liu, and W. Guo, "Block sparse Bayesian learning-based channel estimation for MIMO-OTFS systems," *IEEE Commun. Lett.*, vol. 26, no. 4, pp. 892–896, Apr. 2022.

[112] Q. Ren, Q. Li, Z. Xu, and Z. Pan, "Low overhead pilot design for channel estimation in MIMO-OTFS systems," in *Proc. IEEE/CIC Int. Conf. Commun. (ICCC Workshops)*, Dalian, China, 2023, pp. 1–6.

[113] C. Chen, J. Zhang, Y. Han, J. Lu, and S. Jin, "Channel estimation for massive MIMO-OTFS system in asymmetrical architecture," *IEEE Signal Process. Lett.*, vol. 30, pp. 1412–1416, Oct. 2023.

[114] R. Ouchikh, T. Chonavel, A. Aissa-El-Bey, and M. Djeddou, "Iterative channel estimation and data detection algorithm for MIMO-OTFS systems," *Digit. Signal Process.*, vol. 143, Nov. 2023, Art. no. 104234.

[115] Y. Liu et al., "Evolution of NOMA toward next generation multiple access (NGMA) for 6G," *IEEE J. Sel. Areas Commun.*, vol. 40, no. 4, pp. 1037–1071, Apr. 2022.

[116] V. Khammammetti and S. K. Mohammed, "OTFS-based multiple-access in high Doppler and delay spread wireless channels," *IEEE Wireless Commun. Lett.*, vol. 8, no. 2, pp. 528–531, Apr. 2019.

[117] G. D. Surabhi, R. M. Augustine, and A. Chockalingam, "Multiple access in the delay-Doppler domain using OTFS modulation," 2019, *arXiv:1902.03415*.

[118] O. K. Rasheed, G. D. Surabhi, and A. Chockalingam, "Sparse delay-Doppler channel estimation in rapidly time-varying channels for multiuser OTFS on the uplink," in *Proc. IEEE 91st Veh. Technol. Conf. (VTC)*, Antwerp, Belgium, 2020, pp. 1–5.

[119] M. Li, S. Zhang, P. Fan, and O. A. Dobre, "Multiple access for massive MIMO-OTFS networks over angle-delay-Doppler domain," in *Proc. IEEE Glob. Commun. Conf. (GLOBECOM)*, Taipei, Taiwan, 2020, pp. 1–6.

[120] R. Chong, S. Li, J. Yuan, and D. W. K. Ng, "Achievable rate upper-bounds of uplink multiuser OTFS transmissions," *IEEE Wireless Commun. Lett.*, vol. 11, no. 4, pp. 791–795, Apr. 2022.

[121] R. Chong, S. Li, W. Yuan, and J. Yuan, "Outage analysis for OTFS-based single user and multi-user transmissions," in *Proc. IEEE Int. Conf. Commun. Workshops (ICC Workshops)*, 2022, pp. 746–751.

[122] R. M. Augustine and A. Chockalingam, "Interleaved time-frequency multiple access using OTFS modulation," in *Proc. IEEE 90th Veh. Technol. Conf.*, Honolulu, HI, USA, 2019, pp. 1–5.

[123] V. Khammammetti and S. K. Mohammed, "Spectral efficiency of OTFS based orthogonal multiple access with rectangular pulses," *IEEE Trans. Veh. Technol.*, vol. 71, no. 12, pp. 12989–13006, Dec. 2022.

[124] Z. Ding, R. Schober, P. Fan, and H. V. Poor, "OTFS-NOMA: An efficient approach for exploiting heterogenous user mobility profiles," *IEEE Trans. Commun.*, vol. 67, no. 11, pp. 7950–7965, Nov. 2019.

[125] Z. Ding, "Robust beamforming design for OTFS-NOMA," *IEEE Open J. Commun. Soc.*, vol. 1, pp. 33–40, 2020.

[126] W. Shao, S. Zhang, C. Zhong, X. Lei, and P. Fan, "Angle-delay-Doppler domain NOMA over massive MIMO-OTFS networks," in *Proc. IEEE/CIC Int. Conf. Commun. China (ICCC)*, Chongqing, China, 2020, pp. 74–79.

[127] A. Chatterjee, V. Rangamgari, S. Tiwari, and S. S. Das, "Nonorthogonal multiple access with orthogonal time–frequency space signal transmission," *IEEE Syst. J.*, vol. 15, no. 1, pp. 383–394, Mar. 2021.

[128] Y. Ge, Q. Deng, P. C. Ching, and Z. Ding, "OTFS signaling for uplink NOMA of heterogeneous mobility users," *IEEE Trans. Commun.*, vol. 69, no. 5, pp. 3147–3161, May 2021.

[129] X. Zhou and Z. Gao, "Joint active user detection and channel estimation for grant-free NOMA-OTFS in LEO constellation Internet-of-Things," in *Proc. IEEE/CIC Int. Conf. Commun. China (ICCC)*, Xiamen, China, 2021, pp. 735–740.

[130] X. Zhou et al., "Active terminal identification, channel estimation, and signal detection for grant-free NOMA-OTFS in LEO satellite Internet-of-Things," *IEEE Trans. Wireless Commun.*, vol. 22, no. 4, pp. 2847–2866, Apr. 2023.

[131] Y. Liu, W. Yi, Z. Ding, X. Liu, O. A. Dobre, and N. Al-Dhahir, "Developing NOMA to next generation multiple access: Future vision and research opportunities," *IEEE Wireless Commun.*, vol. 29, no. 6, pp. 120–127, Dec. 2022.

[132] S. M. Pishvaei and B. M. Tazehkand, "Error and outage performance of the FBMC-based OTFS using large-scale and massive MISO-NOMA with millimeter-wave channel by LoS and NLoS paths impact," *Wireless Netw.*, vol. 28, no. 5, pp. 1835–1855, 2022.

[133] J. Hu, J. Shi, X. Wang, X. Lu, Z. Li, and Z. Tie, "Secrecy transmission of NOMA-OTFS based multicast-unicast streaming," *China Commun.*, vol. 20, no. 1, pp. 1–13, Jan. 2023.

[134] S. McWade, A. Farhang, and M. F. Flanagan, "Low-complexity reliability-based equalization and detection for OTFS-NOMA," *IEEE Trans. Commun.*, vol. 71, no. 11, pp. 6779–6792, Nov. 2023.

[135] S. McWade, M. F. Flanagan, and A. Farhang, "Low-Complexity Equalization and Detection for OTFS-NOMA," in *Proc. IEEE Int. Conf. Commun. Workshops (ICC Workshops)*, Rome, Italy, 2023, pp. 530–535.

[136] H. Zhang, K. Niu, J. Xu, J. Dai, and J. Zhang, "Iterative SIC-based multiuser detection for uplink heterogeneous NOMA system," in *Proc. IEEE Globecom Workshops (GC Wkshps)*, Rio de Janeiro, Brazil, 2022, pp. 94–99.

[137] B. Shen, Y. Wu, W. Zhang, G. Y. Li, J. An, and C. Xing, "LEO satellite-enabled grant-free random access with MIMO-OTFS," in *Proc. IEEE Global Commun. Conf. (GLOBECOM)*, Rio de Janeiro, Brazil, 2022, pp. 3308–3313.

[138] X. Lin et al., "Resource allocation for NOMA based OTFS transmission with heterogeneous mobility users," in *Proc. IEEE 10th Int. Conf. Inf., Commun. Netw. (ICICN)*, Zhangye, China, 2022, pp. 91–98.

[139] Y. Xu, Z. Du, W. Yuan, S. Jia, and V. C. M. Leung, "Performance of OTFS-NOMA scheme for coordinated direct and relay transmission networks in high-mobility scenarios," *IEEE Wireless Commun. Lett.*, vol. 12, no. 12, pp. 2268–2272, Dec. 2023.

[140] T. M. C. Chu and H.-J. Zepernick, "Sum rate of OTFS-NOMA systems with K-means clustering of user equipment," in *Proc. IEEE 34th Annu. Int. Symp. Pers., Indoor Mobile Radio Commun. (PIMRC)*, Toronto, ON, Canada, 2023, pp. 1–6.

[141] L. Xiang, K. Xu, J. Hu, C. Masouros, and K. Yang, "Robust NOMA-assisted OTFS-ISAC network design with 3-D motion prediction topology," *IEEE Internet Things J.*, vol. 11, no. 9, pp. 15909–15918, May 2024.

[142] K. Deka, A. Thomas, and S. Sharma, "OTFS-SCMA: A code-domain NOMA approach for orthogonal time frequency space modulation," *IEEE Trans. Commun.*, vol. 69, no. 8, pp. 5043–5058, Aug. 2021.

[143] Z. Kang, H. Zhao, and H. Wang, "An efficient two-dimension OTFS-NOMA scheme based on heterogenous mobility users grouping," in *Proc. IEEE 21st Int. Conf. Commun. Technol. (ICCT)*, Tianjin, China, 2021, pp. 726–730.

[144] A. Thomas, K. Deka, P. Raviteja, and S. Sharma, "Convolutional sparse coding based channel estimation for OTFS-SCMA in uplink," *IEEE Trans. Commun.*, vol. 70, no. 8, pp. 5241–5257, Aug. 2022.

[145] H. Wen, W. Yuan, Z. Liu, and S. Li, "OTFS-SCMA: A downlink NOMA scheme for massive connectivity in high mobility channels," *IEEE Trans. Wireless Commun.*, vol. 22, no. 9, pp. 5770–5784, Sep. 2023.

[146] H. Wen, W. Yuan, and S. Li, "Downlink OTFS non-orthogonal multiple access receiver design based on cross-domain detection," in *Proc. IEEE Int. Conf. Commun. Workshops (ICC Workshops)*, 2022, pp. 928–933.

[147] Y. Ge, Q. Deng, G. D. Gonzalez, Y. L. Guan, and Z. Ding, "OTFS signaling for SCMA with coordinated multi-point vehicle communications," *IEEE Trans. Veh. Technol.*, vol. 72, no. 7, pp. 9044–9057, Jul. 2023.

[148] Q. Deng, Y. Ge, and Z. Ding, "Jamming suppression via resource hopping in high-mobility OTFS-SCMA systems," *IEEE Wireless Commun. Lett.*, vol. 12, no. 12, pp. 2138–2142, Dec. 2023.

[149] Y. Ma, G. Ma, B. Ai, N. Wang, and Z. Zhong, "Orthogonal time frequency code space modulation enabled multiple access under compactness-reduced channel spreading function," *IEEE Trans. Wireless Commun.*, vol. 23, no. 3, pp. 1810–1826, Mar. 2024.

[150] Y. Ma, G. Ma, B. Ai, J. Liu, N. Wang, and Z. Zhong, "OTFCS-modulated waveform design for joint grant-free random access and positioning in C-V2X," *IEEE J. Sel. Areas Commun.*, vol. 42, no. 1, pp. 103–119, Jan. 2024.

[151] Y. Ge, L. Liu, S. Huang, D. Gonzalez, Y. L. Guan, and Z. Ding, "Low-complexity memory AMP detector for high-mobility MIMO-OTFS SCMA systems," in *Proc. IEEE Int. Conf. Commun. (ICC)*, Rome, Italy, 2023, pp. 1–6.

[152] J. Li and Y. Hong, "Performance analysis and phase shift design of IRS-aided uplink OTFS-SCMA," *IEEE Access*, vol. 11, pp. 133059–133069, 2023.

[153] Y. Ma, G. Ma, N. Wang, Z. Zhong, and B. Ai, "OTFS-TSMA for massive Internet of Things in high-speed railway," *IEEE Trans. Wireless Commun.*, vol. 21, no. 1, pp. 519–531, Jan. 2022.

[154] G. Ma, B. Ai, F. Wang, and Z. Zhong, "Tandem spreading network-coded division multiple access," *IEEE Trans. Ind. Informat.*, vol. 13, no. 1, pp. 390–398, Feb. 2017.

[155] Y. Ma, G. Ma, N. Wang, Z. Zhong, J. Yuan, and B. Ai, "Enabling OTFS-TSMA for smart railways mMTC over LEO satellite: A differential Doppler shift perspective," *IEEE Internet Things J.*, vol. 10, no. 6, pp. 4799–4814, Mar. 2023.

[156] H. Li, C. Gong, Q. Li, S. Hao, X. Wang, and X. Dai, "OTFS-PDMA scheme with EPA-based receivers for high-mobility IoT networks," *IEEE Trans. Wireless Commun.*, vol. 23, no. 5, pp. 4950–4963, May 2024.

[157] Y. Zhang and P. Du, "Decomposition of uplink multi-user OTFS channel with partial CSI feedback," *Phys. Commun.*, vol. 55, Dec. 2022, Art. no. 101911.

[158] B. V. S. Reddy, C. Velampalli, and S. S. Das, "Performance analysis of multi-user OTFS, OTSM, and single carrier in uplink," *IEEE Trans. Commun.*, vol. 72, no. 3, pp. 1428–1443, Mar. 2024.

[159] J. Feng, H. Q. Ngo, and M. Matthaiou, "Rectangular pulse-shaped OTFS with fractional delay and Doppler shift for MU-MIMO systems," in *Proc. IEEE Int. Conf. Commun. Workshops (ICC Workshops)*, Rome, Italy, 2023, pp. 788–793.

[160] M. Y. Abdelsadek et al., "Future space networks: Toward the next giant leap for humankind," *IEEE Trans. Commun.*, vol. 71, no. 2, pp. 949–1007, Feb. 2023.

[161] Y. Su, Y. Liu, Y. Zhou, J. Yuan, H. Cao, and J. Shi, "Broadband LEO satellite communications: Architectures and key technologies," *IEEE Wireless Commun.*, vol. 26, no. 2, pp. 55–61, Apr. 2019.

[162] J. Shi et al., "OTFS enabled LEO satellite communications: A promising solution to severe Doppler effects," *IEEE Netw.*, vol. 38, no. 1, pp. 203–209, Jan. 2024

[163] Z. Xiao et al., "LEO satellite access network (LEO-SAN) toward 6G: Challenges and approaches," *IEEE Wireless Commun.*, vol. 31, no. 2, pp. 89–96, Apr. 2024

[164] M. Caus, M. Shaat, A. I. Pérez-Neira, M. Schellmann, and H. Cao, "Reliability oriented OTFS-based LEO satellites joint transmission scheme," in *Proc. IEEE Globecom Workshops (GC Wkshps)*, Rio de Janeiro, Brazil, 2022, pp. 1406–1412.

[165] X. Wang, W. Shen, C. Xing, J. An, and L. Hanzo, "Joint Bayesian channel estimation and data detection for OTFS systems in LEO satellite communications," *IEEE Trans. Commun.*, vol. 70, no. 7, pp. 4386–4399, Jul. 2022.

[166] C. Xu et al., "OTFS-aided RIS-assisted SAGIN systems outperform their OFDM counterparts in doubly selective high-Doppler scenarios," *IEEE Internet Things J.*, vol. 10, no. 1, pp. 682–703, Jan. 2023.

[167] Z. Gao et al., "Grant-Free NOMA-OTFS paradigm: Enabling efficient ubiquitous access for LEO satellite Internet-of-Things," 2022, *arXiv:2209.12159*.

[168] J. Hu, Y. Jin, J. Shi, X. Liu, Z. Dai, and Z. Li, "Reliability analysis of stochastic geometry-based multi-UAV-aided LEO-Satcom under OTFS," in *Proc. Int. Symp. Wireless Commun. Syst. (ISWCS)*, Hangzhou, China, 2022, pp. 1–6.

[169] "Framework and overall objectives of the future development of IMT for 2030 and beyond," ITU-Rec. M.2160-0, Int. Telecommun. Union, Geneva, Switzerland, 2023. [Online]. Available: https://www.itu.int/dms_pubrec/itu-r/rec/m/R-REC-M.2160-0-202311-I

[170] W. Yuan, Z. Wei, S. Li, J. Yuan, and D. W. K. Ng, "Integrated sensing and communication-assisted orthogonal time frequency space transmission for vehicular networks," *IEEE J. Sel. Topics Signal Process.*, vol. 15, no. 6, pp. 1515–1528, Nov. 2021.

[171] S. Li et al., "A novel ISAC transmission framework based on spatially-spread orthogonal time frequency space modulation," *IEEE J. Sel. Areas Commun.*, vol. 40, no. 6, pp. 1854–1872, Jun. 2022.

[172] Z. Tang, Z. Jiang, W. Pan, and L. Zeng, "The estimation method of sensing parameters based on OTFS," *IEEE Access*, vol. 11, pp. 66035–66049, 2023.

[173] X. Xia, K. Xu, Y. Wang, Y. Xu, and W. Xie, "Achieving better accuracy with less computations: A delay-Doppler spectrum matching assisted active sensing framework for OTFS based ISAC systems," *IEEE Trans. Wireless Commun.*, vol. 23, no. 6, pp. 6204–6220, Jun. 2024.

[174] Y. Shi and Y. Huang, "Integrated sensing and communication-assisted user state refinement for OTFS systems," *IEEE Trans. Wireless Commun.*, vol. 23, no. 2, pp. 922–936, Feb. 2024.

[175] X. Liu, Y. Yang, J. Gong, N. Xia, J. Guo, and M. Peng, "Amplitude barycenter calibration of delay-Doppler spectrum for OTFS signal—An endeavor to integrated sensing and communication waveform design," *IEEE Trans. Wireless Commun.*, vol. 23, no. 4, pp. 2622–2637, Apr. 2024.

[176] Y. Yang, Y. Pan, X. Liu, and M. Peng, "Barycenter calibration with high order spectra of windowed delay-Doppler signals for OTFS based ISAC systems," *IEEE Trans. Signal Process.*, vol. 72, pp. 2450–2466, 2024.

[177] T. P. Zieliński et al., "Wireless OTFS-based integrated sensing and communication for moving vehicle detection," *IEEE Sensors J.*, vol. 24, no. 5, pp. 6573–6583, Mar. 2024.

[178] X. Yang, H. Li, Q. Guo, J. A. Zhang, X. Huan, and Z. Cheng, "Sensing aided uplink transmission in OTFS ISAC with joint parameter association, channel estimation and signal detection," *IEEE Trans. Veh. Technol.*, vol. 73, no. 6, pp. 9109–9114, Jun. 2024.

[179] S. E. Zegrar, H. Haif, and H. Arslan, "OTFS-based ISAC for super-resolution range-velocity profile," *IEEE Trans. Commun.*, early access, Feb. 26, 2024, doi: 10.1109/TCOMM.2024.3369672.

[180] M. F. Keskin, C. Marcus, O. Eriksson, A. Alvarado, J. Widmer, and H. Wymeersch, "Integrated sensing and communications with MIMO-OTFS: ISI/ICI exploitation and delay-Doppler multiplexing," *IEEE Trans. Wireless Commun.*, early access, Mar. 8, 2024, doi: 10.1109/TWC.2024.3370501.

[181] K. Zhang, W. Yuan, P. Fan, and X. Wang, "Dual-functional waveform design with local sidelobe suppression via OTFS signaling," *IEEE Trans. Veh. Technol.*, early access, May 6, 2024, doi: 10.1109/TVT.2024.3395373.

[182] X. Feng et al., "Underwater acoustic communications based on OTFS," in *Proc. 15th IEEE Int. Conf. Signal Process. (ICSP)*, 2020, pp. 439–444.

[183] D. Varshney, M. Agrawal, and A. S. Gupta, "Orthogonal time frequency space modulation: Analysis in noisy underwater acoustic channels," in *Proc. IEEE Int. Symp. Ocean Technol. (SYMPOL)*, 2023, pp. 1–5.

[184] T. P. S. Babu, J. Francis, and R. D. Koilpillai, "OTFS and OCDM based underwater acoustic communication: System design and evaluation," in *Proc. OCEANS*, pp. 1–6, 2022.

[185] X. Guo, B. Wang, Y. Zhu, Z. Fang, and S. Zhang, "Underwater acoustic communication based on OTFS-IM," in *Proc. 14th Int. Conf. Signal Process. Syst. (ICSPS)*, 2022, pp. 216–219.

[186] K. P. Arunkumar and C. R. Murthy, "Orthogonal delay scale space modulation: A new technique for wideband time-varying channels," *IEEE Trans. Signal Process.*, vol. 70, pp. 2625–2638, May 2022.

[187] S. Hanga and W. Li, "OTFS for underwater acoustic communications: Practical system design and channel estimation," in *Proc. OCEANS*, 2022, pp. 1–7.

[188] L. Jing, Q. Wang, C. He, and X. Zhang, "A learned denoising-based sparse adaptive channel estimation for OTFS underwater acoustic communications," *IEEE Wireless Commun. Lett.*, vol. 13, no. 4, pp. 969–973, Apr. 2024.

[189] Y. Zhang, Q. Zhang, C. He, and C. Long, "Channel estimation for OTFS system over doubly spread sparse acoustic channels," *China Commun.*, vol. 20, no. 1, pp. 50–65, Jan. 2023.

[190] S. Zhang, Y. Zhang, J. Chang, B. Wang, and W. Bai, "DNN-based signal detection for underwater OTFS systems," in *Proc. IEEE/CIC Int. Conf. Commun. China (ICCC Workshops)*, 2022, pp. 348–352.

[191] L. Jing, N. Zhang, C. He, J. Shang, X. Liu, and H. Yin, "OTFS underwater acoustic communications based on passive time reversal," *Appl. Acoust.*, vol. 185, Jan. 2022, Art. no. 108386.

[192] X. Wang, X. Shi, J. Wang, and Z. Sun, "Iterative LMMSE-SIC detector for DSE-aware underwater acoustic OTFS systems," *IEEE Trans. Veh. Technol.*, early access, Feb. 6, 2024, doi: 10.1109/TVT.2024.3362894.

[193] Z. Xue, Q. Wang, L. Jing, C. Zhou, and C. He, "Unitary approximate message passing detection method for OTFS underwater acoustic communication system," in *Proc. IEEE Int. Conf. Signal Process., Commun. Comput. (ICSPCC)*, 2023, pp. 1–5.

[194] R. Han, J. Ma, and L. Bai, "Trajectory planning for OTFS-based UAV communications," *China Commun.*, vol. 20, no. 1, pp. 114–124, Jan. 2023.

[195] F. Linsalata, A. Albanese, V. Sciancalepore, F. Roveda, M. Magarini, and X. Costa-Perez, "OTFS-superimposed PRACH-aided localization for UAV safety applications," in *Proc. IEEE Global Commun. Conf. (GLOBECOM)*, 2021, pp. 1–6.

[196] A. Nordio, C. F. Chiasserini, and E. Viterbo, "Robust localization of UAVs in OTFS-based networks," in *Proc. IEEE Global Commun. Conf. (GLOBECOM)*, 2023, pp. 7471–7477.

[197] H. Niu, J. Hu, J. Shi, and Z. Li, "Secrecy performance analysis for OTFS modulation based downlink LEO satellite communication," in *Proc. IEEE Globecom Workshops (GC Wkshps)*, 2023, pp. 2135–2139.

[198] X. Xu, M.-M. Zhao, M. Lei, and M.-J. Zhao, "A damped GAMP detection algorithm for OTFS system based on deep learning," in *Proc. IEEE 92nd Veh. Technol. Conf.*, Victoria, BC, Canada, 2020, pp. 1–5.

[199] M. Liu, M.-M. Zhao, M. Lei, and M.-J. Zhao, "Autoencoder based PAPR reduction for OTFS modulation," in *Proc. IEEE 94th Veh. Technol. Conf.*, Norman, OK, USA, 2021, pp. 1–5.

[200] J. Park, J.-P. Hong, H. Kim, and B. J. Jeong, "Auto-encoder based orthogonal time frequency space modulation and detection with meta-learning," *IEEE Access*, vol. 11, pp. 43008–43018, 2023.
[201] Y. K. Enku et al., "Two-dimensional convolutional neural network-based signal detection for OTFS systems," *IEEE Wireless Commun. Lett.*, vol. 10, no. 11, pp. 2514–2518, Nov. 2021.
[202] Y. K. Enku, B. Bai, S. Li, M. Liu, and I. N. Tiba, "Deep-learning based signal detection for MIMO-OTFS systems," in *Proc. IEEE Int. Conf. Commun. Workshops (ICC Workshops)*, 2022, pp. 1–5.
[203] Z. Zhou, L. Liu, J. Xu, and R. Calderbank, "Learning to equalize OTFS," *IEEE Trans. Wireless Commun.*, vol. 21, no. 9, pp. 7723–7736, Sep. 2022.
[204] X. Zhang, L. Xiao, S. Li, Q. Yuan, L. Xiang, and T. Jiang, "Gaussian AMP aided model-driven learning for OTFS system," *IEEE Commun. Lett.*, vol. 26, no. 12, pp. 2949–2953, Dec. 2022.
[205] S. Li, C. Ding, L. Xiao, X. Zhang, G. Liu, and T. Jiang, "Expectation propagation aided model driven learning for OTFS signal detection," *IEEE Trans. Veh. Technol.*, vol. 72, no. 9, pp. 12407–12412, Sep. 2023.
[206] M. H. Abid, I. A. Talin, and M. I. Kadir, "Reconfigurable intelligent surface-aided orthogonal time frequency space and its deep learning-based signal detection," *IEEE Access*, vol. 11, pp. 47321–47338, 2023.
[207] L. Guo, P. Gu, J. Zou, G. Liu, and F. Shu, "DNN-based fractional doppler channel estimation for OTFS modulation," *IEEE Trans. Veh. Technol.*, vol. 72, no. 11, pp. 15062–15067, Nov. 2023.
[208] C. Liu, S. Li, W. Yuan, X. Liu, and D. W. K. Ng, "Predictive precoder design for OTFS-enabled URLLC: A deep learning approach," *IEEE J. Sel. Areas Commun.*, vol. 41, no. 7, pp. 2245–2260, Jul. 2023.
[209] A. Singh, S. Sharma, K. Deka, and V. Bhatia, "DL-based OTFS signal detection in presence of hardware impairments," *IEEE Wireless Commun. Lett.*, vol. 12, no. 9, pp. 1533–1537, Sep. 2023.
[210] X. Zhang, S. Zhang, L. Xiao, S. Li, and T. Jiang, "Graph neural network assisted efficient signal detection for OTFS systems," *IEEE Commun. Lett.*, vol. 27, no. 8, pp. 2058–2062, Aug. 2023.
[211] A. Kumar and U. Satija, "Residual stack-aided hybrid CNN-LSTM-based automatic modulation classification for orthogonal time-frequency space system," *IEEE Commun. Lett.*, vol. 27, no. 12, pp. 3255–3259, Dec. 2023.
[212] Y. Yue, J. Shi, Z. Li, J. Hu, and Z. Tie, "Model-driven deep learning assisted detector for OTFS With channel estimation error," *IEEE Commun. Lett.*, vol. 28, no. 4, pp. 842–846, Apr. 2024.
[213] S. R. Mattu and A. Chockalingam, "Learning in time-frequency domain for fractional delay-Doppler channel estimation in OTFS," *IEEE Wireless Commun. Lett.*, vol. 13, no. 5, pp. 1245–1249, May 2024.
[214] Y. Liang, L. Li, P. Fan, and Y. Guan, "Doppler resilient orthogonal time-frequency space (OTFS) systems based on index modulation," in *Proc. IEEE 91st Veh. Technol. Conf.*, Antwerp, Belgium, 2020, pp. 1–5.
[215] H. Ren, W. Xu, and L. Wang, "Orthogonal time-frequency space with improved index modulation," in *Proc. 15th Int. Conf. Signal Process. Commun. Syst. (ICSPCS)*, 2021, pp. 1–6.
[216] H. Zhao, D. He, Z. Kang, and H. Wang, "Orthogonal time frequency space (OTFS) with dual-mode index modulation," *IEEE Wireless Commun. Lett.*, vol. 10, no. 5, pp. 991–995, May 2021.
[217] L. Li, L. Xiao, X. Zhang, G. Liu, S. Li, and T. Jiang, "An efficient symbol-by-symbol aided expectation propagation detector for OTFS with index modulation," *IEEE Wireless Commun. Lett.*, vol. 11, no. 10, pp. 2046–2050, Oct. 2022.
[218] D. Feng, J. Zheng, B. Bai, J. Jiang, and L. Zheng, "In-phase and quadrature index modulation aided OTFS transmission," *IEEE Commun. Lett.*, vol. 26, no. 6, pp. 1318–1322, Jun. 2022.
[219] M. Qian, F. Ji, Y. Ge, M. Wen, X. Cheng, and H. V. Poor, "Block-wise index modulation and receiver design for high-mobility OTFS communications," *IEEE Trans. Commun.*, vol. 71, no. 10, pp. 5726–5739, Oct. 2023.
[220] K. Ma, Z. Gao, J. Wang, and L. Cheng, "Physical layer security design for FDD IM-OTFS transmissions based on secure mapping," *IEEE Access*, vol. 11, pp. 98293–98304, 2023.
[221] K. Zhang, X.-Q. Jiang, H. Hai, R. Qiu, and S. Mumtaz, "Enhanced index modulation aided orthogonal time frequency space with variable active grids and multiple constellations," *IEEE Trans. Veh. Technol.*, early access, Mar. 7, 2024, doi: 10.1109/TVT.2024.3373591.
[222] Y. I. Tek and E. Basar, "Joint delay-Doppler index modulation for orthogonal time frequency space modulation," *IEEE Trans. Commun.*, early access, Feb. 26, 2024, doi: 10.1109/TCOMM.2024.3370827.
[223] Y. Wu, L. Xiao, Y. Xie, G. Liu, and T. Jiang, "Efficient signal detector design for OTFS with index modulation," *Digital Commun. Netw.*, to be published.
[224] V. S. Bhat and A. Chockalingam, "OTFS-IM with decode and forward relaying," in *Proc. IEEE 98th Veh. Technol. Conf.*, 2023, pp. 1–6.
[225] C. Zhang, D. Feng, M. Liu, and B. Bai, "Spatial modulation based MIMO-OTFS transmissions," in *Proc. IEEE/CIC Int. Conf. Commun. China (ICCC Workshops)*, Xiamen, China, 2021, pp. 427–432.
[226] S. Li, L. Xiao, X. Zhang, L. Li, and T. Jiang, "Spatial multiplexing aided OTFS with index modulation," *IEEE Trans. Veh. Technol.*, vol. 72, no. 6, pp. 8192–8197, Jun. 2023.
[227] Y. Yang et al., "Design and analysis of spatial modulation based orthogonal time frequency space system," *China Commun.*, vol. 18, no. 8, pp. 209–223, Aug. 2021.
[228] Y. Qian, L. Xiao, and T. Jiang, "SM-STBC aided orthogonal time frequency space modulation," in *Proc. IEEE Wireless Commun. Netw. Conf. (WCNC)*, Austin, TX, USA, 2022, pp. 2172–2177.
[229] Y. Yang, Z. Bai, H. Liu, K. Pang, X. Hao, and K. J. Kim, "Design and performance analysis of spatial-index modulation based orthogonal time frequency space system," in *Proc. IEEE Int. Conf. Commun. Workshops (ICC Workshops)*, 2022, pp. 922–927.
[230] Y. Yang, Z. Bai, K. Pang, S. Guo, H. Zhang, and K. S. Kwak, "Spatial-index modulation based orthogonal time frequency space system in vehicular networks," *IEEE J. Intell. Transport. Syst.*, vol. 24, no. 6, pp. 6165–6177, Jun. 2023.
[231] X. Zou, S. Fan, H. Chen, Y. Xiao, C. Di, and J. Ji, "Orthogonal time frequency space with generalized spatial modulation," *in Proc. IEEE Veh. Technol. Conf.*, Helsinki, Finland, 2022, pp. 1–5.
[232] Z. Sui, H. Zhang, Y. Xin, T. Bao, L.-L. Yang, and L. Hanzo, "Low complexity detection of spatial modulation aided OTFS in doubly-selective channels," *IEEE Trans. Veh. Technol.*, vol. 72, no. 10, pp. 13746–13751, Oct. 2023.
[233] D. Feng, B. Bai, and F. Wan, "Generalised space-delay-Doppler index modulated OTFS transmission," in *Proc. IEEE Wireless Commun. Netw. Conf. (WCNC)*, 2023, pp. 1–5.
[234] D. Feng, J. Zheng, B. Bai, J. Jiang, and H. Chu, "Generalized index modulation for MIMO-OTFS transmission," *IEEE Wireless Commun. Lett.*, vol. 12, no. 5, pp. 907–911, May 2023.
[235] Z. Sui, H. Zhang, S. Sun, L.-L. Yang, and L. Hanzo, "Space-time shift keying aided OTFS modulation for orthogonal multiple access," *IEEE Trans. Commun.*, vol. 71, no. 12, pp. 7393–7408, Dec. 2023.
[236] S. Doğan-Tusha, A. Tusha, S. Althunibat, and K. Qaraqe, "Orthogonal time frequency space multiple access using index modulation," *IEEE Trans. Veh. Technol.*, vol. 72, no. 12, pp. 15858–15866, Dec. 2023.
[237] A. Tariq, M. S. Sarwar, and S. Y. Shin, "Orthogonal time frequency space index modulation based on non-orthogonal multiple access," in *Proc. 14th Int. Conf. Inf. Commun. Technol. Converg. (ICTC)*, 2023, pp. 838–841.
[238] E. Nayebi, A. Ashikhmin, T. L. Marzetta, H. Yang, and B. D. Rao, "Precoding and power optimization in cell-free massive MIMO systems," *IEEE Trans. Wireless Commun.*, vol. 16, no. 7, pp. 4445–4459, Jul. 2017.